Université de Montréal

The psychophysics of decision making in a two-direction random dot motion target selection task

par

Edmund Lam

Département de neurosciences
Faculté de médecine

Mémoire présenté à la Faculté des études supérieures et postdoctorales en vue de l'obtention du grade de la Maîtrise en sciences neurologiques

Avril 2014

Université de Montréal
Faculté des études supérieures et postdoctorales

Ce mémoire intitulé :

The psychophysics of decision making in a two-direction random dot motion target selection task

Présenté par :

Edmund Lam

a été évalué par un jury composé des personnes suivantes :

Numa Dancause, Ph.D.
président-rapporteur

John F. Kalaska, Ph.D.
directeur de recherche

Erik P. Cook, Ph.D.
membre du jury

Résumé

La tâche de kinématogramme de points aléatoires est utilisée avec le paradigme de choix forcé entre deux alternatives pour étudier les prises de décisions perceptuelles. Les modèles décisionnels supposent que les indices de mouvement pour les deux alternatives sont encodés dans le cerveau. Ainsi, la différence entre ces deux signaux est accumulée jusqu'à un seuil décisionnel. Cependant, aucune étude à ce jour n'a testé cette hypothèse avec des stimuli contenant des mouvements opposés. Ce mémoire présente les résultats de deux expériences utilisant deux nouveaux stimuli avec des indices de mouvement concurrentiels. Parmi une variété de combinaisons d'indices concurrentiels, la performance des sujets dépend de la différence nette entre les deux signaux opposés. De plus, les sujets obtiennent une performance similaire avec les deux types de stimuli. Ces résultats supportent un modèle décisionnel basé sur l'accumulation des indices de mouvement net et suggèrent que le processus décisionnel peut intégrer les signaux de mouvement à partir d'une grande gamme de directions pour obtenir un percept global de mouvement.

Mots-clés : prise de décision, psychophysique, intégration sensorimotrice, kinématogramme de points aléatoires, choix forcé entre deux alternatives

Abstract

Random dot kinematograms are used in visual psychophysics with the two-alternative forced-choice paradigm to study the process of simple perceptual decisions. Mathematical models of this process assume that stochastic motion evidence for the two alternative choices is encoded in the brain, and that the difference in evidence is accumulated towards a decision bound. However, no study to date has tested this assumption using stimuli with different levels of mutually opposing evidence in both directions. This thesis presents the results of two experiments using two novel stimuli with opposing coherent motion evidence. Over a variety of competing evidence combinations, subject performance was based on the net difference in the opposing signals. Furthermore, task performance was similar with both types of stimuli. These results support a decision model based on the accumulation of net evidence, and suggest that the decision process is capable of integrating motion evidence from a wide range of directions to obtain a global percept of motion.

Keywords: Decision making, psychophysics, sensorimotor integration, random dot motion, two-alternative forced-choice.

Table of Contents

List of Tables

List of Figures

I. Introduction

II. Article

III. Discussion

List of Abbreviations

2AFC	Two-alternative forced-choice
BD	Brownian Drift
dlPFC	Dorso-lateral prefrontal cortex
DPC	Dorsal premotor cortex
DV	Decision variable
FEF	Frontal eye fields
FPD	Framewise Pixel Displacement
LATER	Linear Accumulation to Threshold with Ergodic Rate
LBA	Linear Ballistic Accumulator
LIP	Lateral intraparietal area
LFP	Local field potential
M1	Primary motor cortex
MPC	Medial premotor cortex
MT	Middle temporal area
NC	Narrow Coherence
PFC	Prefrontal cortex
RDK	Random dot kinematogram
ROC	Receiver operating characteristic
RT	Reaction time
SC	Superior colliculus
S1	Primary somatosensory cortex
S2	Secondary somatosensory cortex
V1	Primary visual cortex
VPC	Ventral premotor cortex

Acknowledgements

I would like to express my most sincere gratitude to my director Dr. John F. Kalaska for his guidance, support and encouragement throughout the duration of my project. I would also like to thank my project committee members Dr. Numa Dancause and Dr. Paul Cisek for their advice during my research. I would like to extend my appreciation to all the members of the lab for their company and support. I would like to thank to my parents, who have always encouraged me to pursue academic excellence. Finally I wish to express my gratitude to Rosa for her constant love and presence in my life.

I. Introduction

Decision making is a fundamental cognitive process that is studied in many disciplines, from political science, management science, and computer science, to economics, sociology and cognitive psychology. While each discipline studies different forms of decision making, the general decision process is similar: it involves "a commitment to a proposition or plan of action based on information and values associated with the possible outcomes" (Shadlen and Kiani, 2013). Decisions could concern such seemingly simple questions such as whether or not a sensory event had occurred ("signal detection"), what was the nature of the stimulus ("signal discrimination"), what action to take in response to the stimulus ("action selection"), or more complex questions such as what stocks to buy or sell, what restaurant to go to for dinner or for which political party to vote. The scope of this present work is to study the process of simple perceptual decision making, and to study the properties of the neural mechanisms underlying this process.

In this research project, I will examine how subjects making perceptual decisions about dots moving in different directions on a screen can give insight into how the brain integrates evidence for alternative choices. I start by giving an overview of several topics to provide context for the project. This introduction will consist of three sections. The first section is an overview of the psychophysics of decision making and random dot kinematograms. The second part will be an overview of the theoretical models of decision making. In the third part I will describe the objectives and hypotheses of the project. This introductory section is followed by one article detailing part of my work on the project. Finally I will conclude with

an overall discussion and a summary of the main findings, as well as a brief description of the further analyses of the experimental data that I am pursuing.

I.1. The Psychophysics of Decision Making

In the field of experimental psychology, the term "psychophysics" is typically used to characterize the study of how a sensory stimulus is experienced by an observer. Psychophysical experiments involve perceptual tasks in which individual properties of a sensory stimulus are systematically manipulated to examine how these properties affect the observer's experience of that stimulus (Fechner, 1966). Among the many properties of sensory processing, two have been heavily studied: the point at which an observer can detect a stimulus, called the detection threshold, and the point at which an observer can detect a difference in two similar stimuli, called the discrimination threshold (Gescheider, 2013). These properties can be measured using a simple "yes-no" task paradigm. For example, a simple auditory stimulus detection task could involve playing a tone at different intensities ranging from sub-threshold values to above threshold values and asking an observer to report whether or not they heard the tone. This task produces a psychometric function, as illustrated in **Figure I.1a**. By convention, the threshold for detection is set to the stimulus intensity at which observers report hearing the tone 50% of the time. In an auditory stimulus discrimination task, on the other hand, two tones could be presented to the observer with varying relative differences in the intensity of the two tones. The observer is then asked to report whether the intensity of the two tones was the same or different. Stimulus discrimination tasks can also measure other properties of musical tones, such as pitch and

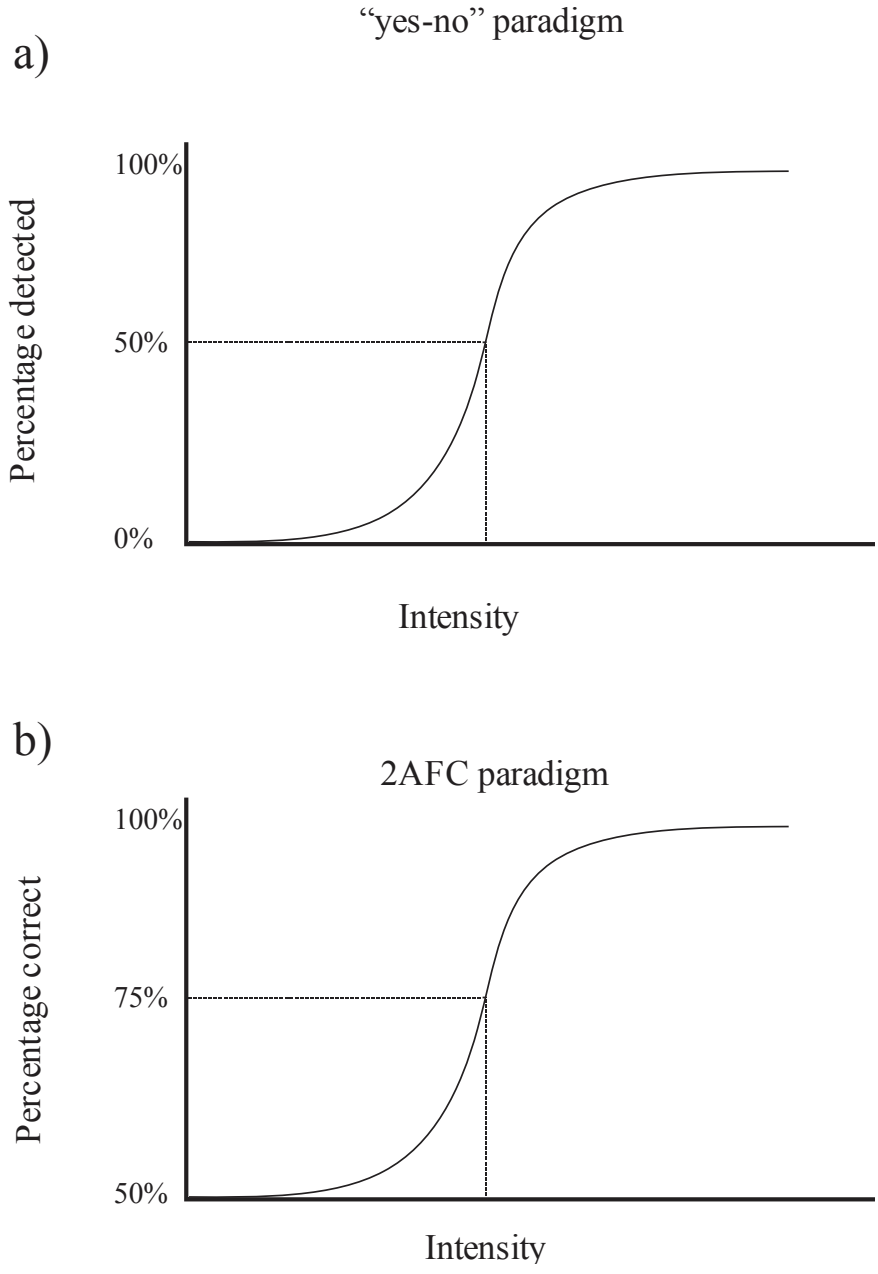

Figure I.1: Illustration of psychometric functions for "yes-no" and 2AFC paradigms

timbre (Hirsh and Watson, 1996). Similar to the detection task, the threshold for discrimination is set to the point at which observers report that the two tones are different 50% of the time. This simple "yes-no" paradigm has been used to study the stimulus properties of all sensory domains, from vision, hearing and touch to taste and smell. For example, in the domain of vision, this task has been used to measure detection and discrimination thresholds for luminance, contrast, and color as well as more complex percepts such as orientation and visual motion.

One of the limitations to the "yes-no" paradigm is that the observer must choose between reporting the presence or absence of an event. This can introduce a response bias, in which the observer might be more biased towards reporting a "yes" or "no" based on an internally defined response criterion (Swets, 1961; Macmillan and Creelman, 1996). Furthermore, this response criterion could vary over time for the same observer. Therefore the measurement of sensory sensitivity can be contaminated by centrally-generated influences on the decision process. One paradigm that was developed in order to reduce the bias in the measure of sensory sensitivity is the two-alternative forced-choice task (Linschoten et al., 2001).

I.1.1.Two-Alternative Forced-Choice Tasks

The two-alternative forced-choice (2AFC) task asks a participant to make a decision between two alternative choices based on the sensory stimuli shown (Green and Swets, 1966; Swets, 1986; Macmillan and Creelman, 1996). While the "yes-no" paradigm presents the observers with a choice between the presence or absence of an event, the 2AFC task presents the observers with a choice between two possible event alternatives. For example, consider a 2AFC auditory stimulus discrimination task: Instead of the "yes-no" paradigm, where

observers are asked whether two tones have the same or different intensities, in the 2AFC paradigm, observers would be asked to indicate whether the first or second tone was more intense. As a further example, a vibrotactile stimulus detection task could involve a near-threshold vibration that is presented randomly to an observer's right or left index finger. The observer must then report which index finger received the vibration stimulus. Similarly, a vibrotactile frequency discrimination task could involve two vibrations that are presented in two sequential time intervals to the observer. The observer is then asked to compare the frequencies of the two vibrations and report whether the first or second stimulus had a higher frequency vibration. By adjusting the difference in the vibration frequencies presented to the observer, one could generate a similar psychophysical curve to the ones generated with the "yes-no" paradigm. Since the observer must always choose one of the alternatives, their performance on 2AFC tasks will range from chance probability (50%) to perfect discrimination (100%) and the discrimination threshold is set to 75% (**Figure I.1b**).

With the development of neural recording techniques, psychophysics tasks were adopted by neurophysiologists to study the neural mechanisms of sensory processing. Mountcastle and colleagues pioneered this approach in the 1960s, and were among the first to relate neural activity recorded in non-human primates with human psychophysics. They showed that neural activity in the primary afferents of anesthetized monkeys varied with the properties of a vibrational stimulus, and that this neural activity had a measurable quantitative association with the psychophysical performance of human observers performing a detection task with the same vibrotactile stimuli (Werner and Mountcastle, 1965; Mountcastle et al., 1967; Talbot et al., 1968).

Furthermore, the 2AFC paradigm proved to be useful in the study of the neural basis of decision making by allowing experimental neurophysiologists to study the activity of neurons during the deliberation process of a decision while it is being made (Gold and Shadlen, 2001; Cisek and Kalaska, 2002; Roitman and Shadlen, 2002; Cisek and Kalaska, 2005; Gold and Shadlen, 2007; Churchland et al., 2008). For example, Romo and colleagues used the vibrotactile frequency discrimination task to study the activity of neurons in the somatosensory cortex (primary, S1; secondary S2), the premotor cortex (ventral, VPC; dorsal DPC; and medial, MPC), the prefrontal cortex (PFC) and the primary motor cortex (M1). While neurons in S1 encoded the sensory properties of the two vibration stimuli as they were presented (Hernández et al., 2000; Salinas et al., 2000), the activity of neurons in S2, VPC, DPC, MPC, PFC and M1 were correlated with later stages in the decision process, such as the encoding of the first vibration into working memory, the comparison of the two vibrational stimuli, as well as the animal's final decision (Romo et al., 1999; Hernández et al., 2002; Brody et al., 2003; Romo et al., 2004; Hernández et al., 2010). In summary, researchers have embraced the combination of psychophysical measurements and neurophysiological recordings in order to understand the neural basis of decision making.

I.1.2. Random Dot Kinematograms

One stimulus commonly used in conjunction with 2AFC tasks to study decision making is the random dot kinematogram (RDK). Random dot motion was used as early as the 1970s to study the process of visual motion detection and discrimination (Braddick, 1974; Lappin and Bell, 1976; Ball and Sekuler, 1979). In a standard RDK (illustrated in **Figure I.2**), a group of dots are displaced randomly on a screen. In order to evoke a percept of coherent visual motion, a portion of these dots are chosen to move coherently in one direction

(Williams and Sekuler, 1984; Downing and Movshon, 1989; Britten et al., 1992). Used in a 2AFC direction discrimination paradigm, observers are asked to view an RDK stimulus and decide between two possible directions of coherent motion among the background of random dot motion.

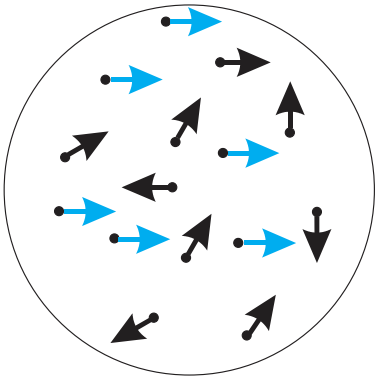

Figure I.2: Random dot kinematogram

RDK stimuli are ideal psychophysical stimuli to study visual motion: they minimize position cues, the individual stimulus elements (dots) usually do not have any easily recognizable features that would make them easy to identify and track individually, and they can be generated with easy control over other visual parameters, such as contrast, luminance, as well as the spatial-temporal frequency content of the stimulus (Newsome and Pare, 1988). Furthermore, RDK stimuli are ideal perceptual stimuli for decision-making studies for several other reasons. First, they tend to lead to longer reaction times than many other sensory stimuli. This led to the development of a reaction-time variant of the 2AFC paradigm in which observers could indicate their choice as soon as they made their perceptual decision. This facilitates the study of the time course of the decision process by using the time of onset of the motor action that signals the subject's decision as a distal surrogate for the time of the end of

the decision process (Roitman and Shadlen, 2002; Gold and Shadlen, 2007). Second, RDKs can easily provide different amounts of visual motion signal ("evidence") by modifying the amount of coherently moving dots in the stimuli. Finally, the RDK stimulus paradigm offers a number of other ways in which to probe the decision-making process. For instance, one can transiently increase or decrease the amount of sensory evidence for different choices at different times in the trial (Huk and Shadlen, 2005; Thura and Cisek, 2014). The coherent-motion evidence signal and random-noise motions can be distributed onto different dots in different ways, such as partitioning them onto two separate sub-groups of dots for the entire duration of a stimulus, or onto continually-changing groups of dots according to different schedules (Williams and Sekuler, 1984; Snowden and Braddick, 1989; Pilly and Seitz, 2009; Schütz et al., 2010).

Similar to the aforementioned studies combining the vibrotactile discrimination task with neural recordings in the somatosensory cortex to study the neural basis of vibrotactile frequency discrimination, RDKs were combined with neurophysiological studies to show that the middle temporal (MT/V5) area of monkeys contributed to the perception of visual motion. MT is an extrastriate visual cortical area in which the majority of neurons are preferentially activated by moving visual stimuli (Dubner and Zeki, 1971; Zeki, 1974; Albright, 1984; Newsome et al., 1986; Mikami et al., 1986a, 1986b). The ability to detect coherent motion in an RDK stimulus was impaired in monkeys after lesions to the MT area (Newsome and Pare, 1988), as well as with a human patient with damage in the corresponding extrastriate visual cortex (Baker et al., 1991). A study by Britten et al. (1993) showed that motion sensitive neurons in area MT of monkeys would discharge at a rate proportional to the amount of coherent motion in their preferred direction of motion. The neurometric sensitivity profile of

these neurons as a function of stimulus motion coherence closely resembled the psychometric curves of the motion sensitivity of the animal observers performing a 2AFC RDK motion discrimination task (Britten et al., 1992), further solidifying the evidence that MT neurons contributed to the perception of visual motion.

RDK stimuli were subsequently used in further 2AFC action-choice tasks to study the relationship between neural activity in area MT and the process of decision making. When analyzed on a trial-to-trial basis, the variability of the firing rates of MT neurons was weakly but significantly correlated to the monkey's choices (Britten et al., 1996; Cook and Maunsell, 2002). Furthermore, Salzman et al. (1992) demonstrated that microstimulation in area MT could bias the observing monkey's decision choice towards the preferred direction of motion of the neurons in the locally stimulated area. In addition, Ditterich et al. (2003) used a reaction-time version of the RDK task to demonstrate that microstimulation would speed up the monkey's reaction times towards the direction of preferred motion of the neurons in the stimulated area, and slow down reaction times in the opposite direction. These studies demonstrated that the activity of MT neurons was causally related to the perceptual decision-making process in the task.

To report their perceptual decisions, the monkeys typically made saccadic eye movements in the direction of the perceived RDK motion. However, MT cells are not related to saccadic eye movements. To study how the monkeys linked the perceptual decision process to the planning and execution of the reporting saccadic eye movements, researchers then focused on saccade-related areas, such as the lateral intraparietal (LIP) in monkeys, where many cells discharge as a function of saccade direction and target spatial location (Robinson et al., 1978; Bushnell et al., 1981; Gnadt and Andersen, 1988; Platt and Glimcher, 1997, 1998).

A series of studies by Shadlen and colleagues subsequently established area LIP as an integral part of the decision making process. In an instructed-delay version of the RDK-stimulus task, Shadlen & Newsome (2001) showed that the time course of changes in the activity of saccade-related neurons in LIP varied with the coherence of the RDK stimuli. Furthermore, unlike MT neurons, the changes in activity of the LIP neurons were related to the monkeys' perceptual decision, whether correct or wrong, that is, how the monkeys interpreted the stimuli rather than their actual physical properties (Shadlen and Newsome, 2001). Using a subsequent reaction-time variant of the RDK paradigm, Roitman & Shadlen (2002) showed that LIP neuronal activity increased gradually over the course of the trial between the onset of the RDK stimuli and the onset of the saccade, at a rate that was proportional to the amount of coherent motion in the neuron's preferred direction. Furthermore, when aligning the neuronal activity to the onset of the saccade, i.e., to the end of the decision process, the firing rate always reached a common level of activity regardless of the motion coherence of the stimuli and rate of accumulation in each trial, suggesting that the decision process was terminated and a saccade initiated once a critical firing rate was reached in LIP.

In another study, Huk & Shadlen (2005) presented brief motion pulses in the RDK stimuli and showed that these pulses increased the firing rate of neurons when the pulse was presented in the neuron's preferred direction, and decreased activity when the pulse was presented in the opposite direction. Furthermore, the changes in neural activity caused by the motion pulses long outlasted the stimulus changes themselves, consistent with a process of accumulation and retention of the sensory evidence during the trial. A subsequent study by Hanks et al. (2006) showed that microstimulation in LIP during a RDK task led to similar choice biases and RT shifts as the microstimulation studies in area MT described earlier,

further supporting the existence of an integration process in LIP and establishing a causal role between activity in LIP and the choice behaviour of the monkeys. A study by Kiani et al. (2008) showed that when the duration of the RDK stimuli was controlled by the experimenter and variable from trial to trial, the performance of the subjects improved as a function of both RDK stimulus coherence and the duration of observation of the stimuli, also consistent with an evidence integration process. Somewhat surprisingly, however, the observers seemed to adopt a strategy of accumulating information towards a critical decision value rapidly after the onset of the RDK stimuli and terminating the decision process before the end of the stimulus presentation and ignoring any subsequent sensory input, thereby not profiting from the extra evidence available at the end of longer RDK stimuli. Finally a study by Churchland et al. (2008) extending the RDK task from two to four alternative choices found that the same principles of evidence accumulation towards a threshold could apply to more a complex four-choice task. They also found a gradual non-directional increase in activity as a function of time, even in trials in which there was no coherent motion signal. This non-directional progressive increase in activity is consistent with an "urgency" signal that is thought to drive the DV closer to the decision bound as time progresses in the trial, causing a shortening of the decision process especially in the situation of weak sensory evidence (Ditterich, 2006; Churchland et al., 2008).

Taken as a whole, these studies presented a strong body of evidence that LIP activity could be related to the accumulation of motion evidence towards a decision, and that the decision process terminated once LIP neuronal activity reached a critical firing rate, triggering the report saccade.

Other studies have used the RDK stimuli to show decision-related activity in the superior colliculus (SC) (Horwitz and Newsome, 1999, 2001), and the dorso-lateral prefrontal cortex (dlPFC) (Kim and Shadlen, 1999). In summary, RDK stimuli have been used with the 2AFC paradigm to study the neural correlates of decision making in a number of eye movement-related structures, and have yielded extensive evidence consistent with a decision-making process that involves the temporal accumulation of sensory evidence to a decision threshold.

I.2. Models of Decision Making

Experimental psychologists have developed mathematical models to understand how the decision making process works in a 2AFC task. More recently, neurophysiologists have also started using variants of the same models to explain how neuronal activity may be involved in the decision process. One of the main frameworks for modeling the computational basis of decision-making involves a diffusion-like process (Ratcliff, 1978; Smith and Ratcliff, 2004). These models have several similarities: they share common assumptions, they all aim to model key features, and they all address similar questions.

There are three fundamental assumptions underlying these diffusion models, which have been formalized by Bogacz et al. (2006). First, evidence supporting the two alternative choices is integrated over time. Second, this integration process is subject to random fluctuations or "noise". Third, a decision is reached once sufficient evidence is integrated to choose one option over the other. The first assumption can be further extended into the neuron/anti-neuron hypothesis, whereby the momentary sensory evidence is encoded by separate "neuron" and "anti-neuron" input populations, with the two populations encoding the

sensory inputs (evidence) for the opposite choices (Gold and Shadlen, 2001). The activity from these pools is then sent to a decision-making mechanism that integrates the encoded evidence for each choice over time either independently, or as a difference in evidence for the two choices, depending on the type of model used.

According to Smith and Ratcliff (2004), there are two features that must be upheld in order to have a plausible model of the 2AFC task. First, the model must accurately represent an observer's reaction times and success rates on varying difficulties of trials. Second, the model must also predict differences in these behavioural measurements when correct or incorrect choices are made. With the advent of neurophysiological research into decision making, a third feature has also emerged - the model should have a plausible neural representation in the brain (Ditterich, 2006).

Finally, these models address several key questions about the decision making process. One question is whether the evidence for the alternative choices is integrated separately by different accumulators, or whether evidence is integrated as a difference between the evidence for the two alternative choices. Another question focuses on the variability of the integration process, the sources of this variability and its ultimate influence on the decision process.

In the following sections I will review four classes of mathematical models of decision making and how they fit with the 2AFC paradigm.

I.2.1. Decision models with noiseless evidence accumulation

The LATER (linear accumulation to threshold with ergodic rate) model, developed by Roger Carpenter, was among the first models to describe the reaction time distributions during simple stimulus detection and movement initiation tasks (Carpenter, 1981; Carpenter and Williams, 1995). In this model, there is no variability in the momentary accumulation of

evidence during a given trial. Instead evidence is accumulated at a constant rate in a ramp-like fashion towards a predefined threshold at which the movement is then initiated. Between trials of the same stimulus strength, however, the rate of accumulation is subject to random variability; this is the only source of noise in the LATER model. As a result, during repeated trials with the same stimulus, the slope and resulting duration of evidence accumulation will vary between trials with a certain mean and standard deviation. The value of the mean and standard deviation changes when the strength of the sensory signals changes. To accommodate differences in response priorities such as speed versus precision, the LATER model assumes that subjects can adjust the height of the decision threshold. Lowering the decision threshold would allow for faster but less accurate responses, while raising the decision threshold would result in slower but more accurate decisions (Reddi and Carpenter, 2000). In addition, the LATER model assumes that subjects can change the start point of the evidence accumulation process in order to adjust their decision process on the basis of prior knowledge, such as the probability of different stimuli or response choices, or the differential reward value of different responses (Carpenter and Williams, 1995). The LATER model can predict distributions of RTs that fit well with reaction-time distributions during simple movement initiation tasks in a wide range of task conditions (Gold and Shadlen, 2007). However, in the context of the 2AFC task, the LATER model has limitations. First - each LATER module only accumulates evidence for one alternative and does not address how evidence between two alternatives would be compared. Second, the single-module version of the LATER model usually does not successfully predict choice probabilities and errors in even simple single-response tasks. In order to address these limitations, two or more LATER units can be linked together into increasingly complex circuits to race against each other towards two alternate choices to

predict response times and success/error rates in a variety of different tasks (Asrress and Carpenter, 2001; Leach and Carpenter, 2001; Reddi et al., 2003; Sinha et al., 2006; Story and Carpenter, 2009; Noorani and Carpenter, 2011; Noorani et al., 2011).

Another model with noiseless within-trial evidence accumulation is the Linear Ballistic Accumulator (LBA) model (Brown and Heathcote, 2005, 2008). Similar to the Carpenter models that use two LATER units, the LBA model accumulates evidence for two competing choices separately in two noiseless "ballistic" accumulators, and the rate of accumulation of evidence varies randomly between trials of similar evidence strength. In addition to the variable rate of accumulation, the LBA model allows for a second source of random inter-trial variability - a variable starting point for the accumulation process from trial to trial. This extra source of variability allows the LBA model to account for reaction times and success/error rates over a range of different task conditions without having to invoke different combinations of computational modules in different tasks, as is the case with the LATER model.

Both the LATER and LBA models assume that the main source of variability in the decision process arises between trials (*inter*-trial variability). However another family of models assumes that the main source of variability occurs within each trial (*intra*-trial variability) in the stochastic accumulation of evidence, which can be described as a random walk drift-diffusion process. The next three classes of models all use noisy instantaneous evidence accumulation in their design.

I.2.2. Drift Diffusion Models

An early precursor to the drift diffusion model was independently developed during WWII by Abraham Wald to test the quality of batches of munitions being manufactured (Wald, 1945, 1973), as well as by Alan Turing to help his code-breaking work (Good, 1979; Donovan,

2014). Called the sequential probability ratio test, this procedure was developed as a way to repeatedly test a hypothesis against its alternative and reach a statistically reliable decision as quickly as possible when presented with sequential samples of ambiguous evidence (Bogacz et al., 2006; Shadlen and Kiani, 2013). Several years later, the drift-diffusion model combined the idea of accumulation of repeated sequential samples of ambiguous evidence with a sequential test procedure based on the mathematics of drift-diffusion (random walk) processes to characterize the reaction time latencies and choice probabilities in a 2AFC task (Stone, 1960; Laming, 1968; Ratcliff, 1978). In the original formulation of the drift diffusion model (illustrated in **Figure I.3a** and **I.4a**), the evidence for the two choices in the 2AFC task is compared, and the difference in evidence supporting the two choices is accumulated by a single decision variable (DV) over time. The model has an upper and lower decision bound, with the upper bound corresponding to the evidence required to choose one choice, and the lower bound corresponding to the second choice. The DV will integrate the difference in evidence over time until it reaches one of these bounds. At that point, the decision process is terminated and the corresponding choice is selected (Ratcliff and McKoon, 2008). According to drift-diffusion models, the mean rate of evidence accumulation across many trials is determined by the quality and quantity of sensory evidence, like the LATER and LBA models. However, unlike the LATER and LBA models, inter-trial variability in response timing and choices for a constant stimulus is due to moment-to-moment stochastic noise in the accumulation process.

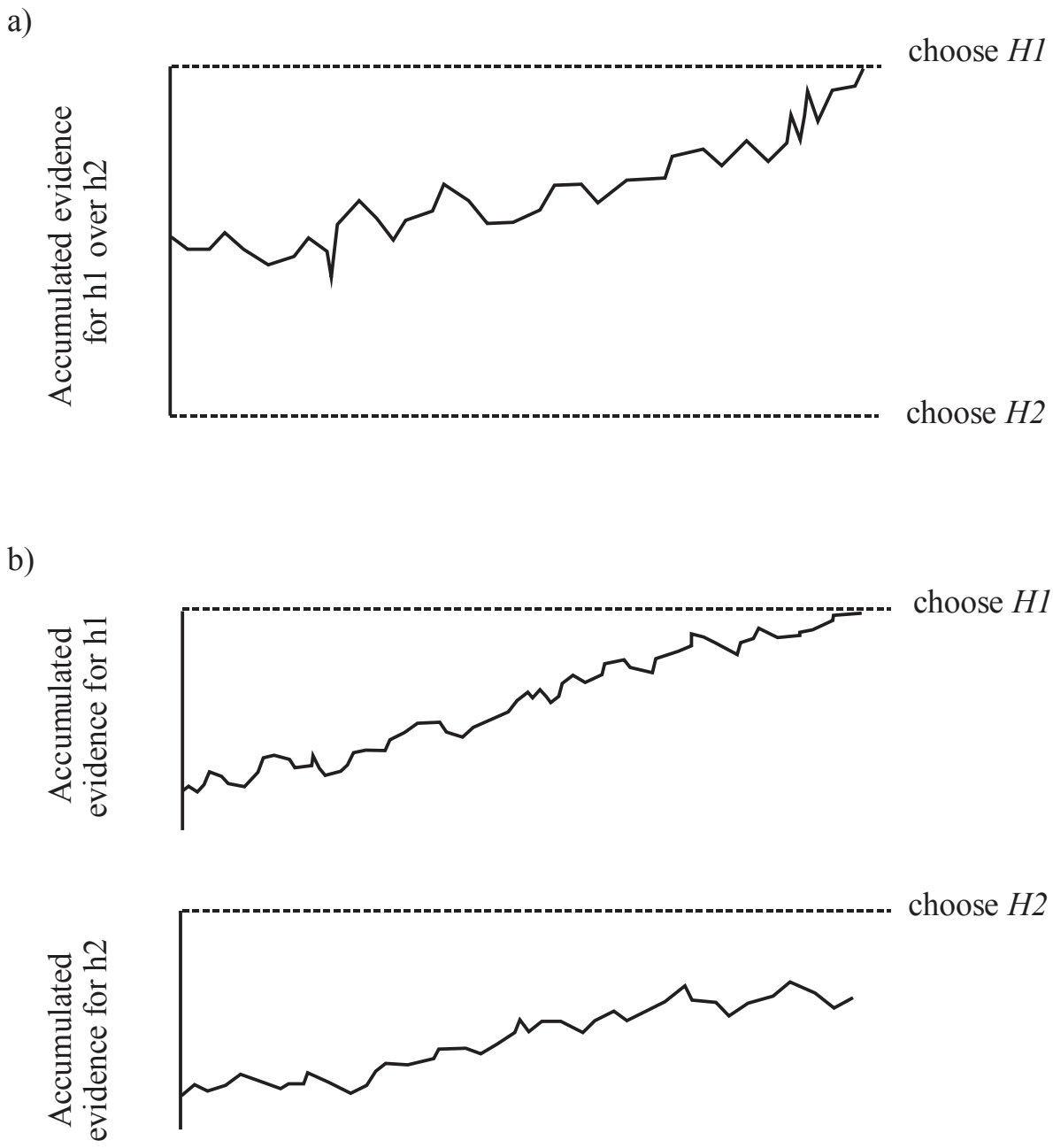

Figure I.3: Single and dual drift-diffusion models

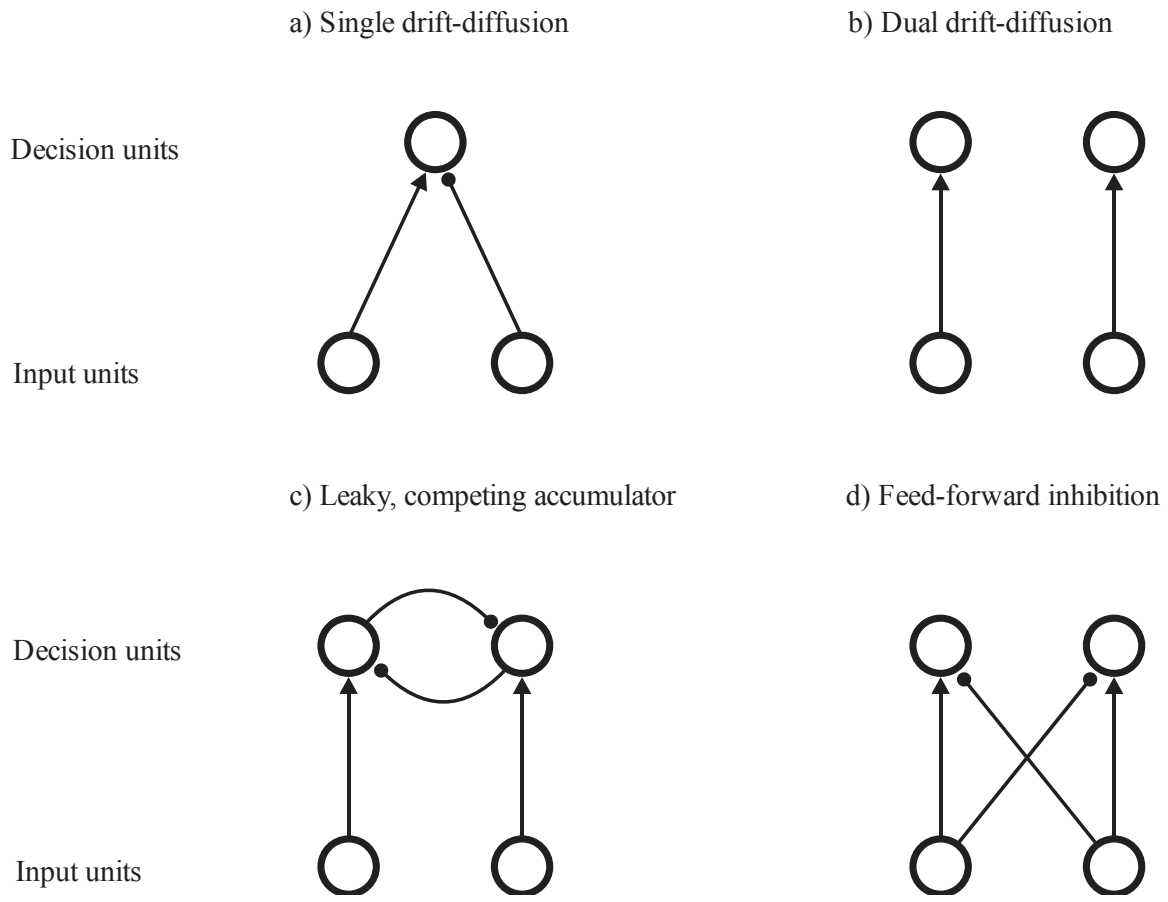

Figure I.4: Network architecture of various decision models

The original formulations of the drift-diffusion models assumed perfect integration, that is, the value of the DV at any given moment accurately reflected the entire stream of sensory evidence accumulated up to that time. A modification of this model was proposed by Busemeyer and Townsend (1993), who introduced a "leakage" factor to the accumulation of evidence. This leak works like a high-pass filter, so that at each moment in time, the leaky accumulator "forgets" a certain amount of the evidence that had been accumulated up to that time while adding the new incoming evidence to the DV. This converted the process into an Ornstein-Uhlenbeck process (Uhlenbeck and Ornstein, 1930; Smith and Ratcliff, 2004) in which earlier evidence is weighed less strongly than the most recent evidence.

Both the perfect and leaky integration versions of this model have been successful at accurately modelling behavioural data in a wide range of variants of the 2AFC task (Smith and Ratcliff, 2004; Ratcliff and McKoon, 2008). However, one of the criticisms with the original drift diffusion model with a single DV and two decision thresholds is that it does not fit very well with the physiological properties of neurons in the brain. While neurons can both increase and decrease their activity, they cannot have a negative firing rate and cannot realistically represent a decision variable that can arrive at two different decisions by crossing over either an upper or lower threshold (Ratcliff et al., 2007).

I.2.3. Dual Drift Diffusion Models

While the original drift diffusion model integrates the difference in evidence for both choices, dual drift diffusion models use two diffusion processes to accumulate evidence for each choice independently (LaBerge, 1962; Vickers, 1970; Bogacz et al., 2006; Ratcliff et al., 2007). The decision process ends once one of the integration processes reaches their respective thresholds. An illustration of this model is shown in **Figure I.3b** and **I.4b**. Like the LATER and LBA models, each drift diffusion module accumulates evidence only for its preferred choice, but the dynamics of the decision process is determined by the stochastic noise of the drift-diffusion process.

The idea of a race between two drift diffusion accumulators was more physiologically plausible than the single-accumulator drift diffusion model. The two accumulators could be represented in the brain as two populations of neurons with opposite choice preferences competing by increasing their activity towards a critical firing rate (Ditterich, 2006; Ratcliff et al., 2007). Furthermore, while the single-accumulator drift diffusion model was limited to two

choices by design, the dual drift diffusion model could be extended to incorporate multiple choices as additional separate accumulators.

However, there were still limitations to the dual drift diffusion model. Psychophysical evidence suggested that subjects' choice behaviour was being driven by the difference in evidence for different response choices (Gold and Shadlen, 2001; Mazurek et al., 2003; Niwa and Ditterich, 2008). The accumulation of the difference in evidence is particularly advantageous because it is approximately equivalent to the calculation of the log likelihood ratio for different alternative hypotheses, which is a robust criterion to make decisions based on noisy or uncertain evidence (Carpenter and Williams, 1995; Gold and Shadlen, 2001, 2007). Moreover, LIP neurons were shown to be positively affected by evidence in their preferred direction, and negatively affected by the opposite direction (Roitman and Shadlen, 2002; Mazurek et al., 2003; Bollimunta and Ditterich, 2012). This suggested that a difference comparison was being made, which was not being used in the dual drift diffusion models. This problem was addressed with dual diffusion models with mutual inhibition.

I.2.4. Dual Diffusion Models with Mutual Inhibition

These models resemble the dual drift diffusion model in which two diffusion processes race against each other, but the two processes each accumulate a decision variable that represents the net evidence for or against their preferred choice. The net evidence is obtained through a process of mutual inhibition between the two integrators. This process of mutual inhibition can be modeled in different ways (Ditterich, 2006). Usher and McClelland (2001) proposed a "leaky, competing accumulator model", in which two sensory input units feed evidence supporting each of the alternate choices separately into two accumulating decision units. These two decision units will then mutually inhibit each other by lateral feedback of their

output signals onto the accumulator of the other decision unit. An illustration of this model is shown in **Figure I.4c**. Alternatively, Mazurek et al. (2003) proposed a feed-forward inhibition model. Instead of having the two accumulating decision units mutually inhibit each other, the two sensory input units coding for evidence for the two choices would each send two projections, one excitatory to the decision unit whose preferred choice corresponds to their preferred sensory input, and one inhibitory to the other decision unit that prefers the alternative choice (Ditterich et al., 2003; Mazurek et al., 2003; Ditterich, 2006). In this manner, each decision unit will receive an excitatory input from the sensory input unit corresponding to its preferred choice, and an inhibitory input from the sensory input unit corresponding to the opposite choice. An illustration of this model is shown in **Figure I.4d**. The convergence of the two oppositely-signed sensory inputs onto each accumulator results in both accumulators receiving a combined input equal to the net difference in sensory evidence favouring the two choices.

Since dual diffusion models with mutual inhibition integrate the difference in evidence for the two choices, these models are largely indistinguishable from a single-accumulator drift diffusion model in their ability to predict and fit behavioural data (Smith and Ratcliff, 2004; Bogacz et al., 2006; Ditterich, 2006). However, as mentioned by Ratcliff et al. (2007), the race process incorporated in mutual inhibition models provide a more biologically plausible framework that more accurately resembles decision related neural activity such as the ramping activity of LIP neurons reported by Roitman and Shadlen (2002).

In summary, many computational models have been proposed to model the process of decision-making in a 2AFC task. Most models satisfy the goals of accurately predicting the psychophysical data and the neural data (Smith and Ratcliff, 2004) and they all have the same

common assumptions: These models assume that evidence is accumulated towards a threshold, this accumulation process is noisy, and that a decision is made once enough evidence is accumulated for one choice over the other (Bogacz et al., 2006).

I.3 Objectives

I.3.1 Effect of directly competing motion

The first objective of my research project was to determine the effect of directly competing motion on the decision process in a 2AFC RDK task. While RDKs have been one of the most common stimuli used in perceptual decision-making studies, in most cases these stimuli only used coherent motion in one direction in a given trial. Meanwhile, 2AFC decision-making models assume that evidence is integrated for both possible choices. In these conventional RDK stimuli, the only evidence for the choice in the non-coherent direction would be stochastic noise due to the random dot motions that happen to be in the direction opposite to the coherent motion signal.

Furthermore, for decision-making models that assume that the decision variable accumulates the net difference in the activity of the neuron and anti-neuron input populations, the decision variable should be insensitive to factors that might affect both input populations equally (Gold and Shadlen, 2001). Extensive psychophysical and neurophysiological evidence is consistent with a decision variable that accumulates the net sensory evidence provided by the neuron/anti-neuron input populations (Britten et al., 1993; Roitman and Shadlen, 2002; Ratcliff et al., 2007; Bosking and Maunsell, 2011; Bollimunta and Ditterich, 2012; Bollimunta et al., 2012). However, this fundamental assumption of the drift-diffusion model cannot be fully validated by the standard RDK stimuli used in decision-making studies, because they

only use one direction of coherent motion against a background of random visual motion. As a result, the difference in evidence for the two alternative choices is essentially equivalent to the total coherent motion provided in only one direction in the standard RDK stimuli.

Furthermore, Liston and Stone (2013) recently critiqued the conventional RDK stimuli used in decision-making studies as not being a "true" 2AFC decision because these RDK do not show evidence for both of the alternative choices in each trial. This assertion was based on the original definition of the 2AFC task, in which the term "alternative" was meant to indicate the perceptual comparison of two alternative stimuli or signals, and not just the a priori existence of two alternative choices (Green and Swets, 1966; Macmillan and Creelman, 1996). If only one signal is presented, the task can still be performed as a yes-no paradigm task. For example, an observer of a single coherent motion RDK could use a strategy in which they observe each stimulus and attempt to discern whether or not it contains evidence for only one of the two choices, such as rightward motion. If they perceive motion in that direction ("yes"), they choose the rightward target, but if they do not perceive rightward motion, they reject that choice ("no") and choose the leftward target by default. This introduces the same potential choice biases due to a priori response criteria that were one of the limitations of "yes-no" paradigms. According to Liston and Stone (2013), a "true" 2AFC RDK motion discrimination task would require an RDK stimulus in which two signals of evidence compete against each other in the same trial.

Opposing motion has been used in RDK stimuli to study the psychophysics and neurophysiology of visual motion perception, especially the perception of so-called "transparent motion", that is, simultaneous motion in different directions in the same spatial location (Snowden et al., 1991; Snowden et al., 1992; Qian and Andersen, 1994, 1995).

However, directly opposing motion RDK stimuli have not yet been used to study its effect on the process of perceptual decisions about the direction of global motion (see next section).

This knowledge gap leads to the following questions: What happens to the behavioural psychophysics if we present stimuli with mutually-competing opposing motion? Is the process really dependent on the net difference in evidence, or could the mutually contradictory evidence actually interfere in the decision-making process? In order to explore these questions we generated modified RDK stimuli which contained two simultaneous opposing coherent motions. Different amounts of coherent motion in both directions were combined to produce RDK stimuli that had the same relative net coherent motion in one of the two directions, but different amounts of simultaneous coherent motions in both opposing directions. We hypothesized that with competing motion, the decision process will still be mainly driven by the net amount of coherent evidence towards the correct choice.

I.3.2 Integration of the global motion signal

Standard RDK stimuli used in decision-making research provide coherent motion in only one of two opposite directions. In addition, all of the coherent dots move in parallel, by definition. As a result, the coherent motion signal is carried explicitly by the parallel motions of a subset of moving dots. What would happen if the coherent motion signal was instead implicitly embedded in the motions of dots moving in many different directions to create a net bias in the distribution of dot motions? Would observers be able to integrate the distributed motion signals in order to get a single global percept of net motion direction? This has been tested in a series on studies of the ability of human subjects to perceive the net global motion signal from a wide range of local motion signals (e.g. Williams and Sekuler, 1984; Watamaniuk et al., 1989; Watamaniuk and Sekuler, 1992; Smith et al., 1994; Pilly and Seitz,

2009; Schütz et al., 2010). These studies used RDK stimuli in which moving dots were displaced in a range of directions that was selected from a uniform or Gaussian distribution of directions centered on one true direction of global motion bias. Human observers were able to integrate the local motion signals spread in many directions to perceive the net direction of global motion.

However, again like conventional RDK stimuli with coherent motion in only one direction, the global motion stimuli did not contain an opposing component of coherent dots moving in the anti-direction. Indeed, if the width of the distribution of motion signals got too broad and started to include motions in nearly opposite directions, the ability of subjects to perceive a global motion direction decreased. At the limit, when the motions were selected uniformly from the full 360 degree continuum, subjects unsurprisingly failed to perceive any net global motion (Williams and Sekuler, 1984). Therefore the second objective of my work was to explore the effect of presenting different amounts of two opposing coherent motion signals whose presence was implicitly embedded across a broad range of dot motion directions in the RDK stimuli.

A more recent study by Niwa and Ditterich (2008) used varying amounts of coherent motion in three equidistant directional axes separated by 120 degrees. Observers' reaction times and target choices were driven by the net direction of motion evidence pooled across the three streams of coherent motion presented in each trial. This indicated that the decision was based on the total distribution of responses across populations of input neurons with a broad range of motion direction preferences. Moreover, the choice behaviour of the subjects could be simulated successfully by a three-accumulator drift-diffusion model driven by the net output of three neuron/anti-neuron populations. In this model, each accumulator integrated the

difference between the motion signal generated by its own sensory input "neurons" that preferred the same direction of motion and the average signal of the two other sensory input sources preferring the other two directions of motion (Niwa and Ditterich, 2008). Neurons in the area LIP of monkeys performing the same task appeared to sum that net motion signal (Bollimunta and Ditterich, 2012; Bollimunta et al., 2012). However, as with other global motion studies using RDK stimuli, the stimuli in the Niwa and Ditterich (2008) study did not explicitly contain competing opposing motions in each of the three streams of coherent motion.

To explore how the psychophysics of the 2AFC task was affected by presenting competing coherent motion spread across many directions, we used two different algorithms to generate RDK stimuli. In one of the stimuli, called the "Narrow Coherence" (NC) stimuli, the coherent motion was confined to the left and right directions, so that the two competing coherent motions are explicitly displayed in the dot motions. In contrast, in the "Brownian Drift" (BD) stimulus, this coherent motion signal was distributed implicitly across many directions by adding a coherent-motion vector component to the otherwise random Brownian motion vector of the RDK dots. Our hypothesis was that if the decision process integrates motion signals from a wide range of directions, then observers' psychophysical reaction times and success rates should be identical for both NC and BD stimuli in a 2AFC RDK coherent-motion discrimination task.

II. Article

Title Page

Title: Choosing sides: they psychophysics of target choices using random dot kinematograms with mutually contradictory evidence.

Abbreviated Title: Random dot motion with directly opposing evidence

Author names and affiliations

Edmund Lam[1,2], John F. Kalaska[1,2]
[1]Département de neurosciences, Université de Montréal, Québec, Canada
[2]Groupe de Recherche sur le Système Nerveux Central (GRSNC), Université de Montréal, Québec, Canada

Conflict of Interest: The authors declare no competing financial interests.

Acknowledgements: This work was supported by the Canadian Institutes of Health Research (CIHR) operating grant MOP-97944. E.L. was supported by the Natural Sciences and Engineering Research Council (NSERC) Alexander Graham Bell Canada Graduate Scholarship and the Fonds de recherche du Québec – Santé (FRQS) Master's Training Award. We thank C. Pack and E. Cook for their helpful comments on motion energy analysis.

Abstract

Random-dot kinematograms (RDKs) are often used in two-alternative forced-choice (2AFC) tasks to study how the brain decides among two perceptual or motor choices based on noisy evidence. Some current models assume that two pools of sensory neurons code the motion evidence in two opposite directions; the difference of these inputs is then accumulated in a decision variable. However, conventional RDKs contain only one direction of coherent motion against a background of random "noise" motion. Here, we explored the psychophysics of RDKs with mutually contradictory evidence. Different amounts of coherent motion were presented simultaneously in both directions to produce RDKs that had the same amount of net coherent motion, but different combinations of coherent motions in opposing directions. The two competing coherent-motion components were either confined to the two exactly opposite directions against a background of random motion ("narrow coherence" stimuli, NC), or spread across many directions of motion by adding a coherent-motion vector to the otherwise random motion of some of the dots ("Brownian drift" stimuli, BD). The choice behaviour of 12 human subjects was primarily driven by the net coherence of motion across a range of combinations of opposing coherent motions for both NC and BD stimuli. Nevertheless, reaction times (RTs) decreased for low net-coherence stimuli as the total amount of coherent motion and motion variability increased. This reduction in RTs can be reproduced with a simple two-accumulator drift-diffusion model with feed-forward inhibition by increasing the stochastic noise variability of the accumulation process.

Introduction

The brain continuously accumulates sensory information about the external world and uses it to make decisions about actions with its surrounding environment (Gold and Shadlen, 2007; Cisek and Kalaska, 2010). Random-dot kinematogram (RDK) visual-motion stimuli have been widely used in two-alternative forced-choice (2AFC) tasks to study how the brain decides among two competing sensory or motor choices (Newsome et al., 1989; Kim and Shadlen, 1999; Roitman and Shadlen, 2002; Ratcliff et al., 2003a; Palmer et al., 2005; Ratcliff et al., 2007; Niwa and Ditterich, 2008; Resulaj et al., 2009; Kiani et al., 2013).

One computational framework for modeling decision making proposes a decision variable which accumulates noisy evidence across time and can be simulated mathematically by a bounded drift-diffusion process (Ratcliff, 1978; Gold and Shadlen, 2001; Mazurek et al., 2003; Smith and Ratcliff, 2004; Bogacz et al., 2006; Gold and Shadlen, 2007; Eckhoff et al., 2008; Ditterich, 2010). In 2AFC tasks, the models assume that a pair of neuron and "anti-neuron" populations with opposite motion direction preferences separately encode the sensory evidence supporting each choice (Gold and Shadlen, 2001; Mazurek et al., 2003; Gold and Shadlen, 2007). The decision variable then integrates the moment-to-moment difference in activity between these two sensory inputs.

While extensive psychophysical and neurophysiological evidence is consistent with a decision variable that accumulates the difference in sensory evidence provided by the neuron/anti-neuron inputs (Roitman and Shadlen, 2002; Ratcliff et al., 2007; Bosking and Maunsell, 2011; Bollimunta and Ditterich, 2012), conventional RDKs contain only one direction of coherent motion against a background of random motion. As a result, the coherent motion

signal is encoded primarily by the neural input population that prefers that motion direction, while any motion signals near the preferred direction of the "anti-neuron" population would result from the stochastic directional variability in the random motion background (Britten et al., 1993; Bosking and Maunsell, 2011). The net motion evidence is essentially equivalent to that of the sensory signal encoded by the one input population that is activated by the coherent motion component of the RDK stimulus, and so does not provide a strong test of the assumption of an accumulation of the net difference in motion evidence (Liston and Stone, 2013).

In this study, we explored the psychophysics of RDK stimuli with mutually contradictory evidence. Different amounts of coherent-motion signals in both directions were presented simultaneously to produce RDKs that had the same amount of net coherent-motion signal in one direction, but different levels of balanced mutually-contradictory "base" coherent motions in both opposing directions. The two competing motion components were either confined to the two exactly opposite directions against a background of residual random motion ("narrow coherence" stimuli , NC), or spread across all possible directions of motion by adding a coherent motion component bias to the otherwise random Brownian motion of the RDK dots ("Brownian drift" stimuli, BD).

Our results show that the choice behaviour of 12 human subjects was primarily driven by the net coherence of motion across a broad range of different levels of opposing coherent motions. Behaviour was very similar for both NC and BD stimuli, which suggests that the decision-making process extracts motion evidence across a wide range of motion directions, whether the motion signal is confined to two opposite directions or broadly distributed across a wide range of dot motion directions (Jazayeri and Movshon, 2006; Bosking and Maunsell, 2011). Furthermore, the total amount of signal motion had a secondary impact on choice behaviour; at

low net-coherence levels, reaction times (RTs) decreased as total motion signal and associated motion variability increased. The choice behaviour of the subjects across different levels of net and total signal strength could be replicated by a simple two-accumulator drift-diffusion process with mutual feed-forward inhibition between the output of the neuron and anti-neuron channels at the input stage of the accumulators, by increasing the level of instantaneous stochastic noise as a function of base coherence level.

Methods

Human Subjects

8 male and 4 female subjects with ages ranging from 20-36 years old were recruited for the present study. Subjects had normal or corrected to normal vision and were naïve to the experimental objectives. All experiments conformed to the rules and guidelines established by the Comité d'éthique de la recherche en santé de l'Université de Montréal. Subjects read and signed an informed consent form before participating in the study.

Experimental Setup

Experiments were conducted in a darkened room with a 19 inch flat-screen TFT LCD monitor (Samsung SyncMaster 191T Plus, 60 Hz). Subjects sat at a viewing distance 60 cm from the monitor and subjects recorded their response choices by moving a computer mouse. The experimental stimuli were generated on a PC computer running Windows 7, and Matlab (R2008b; The Mathworks, Natick MA) with the Psychophysics Toolbox Extension (Brainard, 1997; Pelli, 1997). Data were collected and stored with custom-written Matlab routines.

Experimental Task

Subjects completed a series of trials in which they had to determine the direction of overall motion in a random-dot kinematogram (RDK) stimulus that usually contained two variable-strength opposing motion "signals" to the right or left ("signal-R" and "signal-L", respectively) against a variable-strength background of random-motion "noise", (**Figure 1A**). Each trial had four epochs. The first epoch was the center-fixation epoch, which began when a small central white circle (diam: 0.5 deg visual angle) appeared. The subject had to move the mouse to position an on-screen cursor in the central circle and hold it there for 700ms. Two large white circular peripheral targets then appeared to the left and right of the central cue (diameter: 4 deg, distance from center: 12.5 degrees) for 700ms (target-display epoch). Next, the RDK epoch began when the central circle disappeared and a dynamic RDK motion stimulus appeared in the center of the screen, subtending 5 degrees of visual angle. Subjects were told to look at the stimulus and to determine the direction of the motion stimulus. The subjects' head was not fixed and no explicit eye fixation controls were used. Once the subjects made a decision about the net direction of visual motion, they reported the decision by moving the mouse to displace the on-screen cursor from the center circle to the peripheral target located in the same direction as their estimate of the signal motion. Once the cursor exited the center circle, the RDK stimulus froze on the last presented frame and the RDK epoch ended. The choice Reaction Time (RT) was measured as the duration of the RDK epoch from the onset of the RDK stimulus to the exit of the cursor from the small central window. The fourth epoch was the movement-time (MVT) epoch from the exit of the central start circle to the entrance into the chosen target circle. At the end of the trial, the subjects where shown the correct target by changing the correct target's color from

white to green. Simultaneously, the subjects received an auditory cue that confirmed whether they had made the correct choice (one short beep, 400Hz) or an incorrect choice (two short beeps, 240Hz and 200Hz).

Subjects were given the general instruction to "move as quickly and as accurately as possible to the target in the direction of perceived motion", but were not given any explicit instructions to bias their behaviour to either speed or accuracy of choices. Furthermore, no hard constraint was made on the duration of the subjects' reaction times (RT), beyond a trial time-out if the subjects did not respond in less than 10 seconds. As a result, each subject established their own preferred speed/accuracy trade-off criterion.

Visual Stimuli – Random dot kinematogram (RDK) algorithms

The RDK-generating algorithms used in this experiment created three interleaved sequences of image frames that presented sets of dots that carried the coherent-motion signal as well as random-noise dots. Similar to some previous RDK algorithms (Shadlen and Newsome, 2001; Roitman and Shadlen, 2002; Niwa and Ditterich, 2008; Pilly and Seitz, 2009; Bollimunta and Ditterich, 2012), three sets of dot sequences were interleaved so that the dots from one sequence were presented every three frames. As such, the first group of dots were plotted on frames [1, 4, 7 …], while the second group of dots were plotted on frames [2, 4, 8 …], and the third group of dots were plotted on frames [3, 4, 9 …] and so on. With a frame rate of 60 Hz, successive frames from one random-dot sequence were plotted every 50 ms. However, unlike those previous RDK algorithms in which coherent motion occurred in only one direction against a background of random motion, most of the stimuli in the present study were designed to present motion signals

of different strengths in two opposite directions simultaneously, against a background of random dot motions. The procedure was as follows.

The algorithm first initialized the dot pattern for each of the 3 dot sequences by randomly distributing the dots in a 5x5 degree square area. The dots were subsequently masked by a circular aperture of 5 degrees in diameter. Each dot filled a square with an edge size of two pixels (0.055 degrees). The dot density was 33.4 dots/($deg^2 \cdot s$). This comprised 3 groups of 14 dots moving in the three separate interleaved frames, for a total of 42 dots in the full RDK sequence. However, because of the circular mask, somewhat fewer than 42 dots were usually visible at any one time. To plot the movement of the dots in the next frame in their sequence, each dot was assigned a Brownian motion vector with a constant length but a random direction. The dots were then divided into three subgroups. The first subgroup of dots conveyed the rightward motion signal (signal-R), while the second subgroup of dots conveyed the leftward motion signal (signal-L). The remaining dots formed the third subgroup, which provided the random-noise component of the visual stimulus. The different stimulus conditions were created by modifying the relative number of dots assigned to these three subgroups.

We used two different methods to displace the signal dot subgroups in the stimuli, illustrated in **Figure 1B**. In the "Narrow-Coherence" (NC) stimulus set, a vector component in the assigned signal direction replaced the assigned Brownian motion vectors of the signal dots for that frame, similar to most standard RDK stimuli. The resulting apparent coherent motions of the two signal dot subgroups in the NC stimuli were narrowly confined to leftward and rightward displacements parallel to the horizontal axis, and were therefore explicitly visible in their frame-wise displacements.

In contrast, in the "Brownian-Drift" (BD) stimulus set, the coherent signal vector component of the signal dots was added to their assigned Brownian motion vector. As a result, the coherent motion component of the signal dot displacements in the BD stimuli was not confined to the horizontal axis, but was instead embedded implicitly in signal dot motions across a broad range of directions, similar to the RDK stimuli often used in global-motion studies (Williams and Sekuler, 1984; Watamaniuk et al., 1989; Watamaniuk and Sekuler, 1992). Furthermore, while the signal dots had a fixed speed (2°/s) in the NC stimuli, the signal dot speeds ranged from 0°/s - 4°/s in the BD stimuli (see below).

Between successive frames of the three sets of random-dot sequences, each dot was randomly chosen to be in one of the 3 dot subgroups. As a result, the displacement of any given dot between two successive image frame pairs could be a signal-R or signal-L vector or a random-noise vector, so that the nature of the motion signal provided by each dot had a short lifetime.

Importantly, however, the dots themselves had extended lifetimes. Unlike many RDK stimuli (Shadlen et al., 1996; Kim and Shadlen, 1999; Shadlen and Newsome, 2001; Pilly and Seitz, 2009; Schütz et al., 2010; Kiani et al., 2013), the dots were not randomly repositioned to new positions in the stimulus array between pairs of frames in a sequence. Instead, the positions of the dots in each of the three interlaced sequences of frames were incremented progressively in each frame according to their random assignment into each of the three dot subgroups. As a result, the dots in the NC and BD stimuli had a long lifetime and created the illusion of sets of dots in continuous noisy motion, with different relative strengths of motion in the two opposing signal directions rather than an evanescent "snow" of transient flickering dots that moved in different directions. The random-replacement procedure has some advantages for studying pure

visual movement direction perception mechanisms (Huk and Meister, 2012). However, most ecologically-natural moving stimuli that the visual system evolved to process are usually generated by the continuous sequential changes in the spatial location of physical objects that exist over periods of time much longer than the 50ms repeat rate of the frames in the RDK dot sequences. Pilot studies using NC, BD and standard RDK stimuli generated with random replacement of dots between successive pairs of frames (not presented here) confirmed that the psychophysical performance of subjects using the NC and BD stimuli were consistent with all the major trends reported many times in subjects responding to RDK stimuli with random replacement (Britten et al., 1992, 1993; Shadlen and Newsome, 2001; Roitman and Shadlen, 2002; Palmer et al., 2005; Niwa and Ditterich, 2008; Pilly and Seitz, 2009; Bollimunta and Ditterich, 2012). Moreover, other comparative studies have reported similar results, supporting the idea that the visual system obtains a global percept of motion direction primarily by processing the directional displacements of the dots between successive corresponding frames, and does not rely solely on the additional motion information that might be available in the temporally evolving spatial paths of individual dots in stimuli with prolonged dot lifetimes (Williams and Sekuler, 1984; Snowden and Braddick, 1989; Watamaniuk et al., 1989; Tripathy and Barrett, 2004; Pilly and Seitz, 2009). This supported the basic generality and robustness of the findings in this study, and indicated that they could not be an idiosyncratic product of the way in which the motion illusions were generated.

Combinations of coherent motions

The main stimulus set was generated by combining different levels of signal motions in one direction (0% - 64%) with different levels (0% - 32%) of contradictory signal motion in the opposite direction (**Table 1**).

Two properties were used to characterize the motion signal of the stimulus. The **net coherence** was the difference between the percentage of signal dots moving in the dominant (correct) and non-dominant (incorrect) direction. The net coherences used in this study ranged from 0% (chance) to 44% in the correct direction. The **base coherence** was defined as the percentage of signal dot displacements moving equally in the two opposite directions, and which should not result in a net global motion percept. **Table 1** lists the 26 different combinations of motion signals whose percentages of coherences ranged from (0/0) to (64/32). Conditions with the same net coherence were grouped into the same column, while those with the same base coherence were grouped in rows. The top row resemble standard RDK motion stimuli in that signal motion was induced in only one mean direction against a background of randomly moving dots. The following rows represent stimulus conditions with the same net coherence but increasing amounts of base coherence. This set of conditions yielded five combinations of different percentages of opposing signal-motion stimuli for each given net coherence level. An additional condition (44/0) was included to extend the range of standard motion conditions.

Note that we are using the terms “base coherence” and “net coherence” here to describe the relative frequencies of signal dots that were assigned a coherent-motion vector component in the two opposite directions and the excess signal dots that had a vector component in one of the two opposite directions, respectively. However, only the signal dots in the NC stimuli moved coherently in the usual sense of parallel motions in one direction.

Task design:

Experiment 1

In the first experiment, six subjects performed the task in blocks of trials during which they received only the NC or BD stimuli. Trials in each block were randomized and counter-balanced to ensure that there were equal numbers of trial conditions with net motion coherence oriented toward the right and left targets. For the stimuli with 0 net coherence (0/0 – 32/32), one of the two targets was arbitrarily designated as the correct target in a given trial. A single block of trials comprised 26 stimulus conditions x 2 targets x 3 replications per target, for a total of 156 trials**.** Subjects performed 15 blocks of trials with each of the NC and BD stimuli over several days, yielding 90 replications of each stimulus combination for each of the 2 stimulus types (4680 trials/subject).

Experiment 2

Because of the blocked structure of the task in Experiment 1, subjects may have adjusted or optimized how they processed the NC versus BD stimuli in response to their different visual appearance. This could either result in differences in the choice behaviour of the subjects, or alternatively similar psychophysical performance despite processing the visual stimuli in different ways. To assess the potential impact of the blocked structure of the first experiment, a second group of six subjects were recruited to perform the task in blocks of trials during which they received both the NC or BD trials randomly interleaved in the same block. A single block of trials comprised 25 stimulus conditions x 2 targets x 2 stimulus types x 5 replications per target, for a total of 500 trials (the 44/0 stimuli were not used in this experiment). Subjects were given a 60 second rest break every 100 trials. Subjects performed 10 blocks of trials over several days,

yielding 100 replications of each stimulus combination for the NC and BD formats (5000 trials/subject). All other details were similar to Experiment 1.

Grouping of trials

Trials were grouped by several different conditions, including the base coherence, the net coherence, the stimulus version, the direction of the correct target, the subject's chosen target, and the trial outcome. To combine equivalent trials separated according to rightward and leftward stimulus motions or target choices, measures of the motion stimuli for leftward trials were mirror reversed and then grouped with the rightward trials.

Repeated-measures analysis of variance

Three-way repeated-measures ANOVA were conducted using IBM SPSS Statistics 21 to measure the main and interaction effects of base coherence, net coherence and stimulus version on reaction times and success rates. In the cases where Mauchly's test indicated that the assumption of sphericity was violated, the degrees of freedom were corrected using the Greenhouse-Geisser estimates of sphericity.

Dot Displacement Distributions

The different algorithms used to generate the NC and BD stimuli resulted in very different distributions of dot displacements between corresponding pairs of frames in the stimulus sequence. We defined the X-axis and Y-axis as being parallel and perpendicular to the mean left-right direction of coherent motion respectively. **Figure 2** shows the frequency distribution of the (X,Y) screen pixel displacements of the dots between pairs of corresponding stimulus frames in the NC stimuli. When there was no coherent-motion signal in the stimuli (0/0 stimulus), the RDK stimulus contained only random-motion vectors that were uniformly distributed across all directions and had a fixed length, resulting in a circular distribution of dot displacements. The remaining graphs in Figure 2 illustrate the separation of the dot displacements into three distinct populations as the base and net coherence increased. The random-noise dots continued to form a circle, while the signal-R and signal-L dots formed two discrete and oppositely oriented columns whose (X,Y) pixel coordinates were (3.64,0) and (-3.64,0) respectively. As the base and net coherence levels increased, the numbers of dot displacements in the signal-R and signal-L columns increased while the numbers of random-noise dot displacements decreased in a corresponding manner. Because the vector displacements of all dots were of a constant length, the net result was three variable-sized sets of dots in different stimuli, one set moving randomly, and two signal sets moving either left or right, all at apparent instantaneous velocities of 2°/s. Note that the row of base-0% coherence stimuli (0/0 – 32/0) have coherent motion in only one direction, similar to the RDK stimuli used in many studies of visual motion perception. Moreover, the base-0% NC stimuli are identical to the “Brownian Motion” RDK stimuli used by Pilly and Seitz (2009) and Schütz et al. (2010).

Figure 3 shows the corresponding frequency distributions of dot displacements for the BD stimuli. In the BD stimuli, the left or right coherent motion vectors assigned to the chosen signal dots were added to their random-motion vector for each frame. This resulted in two adjacent circles of signal dot displacements shifted to the left or right of the origin by the length of the coherent-motion vector, while the random-noise dot displacements continued to form a circle centered on the origin of the graph. The region at which the two circles of signal dot displacements converged near the origin represents the signal dots whose random and coherent motion vectors were nearly opposite in direction, resulting in only a very small net displacement of the dots between frames. As a result, the distributions of dot displacement velocities remained similar along the Y-axis between the NC and BD stimuli, but were spread out continuously over twice as broad a range (-4°/s to +4°/s) along the X-axis in the BD stimuli.

Indeed, one can easily envisage the distributions of the frame-wise velocities (direction and speed) of dot motions by drawing lines from the (x, y) origin of each graph to each point on the circumference of each circle. The result would be a uniform distribution of random-noise vectors with a fixed velocity, and a bi-lobed distribution of signal dot velocities in the two opposite directions, whose relative frequencies would be proportional to the height of each circle of signal displacements. Furthermore, if one were to average the three sets of vectors separately, the net random-noise velocity would be zero, while that for the two signal velocities would be +2°/s for the signal-R dots and -2°/s for the signal-L dots, exactly the same as for the random-noise and signal dots of the NC stimuli.

Figure 4 and 5 present the same data in the form of polar histograms of the frequencies of the directions of dot displacements in the NC and BD stimuli, respectively, independent of their length (speed). These figures further emphasize how the coherent-motion signals are

sharply confined to the two opposing directions in the NC stimuli, but are implicitly embedded in a much more broad range of signal dot motions in the BD stimuli, occupying the entire left and right half-circles centered on the vertical axis for signal-L and signal-R dots respectively. These BD direction distributions are reminiscent of the RDK stimuli used by Williams and Sekuler (1984) to study global motion discrimination. However, they generated their distributions by sampling from uniform distributions of vector directions of different directional bandwidths, whereas the present distributions resulted from the vectorial summation of a coherent-motion vector and a random-motion vector. Note as well that, unlike the NC stimuli, increases in the base coherence in BD stimuli of a given net coherence do not alter the overall frequency distributions of the directions of dot displacements (**Figure 5**, each column), but do change the distributions of velocities of displacements, which become increasingly biased and variable along the horizontal axis as base coherence increases (**Figure 3**).

Auto-correlation Analysis

Figures 2-5 illustrate the motions attributed to each dot in two consecutive matching frames in the stimulus sequence. However, the human observers did not have access to that information, so they could not be certain which dot in the next matching frame of the sequence corresponded to which dot in the previous frame. This introduces uncertainty "noise" into the perceptual process resulting from the so-called correspondence problem (Barlow and Tripathy, 1997). One way to measure the impact of this correspondence uncertainty is to calculate the auto-correlation of the stimulus. In this analysis, the positions of each of the dots from one frame are compared to the positions of all the dots in the next corresponding frame in that sequence. Paired frames were three frames apart, since the motion stimuli had three sets of interleaved dot distributions. For

each dot in a given frame, we generated a set of potential displacement vectors to the positions of all dots in the next corresponding frame in the sequence, not just the displacement designated by the RDK algorithm for that dot (Barlow and Tripathy, 1997). These vectors were collected for all pairs of frames in the stimulus for all trials of the same conditions to produce a frequency distribution of possible dot displacements. For example, **Figure 6A** shows a distribution of 5.92 million vectors of all the possible dot combinations between each pair of corresponding frames in the 600 NC 64/32 trials presented to the subjects in Experiment 2 (50329 frames total). Note that without any a priori knowledge of how individual dots were moved by the algorithm from frame to frame, the autocorrelation revealed two peaks of displacements to the left and right of the origin, superimposed on a broad base of spurious dot displacement vectors (**Figure 6A**). Furthermore, the number of dot displacements in the rightward peak was twice as large as that in the leftward peak, reflecting the 64/32 percent composition of the coherent motions.

It is important to note that this autocorrelation analysis does not take into account the interleaved frames between two corresponding frames of a given dot motion sequence. The dot distributions in the frames of the three separate dot motion sequences were uncorrelated. As a result, an auto-correlation analysis of each sequential frame in the RDK stimulus sequence would have yielded a purely random distribution of potential vector displacements. The coherent motion information was contained in only every third frame, which emphasizes the importance of persistence in the early processing of visual motion inputs.

Framewise Pixel Displacement Analysis

To measure the amount of motion information presented in the NC and BD stimuli as a function of time, we calculated the mean frame-wise pixel displacement (FPD). The FPD is obtained by summing the horizontal components of the potential displacement vectors extracted by the autocorrelation analysis for all combinations of dots in each pair of frames. The resulting FPD is a measure of the instantaneous mean potential dot displacement in the horizontal axis pooled across all dots between corresponding pairs of frames in the RDK stimuli, assuming no a priori knowledge of which dot in a given frame corresponded to which dot in its paired frame. Note that all potential dot displacement vectors that corresponded to a velocity greater than 8°/s were removed from this calculation, since the speed of controlled dot motions in the stimuli was fixed at 2°/s in the NC stimuli and ranged from 0°/s to 4°/s in the BD stimuli. Only some of the vectors with velocities less than 8°/s were the true signal motions in the stimuli (**Figure 6A, B**). All potential displacement vectors with velocities greater than 8°/s would have resulted from spurious pairings of dots between two image frames and would have yielded zero net motion displacement (**Figure 6A**). The distribution of vectors in **Figure 6A** that were actually used for the FPD measurement for the NC stimuli is shown in **Figure 6B**. The FPDs from all pairs of sequential frames in a trial can then be averaged to calculate the mean trial FPD. To combine stimuli with net rightward and leftward signals, all displacement vectors was mirror inverted for the leftward stimuli. This analysis provides a direct physical measure of the potential motion signals contained in the changes in dot positions between successive image frames in the RDK stimuli arriving at the retina, without any assumptions about the nature of the early motion processing in the central visual system.

Ideal observer analysis

The ideal observer analysis models the upper limit of performance on the motion discrimination task based on an "ideal observer" that has direct access to the FPD values (Green and Swets 1966; Britten et al. 1992). **Figure 7A** shows the frequency histograms of the average trial FPD for the NC trials, grouped by net coherence. We computed five receiver operating characteristic (ROC) curves by pairing each net coherence distribution (0%, 4%, 8%, 16%, 32%) with the net 0% distribution (**Figure 7B**). Each point on the ROC curve represented the proportion of trials in the coherent motion group that exceeded a criterion level, plotted against the proportion of trials in the net 0% group that exceeded the same criterion. Each ROC curve was then generated by calculating these proportions while increasing the criterion level from a FPD value of -10 pixels to 30 pixels. The area under the ROC curve corresponded to the expected performance of an ideal observer whose decision was based on the FPD motion information. For example, the area under the net-0% ROC curve covers only 50% of the area, indicating that an ideal observer would perform at a chance (50%) rate. On the other hand, the area under the net-16% and 32% ROC curves cover nearly 100% of the area, indicating that an ideal observer would nearly perfectly detect a 16% or 32% net coherent motion RDK. The expected performance of this model at different net coherences was plotted with the behavioural data in **Figure 10C** and **10D** for the NC and BD trials respectively.

Motion energy analysis

A number of computational models of visual motion perception assume that the visual system extracts signals about the spatiotemporal distribution of motion energy in the temporal sequence of visual inputs without attempting to track the motions of specific elements in the visual scene (Adelson and Bergen, 1985; Qian and Andersen, 1994; Simoncelli and Heeger, 1998). We used the Adelson and Bergen (1985) spatio-temporal motion filter model as a second method to estimate the motion information contained in the RDK stimuli presented to the subjects. This method has been previously used to analyse the RDK stimuli used in decision-making studies (Kiani et al., 2008; Resulaj et al., 2009; Bollimunta et al., 2012; Zylberberg et al., 2012; Kiani et al., 2013). This model uses two pairs of spatiotemporal filters, with one pair of filters selective for leftward direction, and the second pair selective for rightward direction. To construct the spatiotemporal filters, the following spatial filters were used:

$$f_1(x', y') = cos^4(\alpha) \times \cos(4\alpha) \times exp\left(-\frac{y'^2}{2\sigma_g^2}\right)$$

$$f_2(x', y') = cos^4(\alpha) \times \sin(4\alpha) \times exp\left(-\frac{y'^2}{2\sigma_g^2}\right)$$

$$\alpha = tan^{-1}\left(\frac{x'}{\sigma_c}\right)$$

Where σ_g controls the width of the Gaussian envelope in the y dimension and σ_c controls the width of the 4th order Cauchy envelope in the x dimension. As in the study by Kiani et al. (2008), σ_g=0.05 as an approximation of the direction selectivity of MT neurons, and σ_c= 0.35.

The temporal filters used are as follows:

$$g_1(t) = (k \times t)^{n_{slow}} \times \exp(-k \times t) \times \left[\frac{1}{(n_{slow})!} - \frac{(k \times t)^2}{(n_{slow}+2)!}\right]$$

$$g_2(t) = (k \times t)^{n_{fast}} \times \exp(-k \times t) \times \left[\frac{1}{(n_{fast})!} - \frac{(k \times t)^2}{(n_{fast}+2)!}\right]$$

Where k controls the width of both filters while n_{slow} and n_{fast} control the width of the slow $g_1(t)$ and fast $g_2(t)$ filters respectively. As in the filters used by Kiani et al. (2008), k=60, n_{slow}= 3 and n_{fast}= 5.

The two spatial and two temporal filters were then combined to produce the two pairs of directionally selective spatial-temporal motion filters. The leftward pair of selective filters was generated by combining *f1g1 + f2g2* and *f2g1- f1g2*. The rightward pair of selective filters was generated by combining *f2g1 + f1g2* and *f1g1 - f2g2*. These filters are illustrated in **Figure 8**. Both pairs of these filters formed a spatial quadrature pair, i.e. 90 degrees out of phase from each other in the spatial dimension.

The resulting directionally selective motion energy filters spanned -0.7 to 0.7 degrees in the x- and y-dimensions, and 300 ms in the time dimension. Collapsing along the x-y dimensions, the motion energy measured at time t corresponded to the activity of the stimulus in the immediately preceding 300 ms.

These filters were then convolved with the stimulus, which was represented as an x-y-t matrix of pixels. The results of each convolution was then squared and summed over the x and y dimensions to make a measure of motion energy as a function of time for each filter.

The two rightward responses were added to produce the combined motion energy in the rightward direction. The same was done for the leftward responses. Finally the right and left motion energies were subtracted to obtain the net energy as a function of time. The average net energy of the trial was then obtained by summing all the values of this net energy function and dividing by the number of frames.

The off-axis motion energy was also measured using four more mirror symmetrically oriented opponent pairs of filters rotated ±30° and ±60° from the horizontal left-right motion axis. This produced a measure of net motion energy in 5 directions, including the horizontal. No filters were used for the 90°/270° axis orthogonal to the direction of coherent motion in the NC and BD stimuli, since the net output of that pair of filters would be approximately zero. The x-component of these motion vectors were then summed to provide a weighted sum of net motion energy in the x (horizontal) direction.

Results

1. Task Design

We asked human subjects to observe random-dot kinematogram (RDK) stimuli that contained different amounts of mutually contradictory evidence in two opposite directions and to determine the overall directional bias of dot motion. We used two different RDK algorithms to produce the Narrow Coherence (NC) and Brownian Drift (BD) stimuli. In the NC stimuli, differing amounts of opposing motion signals were explicitly visible in the instantaneous rightward or leftward movements of signal-R and signal-L dots, against a background of random-noise dot motion. In the BD stimuli, the rightward and leftward motion signals were carried implicitly by signal-R and signal-L dots that each moved over a 180° range of actual dot motion directions in opposite directions. In both versions of the stimuli we presented varying degrees of stimulus difficulty by presenting different levels of signal evidence simultaneously in the left and right directions.

2.1. Experiment 1

In the first experiment, six subjects were tested with the NC and BD stimuli presented in separate blocks of trials. The mean reaction times (RTs) of the subjects (±95% confidence intervals) are shown as a function of net and base coherence for the NC trials in **Figure 9A** and for the BD trials in **Figure 9B**. Each line links the data for the series of five stimuli at different net coherences but the same base coherence. Data from stimuli with the same net coherence are aligned in columns, but are slightly shifted arbitrarily along the X-axis to increase visibility.

The first prominent feature of the subjects' behaviour was the overall long duration of their RTs. For the NC base-0% stimuli that most closely resembled standard RDK stimuli, mean

RTs ranged from 671ms for net-44% stimuli to 2410ms for net-0% stimuli (**Figure 9A**). This is significantly longer than the RTs often reported for human subjects in RDK tasks (Williams and Sekuler, 1984; Watamaniuk et al., 1989; Reddi and Carpenter, 2000; Ratcliff et al., 2003b; Palmer et al., 2005), but are similar to the RTs of human subjects in at least one other prior study using more complex RDK stimuli with three simultaneous coherent-motion directions (Niwa and Ditterich, 2008). This suggests that our subjects were instinctively cautious in their choice behaviour, and tended to observe the stimuli for longer periods of time than in most studies before making a response choice. Nevertheless, even when there was only random motion in the stimuli (0,0 condition), subjects typically made a response choice with RTs ranging over ~500-5000ms, and rarely took longer than 6000-7000ms for any net-0% stimuli (see later section).

The second prominent feature of their choice behaviour is that despite the significant differences in the nature of the NC and BD motion stimuli, the basic response trends of the subjects were strikingly similar. The grand mean RT for net-0% stimuli was 2136ms for the NC stimuli and 2252ms for the BD stimuli, which decreased to 833ms and 926ms respectively for the net-32% stimuli. For each base coherence series of stimuli (**Figure 9A, B**; solid lines), RTs decreased systematically as a function of the net coherence. The complete RT distributions of individual subjects for different base coherences at a given net coherence were extensively overlapping (data not shown), indicating that subjects' psychophysical performance was more strongly influenced by the net coherence than the base coherence or total motion coherence of each stimulus. This was particularly prominent at higher net coherence levels. For instance, the mean RTs for the net-16% and net-32% NC and BD stimuli were nearly identical across base coherence levels, even though the total percentage of signal dots changed from 16% in the 16/0

condition to 80% in the 48/32 condition, and from 32% (32/0 condition) to 96% (64/32 condition).

The third prominent feature of the choice behaviour of the subjects is that the psychophysical functions relating RTs to net coherence at different base coherence levels overlapped at high net coherence levels, but diverged at low net coherences, especially for the net-4% and net-0% stimuli (**Figure 9A**). More specifically, when net coherence was low, RTs decreased systematically as the base coherence level increased.

We conducted a 3-way, repeated-measures ANOVA to identify the effects of different net coherences, base coherences and stimulus versions on subjects' RTs. There was a significant difference in task performance between different subjects; with single-subject grand mean RTs ranging from 1263ms to 2212ms ($F_{(1,5)} = 146.15$, $p < 0.01$). After accounting for inter-subject differences, there was a significant main effect of net coherence ($F_{(1.08,5.38)} = 17.10$, $p < 0.01$), but not stimulus version ($F_{(1,5)} = 3.40$, $p = 0.124$).

While the net coherence had a strong effect on RTs, there was also a more modest but statistically significant main effect of base coherence ($F_{(1.08,5.41)} = 7.02$, $p < 0.05$), as well as a significant interaction between the base coherence and net coherence, ($F_{(2.90,14.52)} = 4.24$, $p < 0.05$). In particular, at low net coherences (net-0% to net-8%), RTs were generally shorter as base coherence increased (**Figure 9A, B**). As a result, the slope of the psychophysical function for the effect of net coherence (**Figure 9A, B**; solid lines) was steeper for base-0% stimuli than for base-32% stimuli for both the NC and BD stimuli. This was slightly more prominent for the NC stimuli than for the BD stimuli, especially for stimuli with base-32% coherence.

The success rates for the subjects as a function of base and net coherence are shown in **Figure 9C, D**. Success rates increased systematically with net coherence from near chance

performance (success rate 0.5) at the net-0% coherence conditions to asymptote at nearly 100% success for the net-32% coherence conditions, for both the NC and BD stimuli. Furthermore, while the psychometric success-rate functions for different net stimuli were generally similar at different base coherences, they were not overlapping (**Figure 9C, D;** solid lines**)**. A 3-way, repeated-measures ANOVA indicated a significant main effect of net coherence ($F_{(1.17,5.83)}$ = 96.15, $p < 0.01$) but not stimulus version ($F_{(1,5)} = 0.03$, $p = 0.87$). There was a systematic decrease in success rates for all stimuli above net 0% as the base coherence increased (significant effect of base coherence, ($F_{(4,20)} = 7.45$, $p < 0.01$), but there was no significant interaction effect between base and net coherence ($F_{(3.69,18.43)} = 2.485$, $p = 0.83$) for success rates, unlike RTs. This trend was somewhat more pronounced for the NC stimuli than the BD stimuli (significant interaction effect between base coherence and stimulus type; $F_{(4,20)} = 11.75$, $p < 0.01$). In summary, success rates were mainly driven by increasing net coherence, but also decreased modestly with increasing base coherence across all net coherences.

As already stated, one of the striking findings of Experiment 1 was how similar the choice behaviour of the subjects was in response to the NC and BD stimuli. However, one potential confound in the design of this first experiment was that the NC and BD stimuli were presented in separate blocks of trials. It is possible that subjects adjusted their motion discrimination process or decision-making strategy between blocks to accommodate for the differing visual appearance of the two different stimuli, resulting in similar choice behaviour despite potentially different central motion processing mechanisms.

2.2. Experiment 2

To address this potential confound, we conducted a second experiment in which we interleaved the BD and NC stimuli within the same blocks, and presented them to a new group of 6 subjects. At the same time, we saved the complete record of frame-by-frame positions of each dot for each trial. This permitted a detailed analysis of the exact motion evidence presented in each trial. All other details were essentially identical to Experiment 1. The RTs and success rates are shown in **Figure 10A-D**. The general trends in the data were very similar to that in Experiment 1, confirming the basic robustness of the results. The grand mean RT for net-0% stimuli was 1748ms for the NC stimuli and 1800ms for the BD stimuli, which decreased to 868ms and 888ms respectively for the net-32% stimuli, indicating that this second group of subjects responded somewhat more quickly than the first group. Nevertheless, success rate profiles of the two groups largely overlapped.

The RTs and success rates in both the NC and BD trials were once again mainly modulated by the net coherence. A 3-way, repeated-measures ANOVA for RTs indicated that there was a significant difference in task performance between subjects ($F_{(1,5)} = 25.11$, $p < 0.01$). After accounting for the inter-subject differences, there was a significant main effect of net coherence ($F_{(1.02,5.08)} = 9.85$, $p < 0.05$) but not base coherence ($F_{(1.46, 7.32)} = 3.01$, $p = 0.12$) or stimulus type ($F_{(1,5)} = 3.85$, $p = 0.11$). While the base coherence did not have a significant main effect on RTs, the RT curves followed the same trend as Experiment 1, in which mean RTs decreased as the base coherence increased, especially at low coherence conditions (net-0% and net-4%). The resulting slopes of the psychometric RT curves systematically decreased as the base coherence increased. There was a notable increase in reaction times for the NC base-32%

stimuli at high net coherences (net-16% and net-32%) compared to the lower base-coherence conditions, which was not present in the BD trials. However, this is largely due to two subjects in the experiment who showed very flat RT curves for the base 32% conditions in the NC trials (**Figure 11A**) but not the BD trials (**Figure 11B**). This version-specific RT response was paired with a decreased success rate in the NC trials (**Figure 11C**) but not the BD trials (**Figure 11D**) which would suggest that these two subjects were unable to extract the 16% and especially the 32% net coherence signals of the 48/32 and 64/32 NC stimuli against the equal and opposite 32% base coherences in both directions. In contrast, the other four subjects had RT curves that systematically decreased as the net coherence increased in both NC (**Figure 12A**) and BD stimuli (**Figure 12B**), and strikingly resembled the choice behaviour of the subjects in Experiment 1 (**Figure 9**). It is important to note that the outlier data from the two subjects shown in **Figure 11** was in the NC base-16% and base-32% stimuli conditions, and only represented 3.33% of all the data from the 12 subjects studied in Experiment 1 and 2. For all the other stimulus conditions, these two subjects showed similar choice behaviour as the other 10 subjects studied.

Finally, success rates were lower for base-32% conditions in the NC trials (**Figure 10C)** but not the BD trials (**Figure 10D**). A 3-way, repeated-measures ANOVA for success rates indicated significant main effects of net coherence ($F_{(4,20)} = 416.86$, $p < 0.01$) and base coherence ($F_{(2.54, 12.69)} = 7.55$, $p < 0.01$) as well as significant interaction effects between the stimulus type and the base coherence ($F_{(4,20)} = 12.507$, $p < 0.01$).

In summary, when the NC and BD stimuli were presented in an interleaved sequence, all subjects responded to the net and base coherence of most stimuli in Experiment 2 in the same way as the subjects in Experiment 1. The only exception were two subjects who seemed to be

unable to process the base-32% NC stimuli and as a result showed nearly constant RTs and lower success rates with increasing net coherence.

With these two exceptions, the overall results from Experiment 2 indicated that the major trends and small differences seen between NC and BD stimuli in Experiment 1 could not be explained solely by their presentation in separate blocks of trials. Similar trends were still observed when they were presented in interleaved fashion to different subjects in Experiment 2.

3. Framewise pixel displacement analysis

Due to the stochastic nature of RDK generation algorithms, the motion information presented in a sequence of image frames can vary considerably within and between trials, even for stimuli that should ideally present the same level of base and net coherence. As a measure of the motion signal presented to the subjects, we calculated the "frame-wise pixel displacement" (FPD). This analysis yielded a frame by frame sum of the horizontal component of possible horizontal displacements of signal and random-noise dots in the RDK stimulus (see Methods for more details). These values could then be averaged over all frames in a trial and over all trials within a condition to get an average FPD for a particular combination of base coherence and net coherence in each stimulus version. The FPD is proportional to the mean instantaneous horizontal velocity of the pooled motions of all dots in the RDK stimuli.

Note that the FPD calculation was not based only on the dot displacements generated by the RDK algorithm, but takes into account all possible pairings of dots between successive frames in a frame sequence within a certain displacement radius equivalent to 8°/s velocities (c.f. **Figure 6B**), and so is an unbiased measure of the potential motion information in the stimuli without any a priori knowledge of which dots moved where from frame to frame.

The average FPD values pooled across all trials presented to all 6 subjects in Experiment 2 are shown in **Figure 13A**. First, the FPD for net-0% stimuli was essentially zero, and the FPD scaled linearly with increasing net coherence, as intended. Furthermore, the FPD values were very consistent across all base coherence levels for a given net coherence level. This occurred because the mean FPD of the increasing proportions of signal-R and signal-L dots comprising the base coherence was always near zero, leaving only the extra signal dots responsible for the net coherence component of the RDK to contribute to the FPD. Finally, the NC and BD stimuli had virtually identical FPD values for all stimulus combinations, indicating that the amount of horizontal motion input being presented to subjects was the same for both types of stimuli, despite the different algorithms by which they were generated.

With these FPD values, we also performed an ideal observer analysis which establishes an upper limit on the performance on the task (Green and Swets 1966; Britten et al. 1992). The results of this analysis was plotted in the dotted black lines in Figure 10C and Figure 10D and show that an ideal observer would perform similarly on the NC and BD task. This analysis confirmed that the subjects received, on average, the intended net horizontal motion signal across all combinations of net and base coherence level, and between both types of stimuli.

The constant FPD values across all base coherences for a given net coherence level could explain the similarity of the choice behaviour of the subjects for the stimuli with high net coherence (net-16%, net-32%), but does not appear to provide an explanation for the progressive reduction of RTs as base coherence level increased for the stimuli with a given lower net coherence level (from net-8% to net-0%).

4. Framewise pixel displacement variance analysis

We also calculated the variance of the motion signal in the stimuli. **Figure 13B** shows the variance of the FPD as a function of base and net coherence. While the mean FPDs of stimuli with the same net coherence but different base coherences were identical (**Figure 13A**), the variance of the FPDs of these stimuli increased systematically as a function of base coherence and thus of the total motion coherence for both the NC and BD stimuli at all levels of net coherence (**Figure 13B**).

The progressive increase in variance of NC and BD stimuli with base coherence level could be implicated in the shift to faster RTs as the base coherence increased at low net coherences (0% - 8%) (**Figure 10A, B**). However, the effects of base coherence level on RTs was less pronounced for the higher net-coherence stimuli (net-16% and net-32%) in both Experiments 1 and 2, even though the increase in FPD variance with increasing base coherence was as great for those stimuli as it was for net-0% stimuli. Furthermore, the changes in FPD variance with base and net coherence were more pronounced for the BD stimuli than the NC stimuli (**Figure 13**), but the effects of base coherence level on RTs were somewhat more pronounced in the NC stimuli than for the BD stimuli (**Figure 9, 10, 12**). These trends suggest that the signal-dependent variance in dot displacements measured at the level of the sensory input at the retina may have had an impact on RTs at low net coherence levels. However, they were not the main influence on RTs across the full range of net and base motion coherences.

5. Motion energy analysis

In addition to using the frame-wise pixel displacement calculation, we did a motion energy analysis as an alternative measure of motion information in the stimuli. We used a variant of the original Adelson-Bergen (1985) spatial motion energy filter that included two spatial filters and two temporal filters to create a directionally oriented x-y-t spatiotemporal filter that attempts to replicate the visual properties of motion sensitive MT neurons (Kiani et al., 2008).

Using this model and recordings of all the RDK stimuli shown to subjects in Experiment 2, we used 5 pairs of opposing motion filters aligned in five directions centered on the horizontal left-right axis to obtain a single value of motion energy along the horizontal axis at each moment in time in each given trial (see Methods for more details). The results of these motion filter analyses of the RDK stimuli are shown in **Figure 14A**, **B**. The measured motion energies show similarities with the FPD values calculated in the previous section. For example, the mean motion energy scaled linearly with the net coherence, and remained nearly constant across all base coherence levels for a given net coherence (**Figure 14A**). Furthermore, the motion energy variance increased systematically with the base coherence level for each level of net coherence (**Figure 14B**). However, the measured motion energies also show differences from the FPD values. The motion filter measured less mean motion energy for the BD stimuli than the NC stimuli for net-4% to net-32% stimuli (**Figure 14A**), and the effects of base and net coherence level on motion energy variance of NC versus BD stimuli (**Figure 14B**) were reversed from that seen for the FPD measures (**Figure 13B**). Moreover, the motion energy variance of NC stimuli increased more with rising base coherence across all net coherence levels than did the BD stimuli.

These differences between the FPD and motion energy measures were not simply due to the parameter settings of the motion energy filter. We explored a range velocity preferences of the spatiotemporal filter (2°/s – 6°/s) as well as different widths of the y-axis Gaussian envelope of the spatial filters (σ_g from 0.025 – 0.100). While this had an impact on the size of the absolute values of mean motion energy and motion energy variance, they did not eliminate the quantitative differences in motion energy trends between the NC and BD stimuli (data not shown).

The differences between the FPD and motion energy measures are more likely due to the nature of the motion energy analysis itself. The motion energy filters we used were designed to ne optimally activated by motion signals along a particular oriented spatiotemporal trajectory in (x,y,t) space (Adelson and Bergen, 1985; Qian and Andersen, 1994; Kiani et al., 2008). The NC stimuli, in which the entire coherent signal is carried by dots that only move along the horizontal axis at a constant speed will provide a strong activation of motion energy filters with the appropriate tuning properties. However the motion signal embedded in the BD stimuli is carried by signal dots moving in a much broader range of directions. As a result, the local motion signal detected by each motion energy filter will never provide as effective an activation of the filter as the NC stimuli, resulting in less motion energy output.

This indicates that the FPD and motion energy analyses capture two different attributes of the physical properties of the stimuli that differ between the two stimulus versions. While the motion energy analysis models what a single MT neuron might encode from a motion stimulus, the FPD analysis gives a measurement of the global percept of motion in the stimulus.

Figure 15 replots the RTs of Experiment 1 as a function of the FPD (top row) and average motion energy (bottom row), rather than as a function of net coherence as in **Figure 10**.

The FPD graphs in the top row closely resemble **Figure 10A,B** since the mean FPD values scaled with net coherence in the same way for the NC and BD stimuli. However, in the motion energy graphs in the bottom row, the lower motion energies measured in the BD stimuli shifted the RT curves to the left compared to those for the NC stimuli. This indicates that the similar psychophysics of choice behaviour of the subjects in response to NC and BD stimuli is better related to the mean instantaneous motion velocities of the pooled dot motions in the RDK stimuli than to the estimated motion energy contained in the two stimulus sets.

6. Model simulations of the effect of signal-dependent noise on RT distributions

One of the principal findings of this study is that, whereas choice behaviour was primarily driven by the net coherence in the stimuli, RTs nonetheless were also influenced by the background base coherence level, especially for stimuli with lower net coherence strengths (**Figure 9A, 10A-12A**). Comparison of the RT distributions for the base-0% and base-32% NC stimuli from Experiment 1 show that the reduction in mean RTs reflected a greater positive (leftward) skew of the entire RT distribution toward shorter RTs, that was more pronounced for the low net coherence stimuli (**Figure 16**, left column). The same trend was seen for the NC stimuli in Experiment 2, as well as for BD stimuli in both experiments. Because the base coherence comprised equal amounts of coherent motion in both opposing directions, they should in principle cancel and have no effect on the accumulation process if it is driven by the net difference in coherent motion in the two directions.

Niwa and Ditterich (2008) reported a similar effect of the total coherent motion on RTs using RDK stimuli with different amounts of simultaneous coherent motion in three distinctly different directions (see Discussion). They suggested that this could result from signal-

dependent noise that increased the instantaneous stochastic variability of the evidence accumulation process as a function of the total amount of coherent motion signal in their stimuli. They showed that a computational model that included a signal-dependent stochastic noise term, a divisive normalization and other features could account for their subjects' RTs (Niwa and Ditterich, 2008).

Motivated by their findings, we assessed to what degree a simple generative drift-diffusion model could account for the range of behaviour of our subjects in the task. The objective of this exercise was not to create a rigorous computational model that fully explained the presumed computational processes underlying the subjects' decisions in this task, but simply to assess the potential impact of signal-dependent changes in instantaneous stochastic noise on the choice behaviour of the subjects.

The generative model assumed that decisions were made by temporal accumulation of noisy instantaneous sensory evidence by a decision variable (*DV*) to a decision criterion threshold:

$$DV_t = \sum_{i=0}^{t} gain_e \cdot evidence_t + gain_n \cdot noise_t; \;\; for \;\; DV_t < DC \qquad (1)$$

where DV_t is the accumulated amount of evidence up to time t (incrementing in time steps of 1ms), $evidence_t$ is the instantaneous evidence, $noise_t$ is the instantaneous stochastic noise (normal distribution, s.d. = 1.0; Matlab function *randn*), $gain_e$ and $gain_n$ are two gain terms that independently determine the relative size of the increment in DV_t due to sensory evidence and stochastic noise at each time step, and *DC* is the level of the criterion decision bound. The results of the Niwa and Ditterich (2008) study predict that the change in RT distributions from base-0%

to base-32% stimuli should be explained primarily by an increase in the $gain_n$ term, since the increase in base coherence increases the variability of the motion evidence signals while the net motion evidence remains constant across all base coherence levels (**Figure 13, 14**).

The generative drift-diffusion model contained two independent modules that each accumulated the net sensory evidence for or against its preferred choice and momentary stochastic noise until one of the two accumulators exceeded the decision criterion threshold, at which time the decision process was terminated and the subject made their response (Mazurek et al., 2003; Ratcliff et al., 2007; Churchland et al., 2008).

The model also assumed that the observed RT is comprised of the decision time captured by Eqn 1, plus a non-decision time that accounts for input delays resulting from transmitting the sensory signal from the periphery to central visual structures, encoding of the stimulus properties, and output delays required to generate and transmit the motor command for the chosen arm response to the muscles to initiate the movements.

We also implemented a Linear Ballistic Accumulator model with two independent accumulator modules (Brown and Heathcote, 2005, 2008). Each module accumulated noise-free evidence in a given trial at a mean rate that was proportional to the total evidence for its preferred choice, but whose actual single-trial rate varied stochastically between trials (normal distribution), and whose starting point of evidence accumulation also varied between trials (uniform distribution) (Brown and Heathcote, 2005, 2008). This LBA model thus had three gain terms, for the effect of mean evidence level, the magnitude of variability of inter-trial integration rate and the magnitude of the inter-trial variability of the starting point of evidence accumulation. The results for the LBA model were fundamentally similar to that of the drift-diffusion model, so only the latter results will be presented in detail here.

Initial tests using both the drift-diffusion and LBA models to simulate the base-0% RT distributions showed that when the criterion decision bound *DC* had a fixed value across time, values of the gain terms that generated simulated RT distributions that closely matched the observed RT distributions for net-16% and net-32% stimuli predicted RT distributions that were much longer than those observed for the net-4% and net-0% stimuli, and also generated many trials in which DV_t failed to cross the decision bound in either accumulator even after 10,000ms. The incidence of non-decision trials could be reduced or eliminated by increasing the noise gain term $gain_n$ of the drift-diffusion model to a higher value, but this resulted in simulated RT distributions that were unrealistically positively skewed, and predicted RTs that were far too short for net -8% to net 32% stimuli, as well as choice error rates that were too high for all non-zero net-evidence strengths (data not shown). These results indicated that neither the generative drift-diffusion nor LBA model could account for the full range of observed RTs in this task with a fixed decision bound. Therefore, we implemented a generative model with a decision bound that decreased quadratically with time or alternatively an urgency signal that increased non-linearly with time (Ditterich, 2006; Churchland et al., 2008; Resulaj et al., 2009; Thura et al., 2012; Coallier and Kalaska, 2014). This eliminated trials with unrealistically long decision times.

The resulting drift-diffusion model had six potential free parameters – the evidence $gain_e$ and noise $gain_n$ which are the parameters of interest in this simulation, as well as the non-decision time, the starting decision criterion threshold height, the rate of change of the decision bound and the delay after which the decision bound value began to decrease. To estimate the non-decision time and the two collapsing-bound parameters, we fit the observed RT distributions for the base-0% stimuli from each subject separately to a drift-diffusion model with time-

dependent collapsing bounds (Coallier and Kalaska, 2014). Based on those results, we set the non-decision time at 300ms, the starting decision bound at an arbitrary value of 200, the bound decline start time at 500ms and the gain of the quadratic bound decline at each 1ms interval to $1.25x10^{-5}$. Using those parameter values, we then performed an iterative grid search to find the best combination of signal $gain_e$ and noise $gain_n$ for the base-0% and base-32% stimuli separately that could match the median RT values observed for the 5 net-coherence levels for the pooled data across all subjects. In each iteration, we simulated multiple trials for each of the 5 net-evidence levels for a range of pairs of values of $gain_e$ and $gain_n$ and compared the resulting median RT values against those of the observed data (chi-square calculation of the difference between observed and simulated median RT values). We began the iterative search using a large range and a coarse grain of increments of the values for $gain_e$ and $gain_n$ and 2,000-trial simulations, found a range of gain values that yielded the smallest chi-square values, then searched that smaller range of gain values with a finer grain of increments and 5,000-trial simulations. We continued this iterative process until we found a pair of gain values that consistently yielded the smallest chi-squared differences between the observed and simulated median RT values for 10,000 simulated trials each of the net-0% to net-32% stimuli, at gain increments of 0.025 and within the limits of the stochastic variability of the results of repeated simulations using the same gain values. This iterative grid search was robust because the solution space of fits across different combinations of values of the two gain terms had only one local minimum (data not shown). Other, more sophisticated parameter-search algorithms may have found a more theoretically "optimal" pair of gain values, but this approach was reliable, simple and provided the resolution required for this test of the effect of signal-dependent noise.

The best-fit results are shown in **Figure 16**, with $gain_e$=1.425 and $gain_n$= 4.45 for the base-0% stimuli, and $gain_e$=1.40 and $gain_n$ = 6.10 for the base-32% stimuli. As predicted, the simulation captured the reduction in RTs for low net-coherence stimuli between the base-0% and base-32% stimuli by an increase in the instantaneous stochastic noise variability ($gain_n$), while the gain for evidence signal accumulation ($gain_e$) remained nearly constant. The reduction in RTs for base-32% stimuli resulted primarily from an increased positive skew of the distribution of simulated RTs toward shorter values, as was observed in the subjects (**Figure 16**). In contrast, the simulated median RTs and overall RT distributions for the net-16% and net-32% stimuli showed much smaller differences between the base-0%and base-32%, again as was observed in the subjects. The correspondence between the shape of the observed versus predicted RT distributions is all the more striking since the magnitudes of the signal and noise gains were selected by matching predicted to observed data using only one measure of the central tendency of the RTs, their median value.

This simple generative model was quite successful in capturing both the general trends and fine-grained details of the RT distributions simply by increasing the moment-to-moment stochastic variability of the evidence accumulation process between the base-0% and base-32% stimuli. It is possible that the stochastic noise gain term $gain_n$ comprises at least two sources of stochastic noise, one that is dependent on the stochastic properties of neurons independent of signal strength and remains constant across all stimulus conditions, and a second component that is dependent on signal strength. However, we did not attempt to estimate what those two gains might be separately.

The simulations assumed that both accumulators integrated a noisy instantaneous signal proportional to the net coherence of each stimulus. Not surprisingly, when we ran simulations

using the best gain terms for either the base-0% or base-32% data but allowed the two accumulators to independently accumulate evidence proportional to the total coherent motion (base + net) of the base-32% stimuli, the simulated RTs became unrealistically short at all net coherences (data not shown). The LBA model displayed the same results.

Interestingly, the iterative search procedure can find values for $gain_e$ and $gain_n$ that will yield simulated RT distributions whose median values provide a good fit to the observed base-32% median RTs. However, to achieve that match of median RT values, the signal $gain_e$ was reduced from 1.4 to 0.625 to compensate for the greater total coherent motion in each direction in the base-32% stimuli. More importantly, the value of the stochastic noise $gain_n$ was reduced from 6.10 to 0.50. This generated simulated RT distributions that were unrealistically narrow, with very little variability about the median values and very little overlap between RT distributions for the different net-coherence values (data not shown; similar results were obtained for the LBA model). This emphasizes the importance of instantaneous noise in determining the shape of RT distributions in drift-diffusion models, and the potential perils lurking in simulation studies that use only one measure of the central tendency of model simulations (median or mean RTs, for example) to assess model performance (c.f., Ditterich 2006, 2010).

Discussion

In this study, we used two types of RDK stimuli that had different combinations of coherent motion signals in opposing directions. This yielded RDK stimuli with a range of net motion signals towards the correct target against a variable background of balanced motion signals in the two opposite directions. Using these stimuli in a 2AFC paradigm, psychometric reaction-time and success-rate curves for human observers performing this task show that the decision process is mainly driven by the net motion evidence in the RDK stimuli. This is the first study to our knowledge to directly test this fundamental assumption of many decision-making models using RDK stimuli with different amounts of contradictory motion signals in opposite directions. We also found that the level of balanced base motion signals in the two opposite directions also had a smaller effect on performance at low net-coherence levels. Simulations with a simple generative drift-diffusion model showed that this latter effect could be explained by a shift in the distributions of RTs to smaller values resulting from a signal-dependent increase in intra-trial stochastic noise in the evidence accumulation process as the level of contradictory base coherence in both directions increased.

Global motion perception

Our NC and BD stimuli used RDK dots with extended lifetimes, and different dots carried the motion signal in different stimulus frames. They were similar to other Brownian-motion-like stimuli used in previous studies (Williams and Sekuler, 1984; Watamaniuk et al., 1989; Watamaniuk and Sekuler, 1992; Smith et al., 1994; Watamaniuk et al., 1995; Scase et al., 1996; Zohary et al., 1996; Pilly and Seitz, 2009; Schütz et al., 2010). Similar to the present findings,

those studies also found that subjects could perceive the direction of net global motion in RDK stimuli whether the motion signal was confined to a narrow band of directions like our NC stimuli or was distributed over a broad range of local motion directions like our BD stimuli. The general consensus of all these studies is that subjects integrate local motion information across space and time to generate a percept of a single direction of visual motion even when the local-motion signals are readily discriminable and highly diverse. However, many of those studies were concerned with the stimulus properties that influenced the psychophysical threshold for global motion perception, and did not analyze the subjects' overall choice behaviour across a range of stimulus conditions in the context of computational models of decision-making based on noisy sensory evidence. Furthermore, none of those global-motion studies used RDK stimuli in which variable amounts of motion signal were presented simultaneously in opposing directions.

RDK stimuli with sets of dots moving in opposite directions have been used in previous studies, but usually with the goal of determining which stimulus conditions would evoke a percept of two transparent surfaces moving in opposite directions (Snowden et al., 1991; Snowden et al., 1992; Qian et al., 1994a; Qian and Andersen, 1994; Qian et al., 1994b; Snowden and Verstraten, 1999; Takemura et al., 2011). However, our stimuli were non-transparent, because they had balanced signal-R, signal-L and random-motion signals in all local regions of the stimuli that could be also carried by the same dot at different times (Qian et al., 1994a).

Niwa & Ditterich (2008; Bollimunta and Ditterich, 2012) presented subjects with RDK stimuli that contained different levels of coherent motion simultaneously in three different divergent directions separated by 120°. The three uni-directional streams of coherent motion were presented against a background of random motion rather than with differing degrees of

motion in the opposite direction in each of the three directional axes. Nevertheless, consistent with our results they found that observer RTs and success rates were primarily driven by the net motion direction bias summed across all three streams of coherent motion (Niwa and Ditterich, 2008; Bollimunta and Ditterich, 2012). Also similar to the present findings, they observed a secondary effect on RTs as a function of the total motion coherence in the stimuli, whereby RTs decreased as the motion coherence level in each of the three directions increased equally in each direction, i.e., 0% net coherence, but did not show the same decrease when the stimuli had a strong net direction bias (Niwa and Ditterich 2008). The ranges of RTs and success rates across stimulus conditions in that study were also very similar to those found here.

Niwa and Ditterich (2008) proposed that this motion-coherence dependent reduction in RTs at low net motion coherence might be due to signal-dependent noise that increased as the total amount of coherent motion in the stimuli increased. They showed that they could fit their subjects' choice behaviour with a computational model that included a signal-dependent noise variance term whose value increased as the total coherent motion in their stimuli increased. Using a simple generative drift-diffusion model, we showed that we could simulate the changes in median RTs and the total RT distributions between base-0% and base-32% stimuli by increasing the gain of the instantaneous stochastic noise term in the evidence accumulation process. This supports the possibility that signal-dependent variability in the evidence-accumulation process could contribute to the effect of base coherence on choice behaviour, especially when the net motion signal was weak and the stochastic noise had a proportionately greater influence on the decision process. In contrast, when the net motion signal was strong (e.g., net-16% and net-32% stimuli), it dominated the accumulation process and the increased

stochastic noise for the corresponding base-32% stimuli (48/32 and 64/32) has less impact on the decision process.

A key question is whether this signal-dependent noise is of peripheral or central origin. Our FPD and motion energy measures showed clear increases in stimulus variability at higher base coherences, raising the possibility that the stochastic physical variability of the visual stimuli may have contributed to the decrease in RTs as base coherence increased. However, MT neuron discharge rate and variability both follow a near-linear relationship with the strength of the motion signal in the RDK stimuli (Britten et al., 1993; Shadlen et al., 1996). Furthermore, this trial-to-trial variability of MT neuronal activity has been linked with subjects' behavioural choices, such that when an MT neuron had a higher discharge rate in a trial with a given motion strength, the observing monkey had a higher chance of choosing the target in the neuron's preferred direction (Britten et al., 1996). Most importantly, the variability of MT neuronal activity is largely independent of the trial-to-trial variability of the RDK stimuli; their responses are equally variable when the monkeys see exactly the same RDK stimulus in repeated trials (Britten et al., 1992, 1993; Britten et al., 1996; Cook and Maunsell, 2002). This suggests that most of the signal-dependent variability might be central in origin.

Accumulation of net evidence

Our findings show that RTs were primarily modulated by the net evidence in the stimulus across all levels of base coherence, which is in agreement with decision-making models that integrate the net difference in evidence over time. In contrast, our findings cannot be readily explained by simple race models in which non-interacting decision modules each accumulate the total evidence supporting their preferred choice independent of any contradictory evidence supporting

the alternate choice (Carpenter and Williams, 1995; Brown and Heathcote, 2005, 2008; Story and Carpenter, 2009). These race models would predict a systematic decrease in RTs as base coherence increased at all levels of net evidence, which was not observed.

A key question is where the net coherence signal might be calculated. Studies in which subjects used RDK stimuli to choose between two eye saccade targets have implicated motion-sensitive neurons in MT in the encoding of the sensory evidence for each choice and saccade-related neurons in LIP in the net-evidence accumulation process (Shadlen et al., 1996; Shadlen and Newsome, 2001; Roitman and Shadlen, 2002; Mazurek et al., 2003). This implies that the net evidence signal might be calculated in LIP. Consistent with this possibility, Niwa and Ditterich (2008) reported that the sensory input signal to LIP was proportional to the total motion energy in their 3-direction RDK stimuli whereas LIP neuron activity was proportional to the net motion energy.

However, there is no a priori reason to assume that populations of MT "neurons" and "anti-neurons" will each encode the total motion coherence in their preferred motion direction in our stimuli, independent of any conflicting local motion. On the contrary, the opponent-motion properties of MT neurons are well-known. MT responses to RDK dot motions in their preferred direction are strongly suppressed in a direction-dependent manner by simultaneous local-motion stimuli in other directions in their RF (Mikami et al., 1986a; Snowden et al., 1991; Snowden et al., 1992; Qian et al., 1994a; Qian and Andersen, 1994; Qian et al., 1994b; Recanzone et al., 1997). Moreover, motion-energy models that attempt to simulate the properties of MT neurons have an opponent-motion stage to extract the net motion energy in the preferred spatiotemporal orientation of the motion energy filter from the local-motion signals (Adelson and Bergen, 1985;

Simoncelli and Heeger, 1998). This suggests that the computation of the net motion signal begins in MT, but leaves open the possibility that it continues in LIP in saccade-related tasks.

It is therefore reasonable to assume that MT neurons in the subjects in our study generate signals that begin to reflect the net motion signal in each stimulus and not just the total motion signal in each of the opposite directions. Whether and where similar computations might continue in arm- and hand-related neural structures in this task is an open question, since no one to date has studied those structures in decision-making tasks using RDK stimuli. However, Romo and colleagues (Romo et al., 2004; Romo and de Lafuente, 2013) have found strong neural correlates of a tactile vibration-frequency discrimination task in arm-related cortical premotor and prefrontal areas when monkeys report their tactile perceptual decision by pushing on one of two buttons with the non-stimulated hand. This raises the possibility that activity in these same areas resembling that seen in saccade-related LIP neurons might arise when subjects report their perceptions of the global visual motion in RDK stimuli by making differential arm/hand movements.

Implications of the differences in the NC and BD stimuli on the neuronal pools underlying the decision process

The NC and BD stimuli were significantly different. The dots carrying the opposing coherent motions in each image of the NC stimuli moved in parallel along the horizontal axis at a constant speed, while the dots carrying the opposing coherent motion signals in the BD stimuli moved in a broad range of directions with a variable speed. The resulting RDK stimuli had a distinctly different appearance. This was reinforced by the performance of the two subjects in Experiment 2 who displayed the usual response trends for base-32% BD stimuli but could not successfully

extract the net coherence signal in the base-32% NC stimuli. Nevertheless, the FPD calculations confirmed that there were exactly the same amounts of physical displacements of the dots along the horizontal axis in corresponding NC and BD stimuli. In parallel, the subjects had very similar psychometric functions for RTs and success rates as a function of net and base coherence. Finally, the ideal observer analysis using the FPD data also showed that an ideal observer would perform similarly with both stimulus types.

Studies have suggested that MT signals might be pooled in different ways depending on which neurons provide the most reliable signals required for the directional discrimination required in a task, such as coarse discrimination between opposite motion directions versus fine discrimination of similar directions (Snowden et al., 1991; Snowden et al., 1992; Purushothaman and Bradley, 2005; Jazayeri and Movshon, 2006). Although the subjects in this study made coarse direction discriminations to both NC and BD stimuli, the fact that the motion signals were contained in two very different bandwidths of local motion directions raises the possibility that the subjects pooled the MT activity in different ways for the two stimulus sets. This might have been feasible in Experiment 1 when the NC and BD stimuli were presented in different blocks of trials. However, this seems much less feasible in Experiment 2, in which the two stimulus sets were interleaved in different trials of the same block, and which would have required the subject to switch dynamically between two pooling strategies from trial to trial.

A more parsimonious explanation for the similar choice behaviour of most subjects between the two types of stimuli is that they used a common pooling algorithm that combined the output signals from MT neurons with a broad range of spatiotemporal tuning properties to extract the global motion signal from both types of stimuli (Williams and Sekuler, 1984; Jazayeri and Movshon, 2006; Bosking and Maunsell, 2011; Webb et al., 2011). This would not require

the subjects to switch between "optimal" pooling algorithms from trial to trial based on prior knowledge of the statistics of motion signal distributions in the two types of stimuli.

Perception of global motion direction: direction versus position cues

Subjects were asked to report their percept of the direction of global motion in the RDK stimuli in this task. Consistent with a large number of studies using a wide range of different RDK motion algorithms, their choice behaviour suggested that they accumulated evidence about the direction of local motion signals across space and time to determine the global direction of motion (Williams and Sekuler, 1984; Snowden and Braddick, 1989; Watamaniuk et al., 1989; Britten et al., 1992; Watamaniuk and Sekuler, 1992; Britten et al., 1993; Watamaniuk et al., 1995; Britten et al., 1996; Scase et al., 1996; Shadlen et al., 1996; Zohary et al., 1996; Roitman and Shadlen, 2002; Kiani et al., 2008; Niwa and Ditterich, 2008; Pilly and Seitz, 2009; Kiani et al., 2013).

Alternatively, because the dots in our stimuli had an extended lifetime, subjects may have been monitoring and accumulating evidence about the time course of position changes of the dots. The spatial trajectory of each dot is the record of all its frame-wise displacements and its current position is the net result of the accumulated history of all of its frame-wise displacements since the start of the trial, including those reflecting the signal-R and signal-L motion components and the random motions. The change in position of each dot at each moment in time from its initial position at the start of each trial would thus reflect the net motion signal that it had carried up to that time. If indeed the subjects were monitoring the changes in dot positions across time, the present results would indicate that global motion percepts based on the temporal accumulation of evidence about the changing positions of many dots across time displays

strikingly similar psychophysics to that of motion perception presumably extracted from the instantaneous directions of displacements of dots with short lifetimes (Niwa & Ditterich 2008).

However, this would require subjects to monitor the evolving trajectories of motion of many dots across time. In contrast, numerous studies have found that subjects are not very efficient in extracting multi-dot trajectory information (Williams and Sekuler, 1984; Watamaniuk et al., 1989; Watamaniuk and Sekuler, 1992; Watamaniuk et al., 1995; Scase et al., 1996; Tripathy and Barrett, 2004; Pilly and Seitz, 2009). At the extreme, subjects might try to track the motion of a single dot. However, this is not easy to do in these stimuli because dot paths frequently cross, and would not be a very reliable estimate of the global motion signal in the entire population of dots, especially at low net-coherence levels, because each dot carries stochastically variable signal-R, signal-L or random-motion signals in each trial.

Furthermore, the distinction between instantaneous motion direction and position changes may not be as absolute as it might seem. In RDK algorithms with random replacement (Shadlen et al., 1996; Kim and Shadlen, 1999; Shadlen and Newsome, 2001), the lifetime of dots that carries the coherent motion signal increases probabilistically as the level of motion coherence increases. Moreover, sequences of similar instantaneous directions and successive changes in position across the extended spatio-temporal "receptive fields" of motion energy filters are confounded by their spatial and temporal integration functions, suggesting that the temporal evolution of the spatial locations of visual stimuli is inherent in the motion analysis of motion-energy models.

References

Adelson EH, Bergen JR (1985) Spatiotemporal energy models for the perception of motion. J Opt Soc Am A 2:284-299.

Barlow H, Tripathy SP (1997) Correspondence noise and signal pooling in the detection of coherent visual motion. J Neurosci 17:7954-7966.

Bogacz R, Brown E, Moehlis J, Holmes P, Cohen JD (2006) The physics of optimal decision making: a formal analysis of models of performance in two-alternative forced-choice tasks. Psychol Rev 113:700-765.

Bollimunta A, Ditterich J (2012) Local computation of decision-relevant net sensory evidence in parietal cortex. Cereb Cortex 22:903-917.

Bollimunta A, Totten D, Ditterich J (2012) Neural dynamics of choice: single-trial analysis of decision-related activity in parietal cortex. J Neurosci 32:12684-12701.

Bosking WH, Maunsell JH (2011) Effects of stimulus direction on the correlation between behavior and single units in area MT during a motion detection task. J Neurosci 31:8230-8238.

Brainard DH (1997) The psychophysics toolbox. Spat Vis 10:433-436.

Britten KH, Shadlen MN, Newsome WT, Movshon JA (1992) The analysis of visual motion: a comparison of neuronal and psychophysical performance. J Neurosci 12:4745-4765.

Britten KH, Shadlen MN, Newsome WT, Movshon JA (1993) Responses of neurons in macaque MT to stochastic motion signals. Vis Neurosci 10:1157-1169.

Britten KH, Newsome WT, Shadlen MN, Celebrini S, Movshon JA (1996) A relationship between behavioral choice and the visual responses of neurons in macaque MT. Vis Neurosci 13:87-100.

Brown S, Heathcote A (2005) A ballistic model of choice response time. Psychol Rev 112:117-128.

Brown S, Heathcote A (2008) The simplest complete model of choice response time: linear ballistic accumulation. Cogn Psychol 57:153-178.

Carpenter R, Williams M (1995) Neural computation of log likelihood in control of saccadic eye movements. Nature 377:59-62.

Churchland AK, Kiani R, Shadlen MN (2008) Decision-making with multiple alternatives. Nat Neurosci 11:693-702.

Cisek P, Kalaska JF (2010) Neural mechanisms for interacting with a world full of action choices. Annu Rev Neurosci 33:269-298.

Coallier E, Kalaska JF (2014) Reach target selection in humans using ambiguous decision cues. (submitted).

Cook EP, Maunsell JH (2002) Dynamics of neuronal responses in macaque MT and VIP during motion detection. Nat Neurosci 5:985-994.

Ditterich J (2006) Stochastic models of decisions about motion direction: behavior and physiology. Neural Netw 19:981-1012.

Ditterich J (2010) A Comparison between Mechanisms of Multi-Alternative Perceptual Decision Making: Ability to Explain Human Behavior, Predictions for Neurophysiology, and Relationship with Decision Theory. Front Neurosci 4:184.

Eckhoff P, Holmes P, Law C, Connolly P, Gold J (2008) On diffusion processes with variable drift rates as models for decision making during learning. New J Phys 10:015006.

Gold JI, Shadlen MN (2001) Neural computations that underlie decisions about sensory stimuli. Trends Cogn Sci 5:10-16.

Gold JI, Shadlen MN (2007) The neural basis of decision making. Annu Rev Neurosci 30:535-574.

Green DM, Swets JA (1966) Signal detection theory and psychophysics: Wiley New York.

Huk AC, Meister ML (2012) Neural correlates and neural computations in posterior parietal cortex during perceptual decision-making. Front Integr Neurosci 6.

Jazayeri M, Movshon JA (2006) Optimal representation of sensory information by neural populations. Nat Neurosci 9:690-696.

Kiani R, Hanks TD, Shadlen MN (2008) Bounded integration in parietal cortex underlies decisions even when viewing duration is dictated by the environment. J Neurosci 28:3017-3029.

Kiani R, Churchland AK, Shadlen MN (2013) Integration of Direction Cues Is Invariant to the Temporal Gap between Them. J Neurosci 33:16483-16489.

Kim J-N, Shadlen MN (1999) Neural correlates of a decision in the dorsolateral prefrontal cortex of the macaque. Nat Neurosci 2:176-185.

Liston DB, Stone LS (2013) Saccadic brightness decisions do not use a difference model. J Vis 13.

Mazurek ME, Roitman JD, Ditterich J, Shadlen MN (2003) A role for neural integrators in perceptual decision making. Cereb Cortex 13:1257-1269.

Mikami A, Newsome W, Wurtz R (1986a) Motion selectivity in macaque visual cortex. I. Mechanisms of direction and speed selectivity in extrastriate area MT. J Neurophysiol 55:1308.

Newsome WT, Britten KH, Movshon JA (1989) Neuronal correlates of a perceptual decision. Nature.

Niwa M, Ditterich J (2008) Perceptual decisions between multiple directions of visual motion. J Neurosci 28:4435-4445.

Palmer J, Huk AC, Shadlen MN (2005) The effect of stimulus strength on the speed and accuracy of a perceptual decision. J Vis 5:376-404.

Pelli DG (1997) The VideoToolbox software for visual psychophysics: Transforming numbers into movies. Spat Vis 10:437-442.

Pilly PK, Seitz AR (2009) What a difference a parameter makes: a psychophysical comparison of random dot motion algorithms. Vision Res 49:1599-1612.

Purushothaman G, Bradley D (2005) Neural population code for fine perceptual decisions in area MT. Nat Neurosci 8:99.

Qian N, Andersen RA (1994) Transparent motion perception as detection of unbalanced motion signals. II. Physiology. J Neurosci 14:7367-7380.

Qian N, Andersen R, Adelson E (1994a) Transparent motion perception as detection of unbalanced motion signals. I. Psychophysics. J Neurosci 14:7357.

Qian N, Andersen RA, Adelson EH (1994b) Transparent motion perception as detection of unbalanced motion signals. III. Modeling. J Neurosci 14:7381-7392.

Ratcliff R (1978) A theory of memory retrieval. Psychol Rev 85:59.

Ratcliff R, Thapar A, Mckoon G (2003a) A diffusion model analysis of the effects of aging on brightness discrimination. Percept Psychophys 65:523-535.

Ratcliff R, Cherian A, Segraves M (2003b) A comparison of macaque behavior and superior colliculus neuronal activity to predictions from models of simple two-choice decisions. J Neurophysiol 90:1392-1407.

Ratcliff R, Hasegawa YT, Hasegawa RP, Smith PL, Segraves MA (2007) Dual diffusion model for single-cell recording data from the superior colliculus in a brightness-discrimination task. J Neurophysiol 97:1756.

Recanzone G, Wurtz R, Schwarz U (1997) Responses of MT and MST neurons to one and two moving objects in the receptive field. J Neurophysiol 78:2904-2915.

Reddi B, Carpenter R (2000) The influence of urgency on decision time. Nat Neurosci 3:827-830.

Resulaj A, Kiani R, Wolpert DM, Shadlen MN (2009) Changes of mind in decision-making. Nature 461:263-266.

Roitman JD, Shadlen MN (2002) Response of neurons in the lateral intraparietal area during a combined visual discrimination reaction time task. J Neurosci 22:9475-9489.

Romo R, de Lafuente V (2013) Conversion of sensory signals into perceptual decisions. Prog Neurobiol 103:41.

Romo R, Hernández A, Zainos A (2004) Neuronal correlates of a perceptual decision in ventral premotor cortex. Neuron 41:165-173.

Scase M, Braddick O, Raymond J (1996) What is noise for the motion system? Vision Res 36:2579.

Schütz AC, Braun DI, Movshon JA, Gegenfurtner KR (2010) Does the noise matter? Effects of different kinematogram types on smooth pursuit eye movements and perception. J Vis 10:26.

Shadlen MN, Newsome WT (2001) Neural basis of a perceptual decision in the parietal cortex (area LIP) of the rhesus monkey. J Neurophysiol 86:1916-1936.

Shadlen MN, Britten KH, Newsome WT, Movshon JA (1996) A computational analysis of the relationship between neuronal and behavioral responses to visual motion. J Neurosci 16:1486-1510.

Simoncelli EP, Heeger DJ (1998) A model of neuronal responses in visual area MT. Vision Res 38:743-761.

Smith AT, Snowden RJ, Milne AB (1994) Is global motion really based on spatial integration of local motion signals? Vision Res 34:2425-2430.

Smith PL, Ratcliff R (2004) Psychology and neurobiology of simple decisions. Trends Neurosci 27:161-168.

Snowden R, Braddick O (1989) The combination of motion signals over time. Vision Res 29:1621-1630.

Snowden RJ, Verstraten FA (1999) Motion transparency: making models of motion perception transparent. Trends Cogn Sci 3:369-377.

Snowden RJ, Treue S, Andersen RA (1992) The response of neurons in areas V1 and MT of the alert rhesus monkey to moving random dot patterns. Exp Brain Res 88:389-400.

Snowden RJ, Treue S, Erickson RG, Andersen RA (1991) The response of area MT and V1 neurons to transparent motion. J Neurosci 11:2768-2785.

Story GW, Carpenter R (2009) Dual LATER-unit model predicts saccadic reaction time distributions in gap, step and appearance tasks. Exp Brain Res 193:287-296.

Takemura H, Tajima S, Murakami I (2011) Motion integration and segregation modulated by surrounding motion. J Vis 11:739-739.

Thura D, Beauregard-Racine J, Fradet C-W, Cisek P (2012) Decision making by urgency gating: theory and experimental support. J Neurophysiol 108:2912-2930.

Tripathy SP, Barrett BT (2004) Severe loss of positional information when detecting deviations in multiple trajectories. J Vis 4:4.

Watamaniuk S, McKee S, Grzywacz N (1995) Detecting a trajectory embedded in random-direction motion noise. Vision Res 35:65.

Watamaniuk SN, Sekuler R (1992) Temporal and spatial integration in dynamic random-dot stimuli. Vision Res 32:2341-2347.

Watamaniuk SN, Sekuler R, Williams DW (1989) Direction perception in complex dynamic displays: the integration of direction information. Vision Res 29:47-59.

Webb BS, Ledgeway T, Rocchi F (2011) Neural computations governing spatiotemporal pooling of visual motion signals in humans. J Neurosci 31:4917.

Williams DW, Sekuler R (1984) Coherent global motion percepts from stochastic local motions. Vision Res 18:24-24.

Zohary E, Scase M, Braddick O (1996) Integration across directions in dynamic random dot displays: vector summation or winner take all? Vision Res 36:2321.

Zylberberg A, Barttfeld P, Sigman M (2012) The construction of confidence in a perceptual decision. Front Integr Neurosci 6:79.

Tables

Base Coherence \ Net Coherence (%)	0	4	8	16	32	44
0	0/0	4/0	8/0	16/0	32/0	44/0
4	4/4	8/4	12/4	20/4	36/4	
8	8/8	12/8	16/8	24/8	40/8	
16	16/16	20/16	24/16	32/16	48/16	
32	32/32	36/32	40/32	48/32	64/32	

Table 1: The 26 motion conditions

Figures

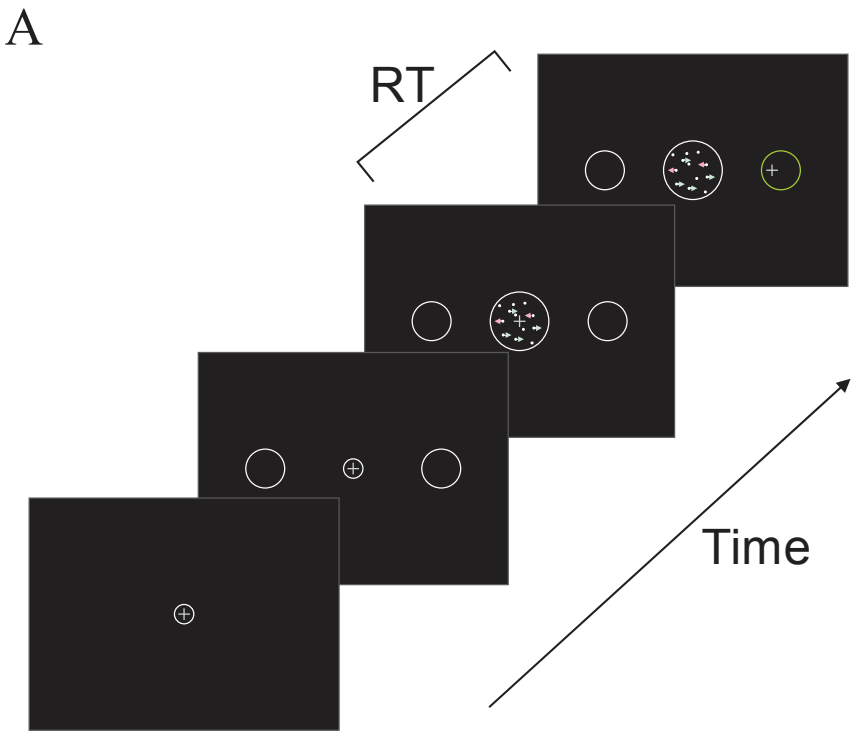

Figure 1: Experimental paradigm

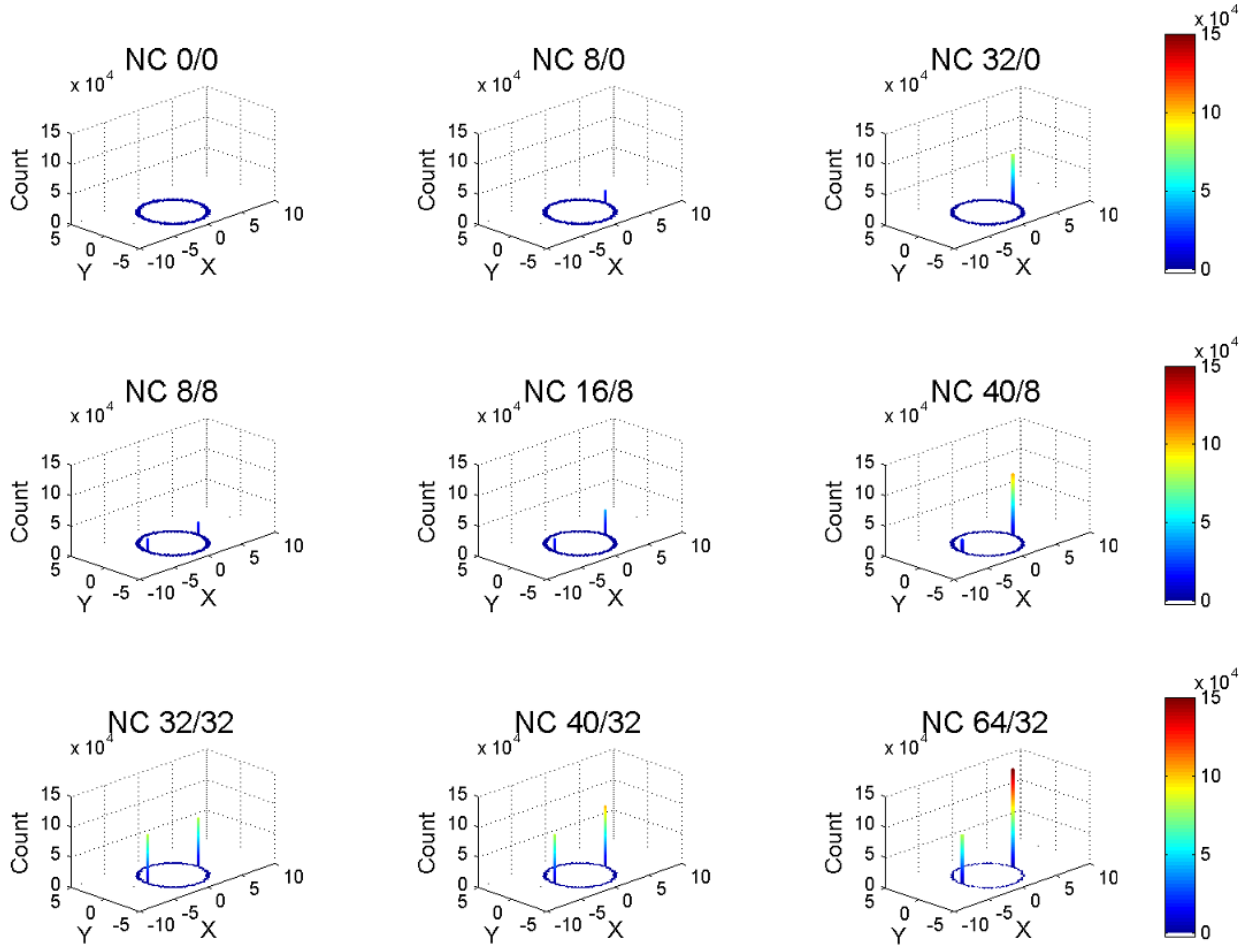

Figure 2: Spatial distributions of dot pixel displacements for the Narrow Coherence task

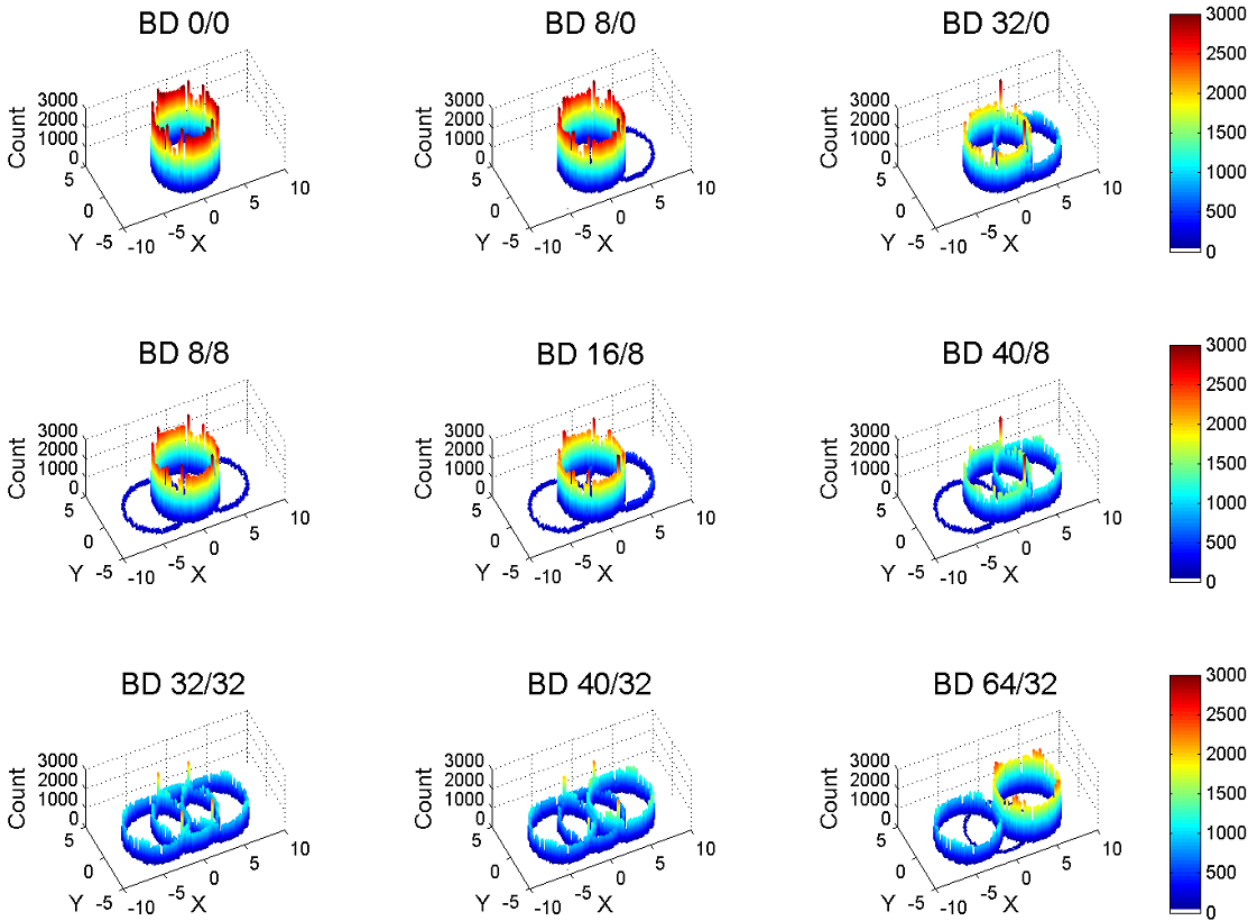

Figure 3: Spatial distributions of dot pixel displacements for the Brownian Drift task

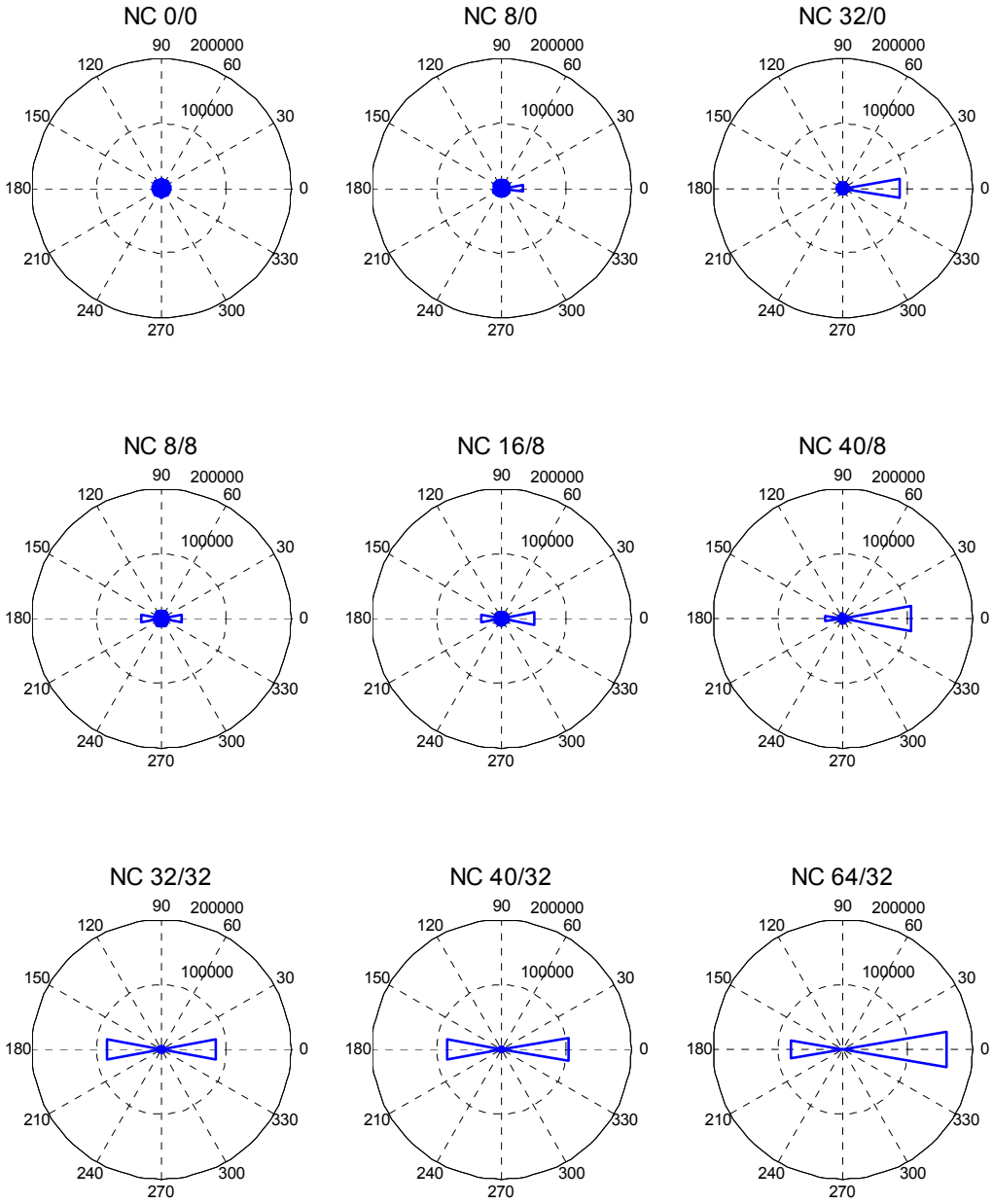

Figure 4: Polar histograms of the frequencies of the directions of dot displacements for the Narrow Coherence (NC) task

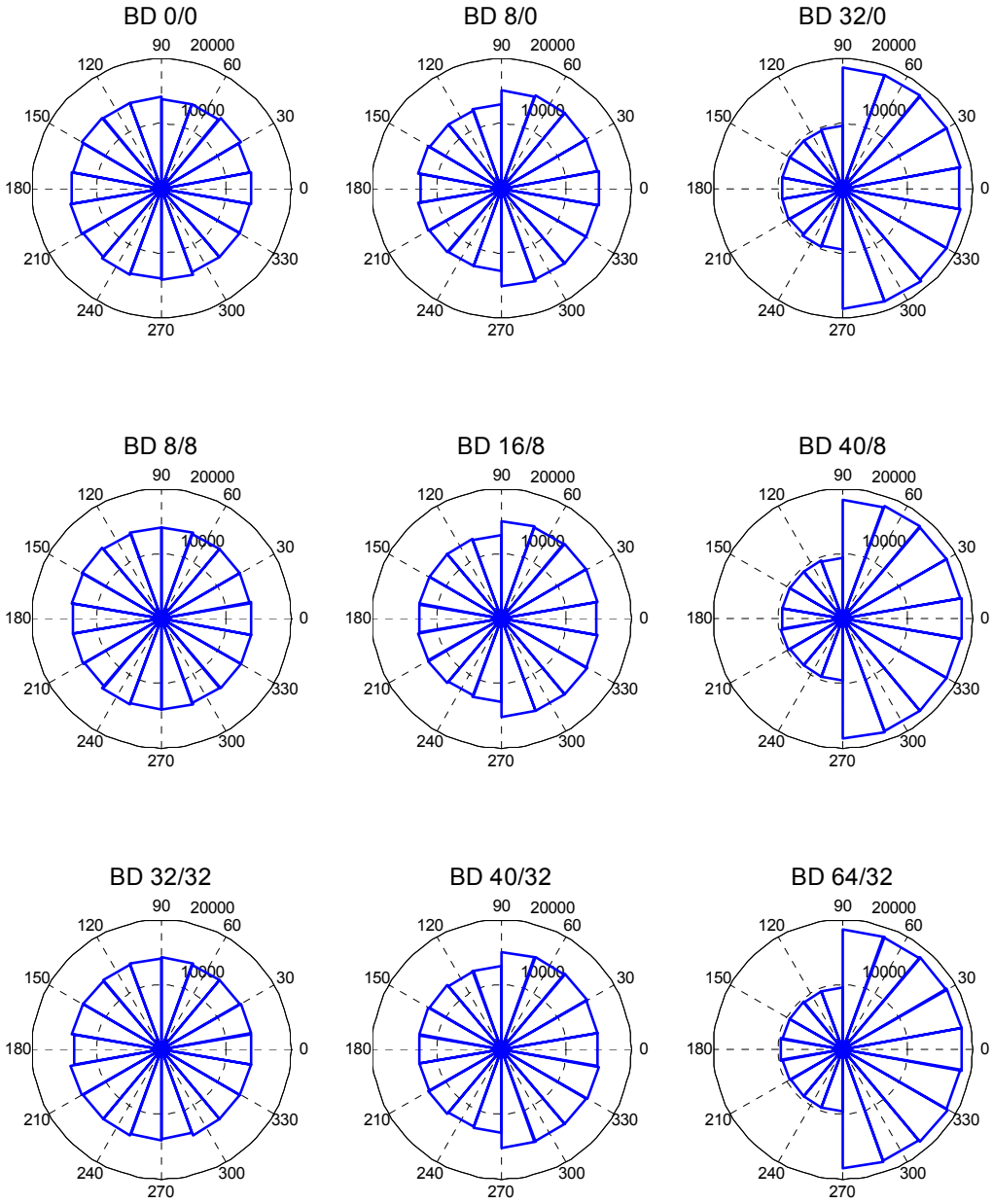

Figure 5: Polar histograms of the frequencies of the directions of dot displacements for the Brownian Drift (BD) task

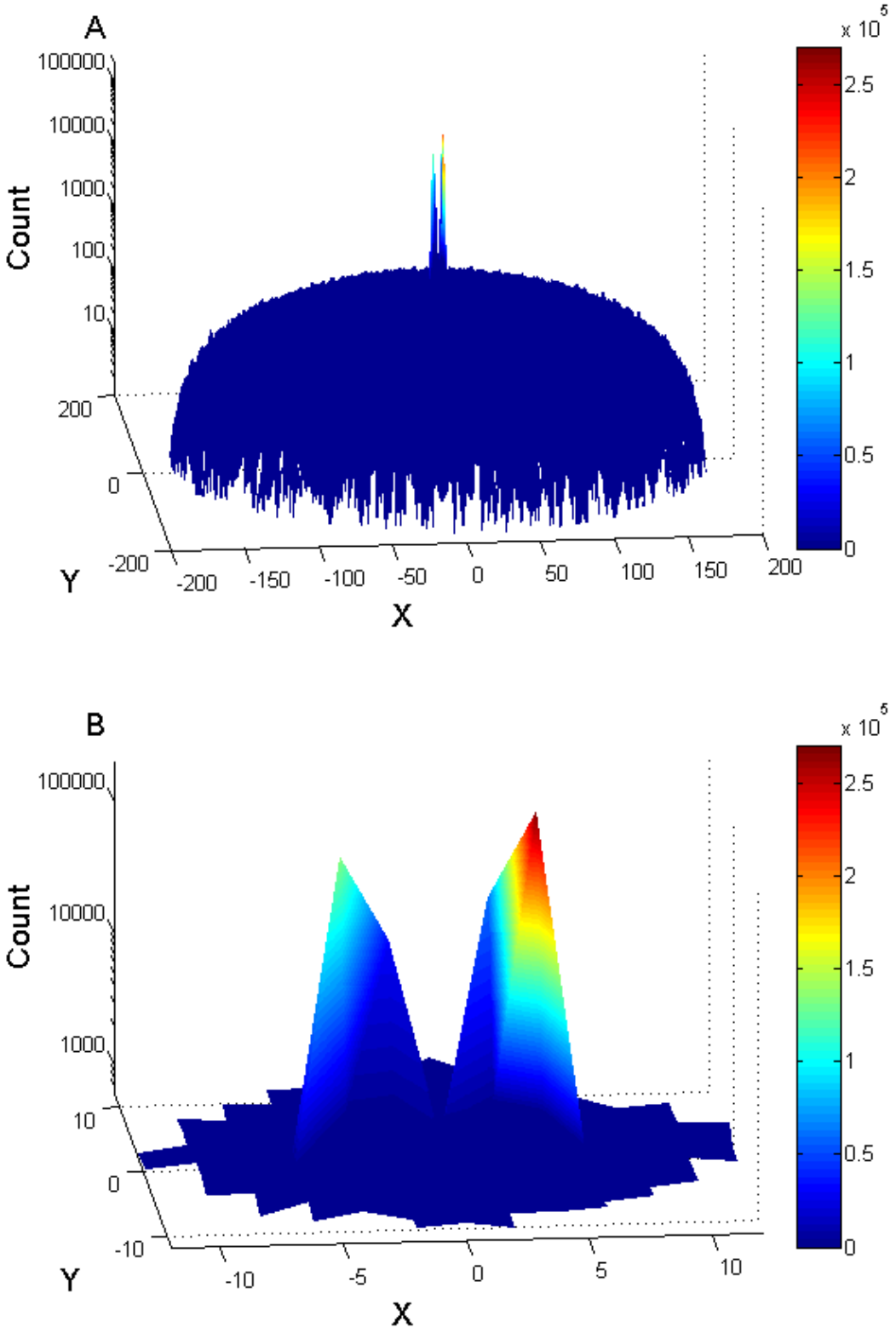

Figure 6: Auto-correlation analysis

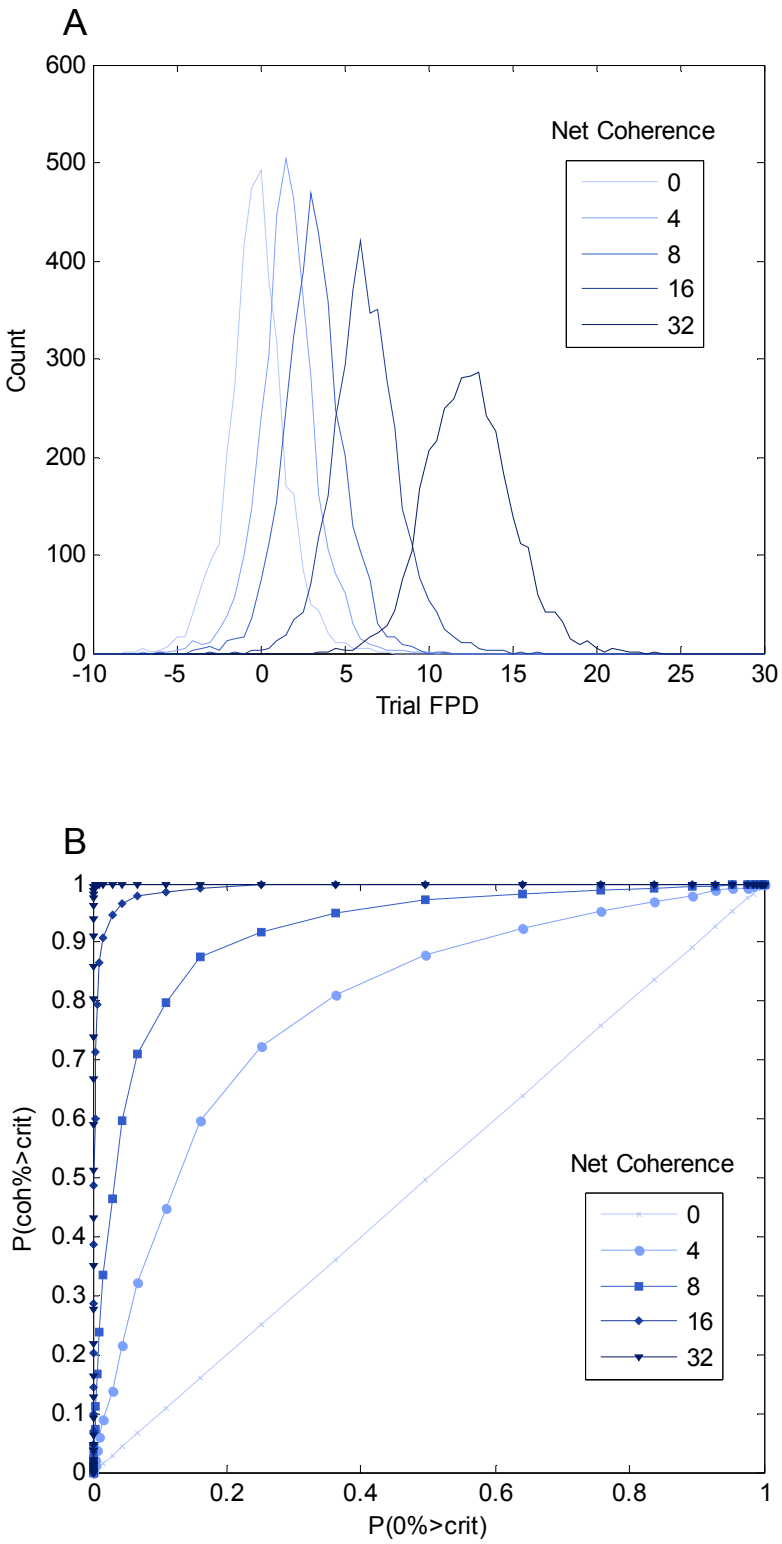

Figure 7: Ideal observer analysis

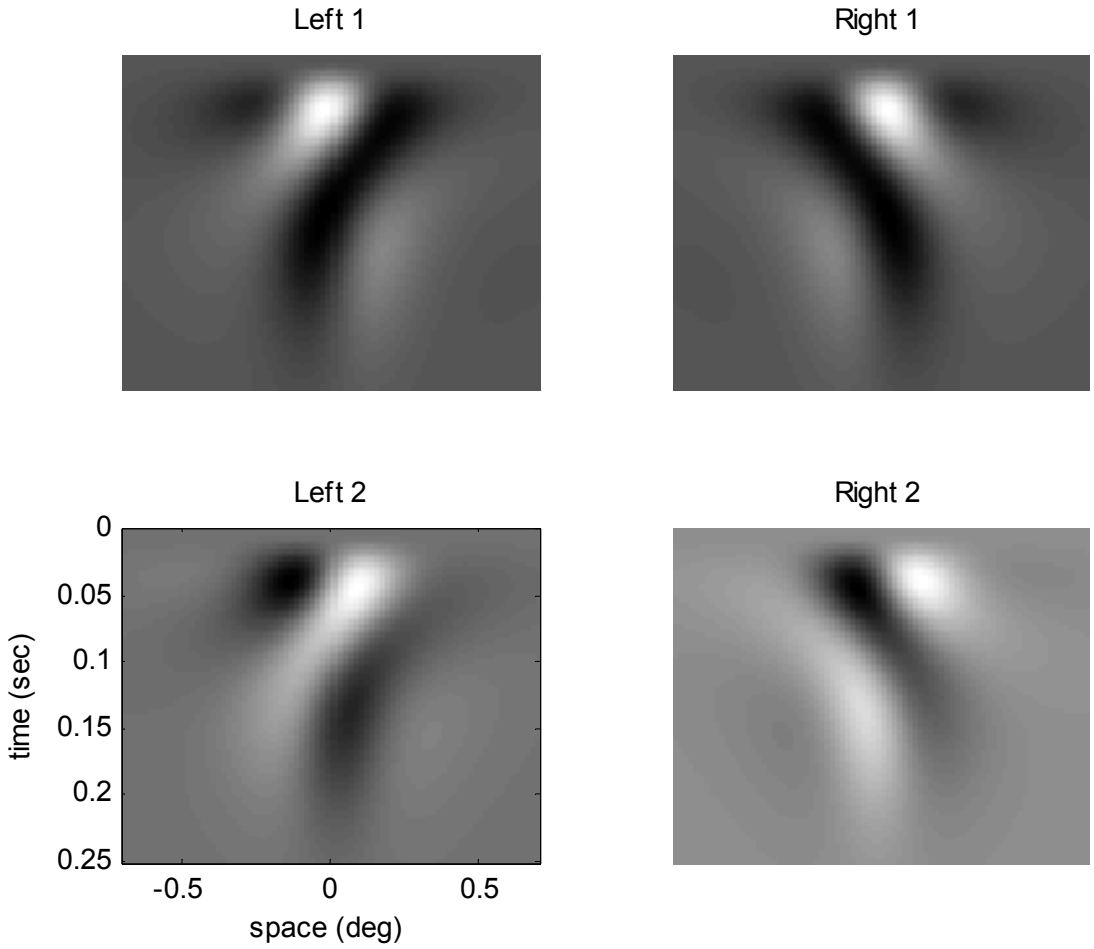

Figure 8: The spatiotemporal motion filters used in the motion energy analysis

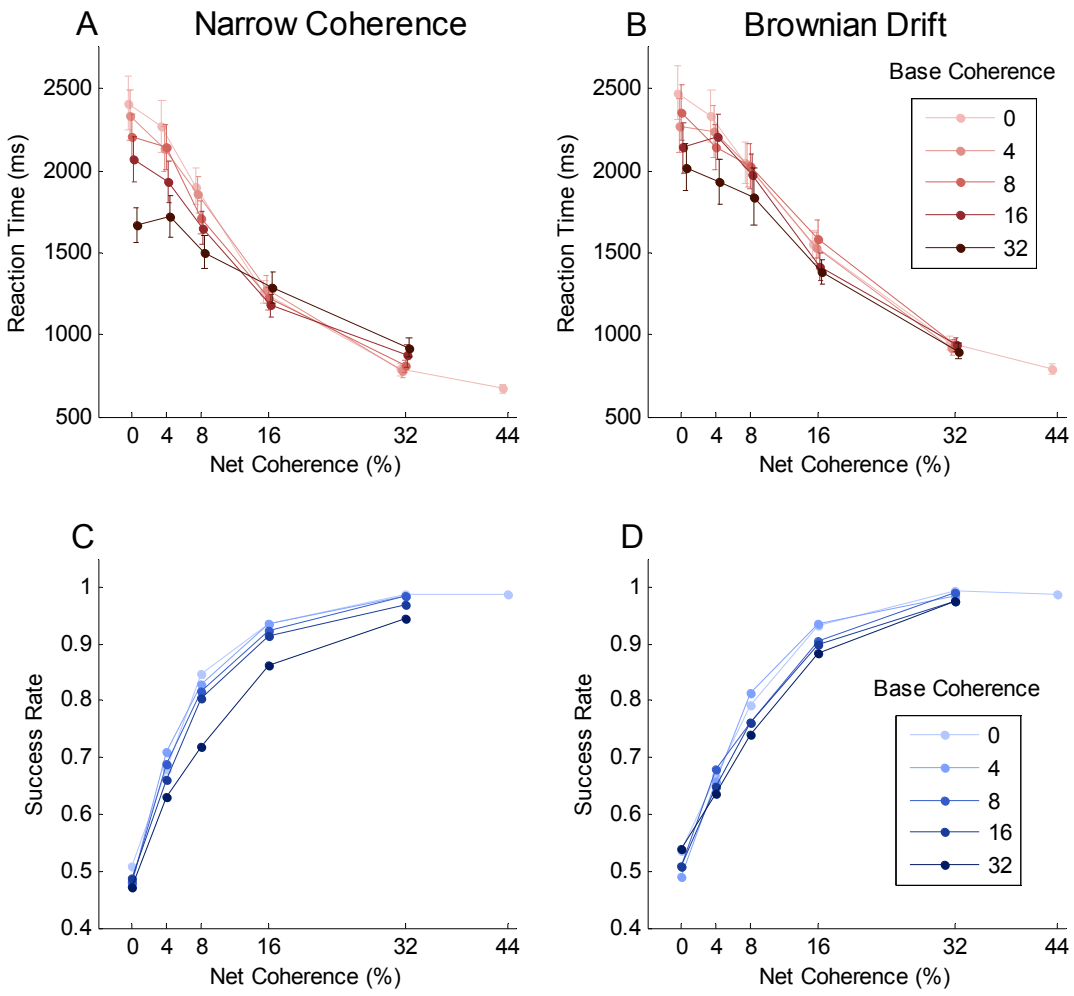

Figure 9: Psychometric curves for Experiment 1

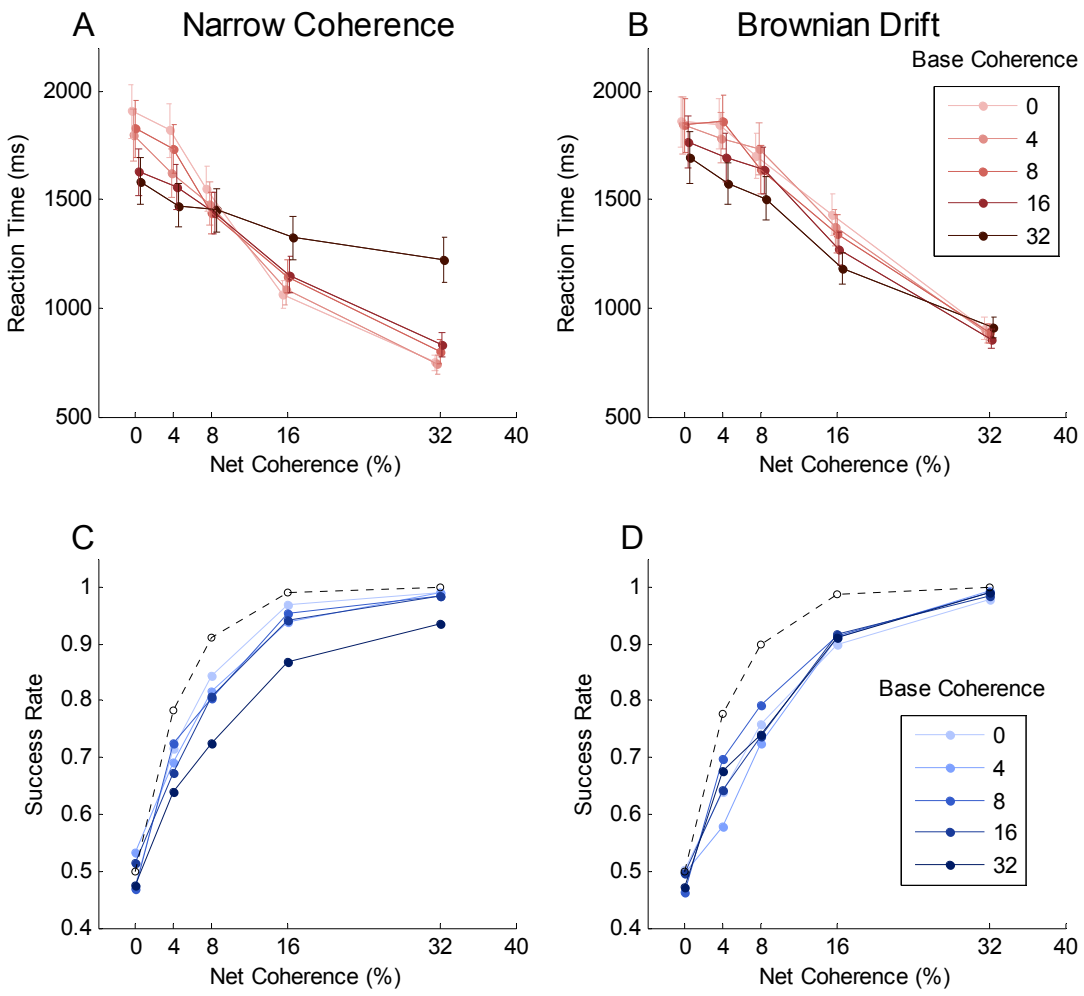

Figure 10: Psychometric curves for Experiment 2

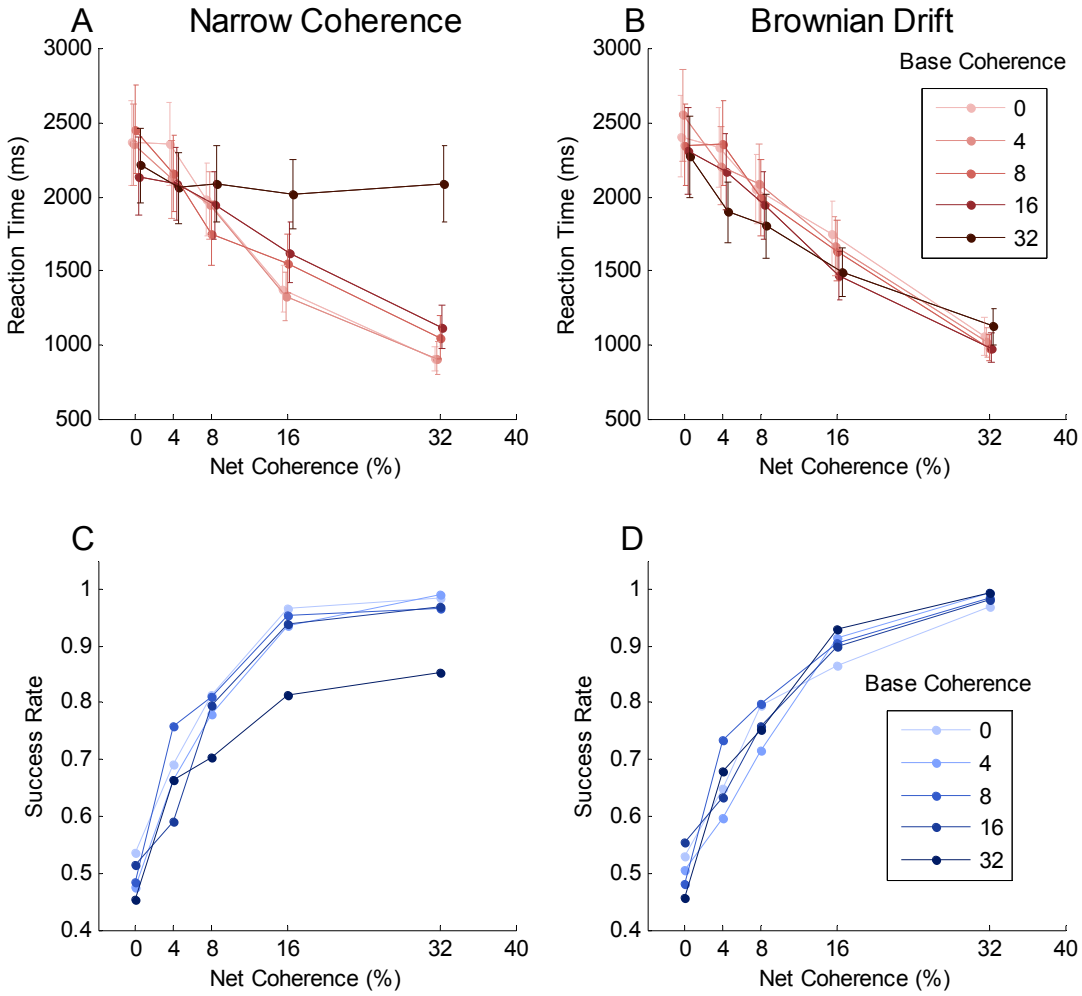

Figure 11: Psychometric curves for the two outlier subjects in Experiment 2

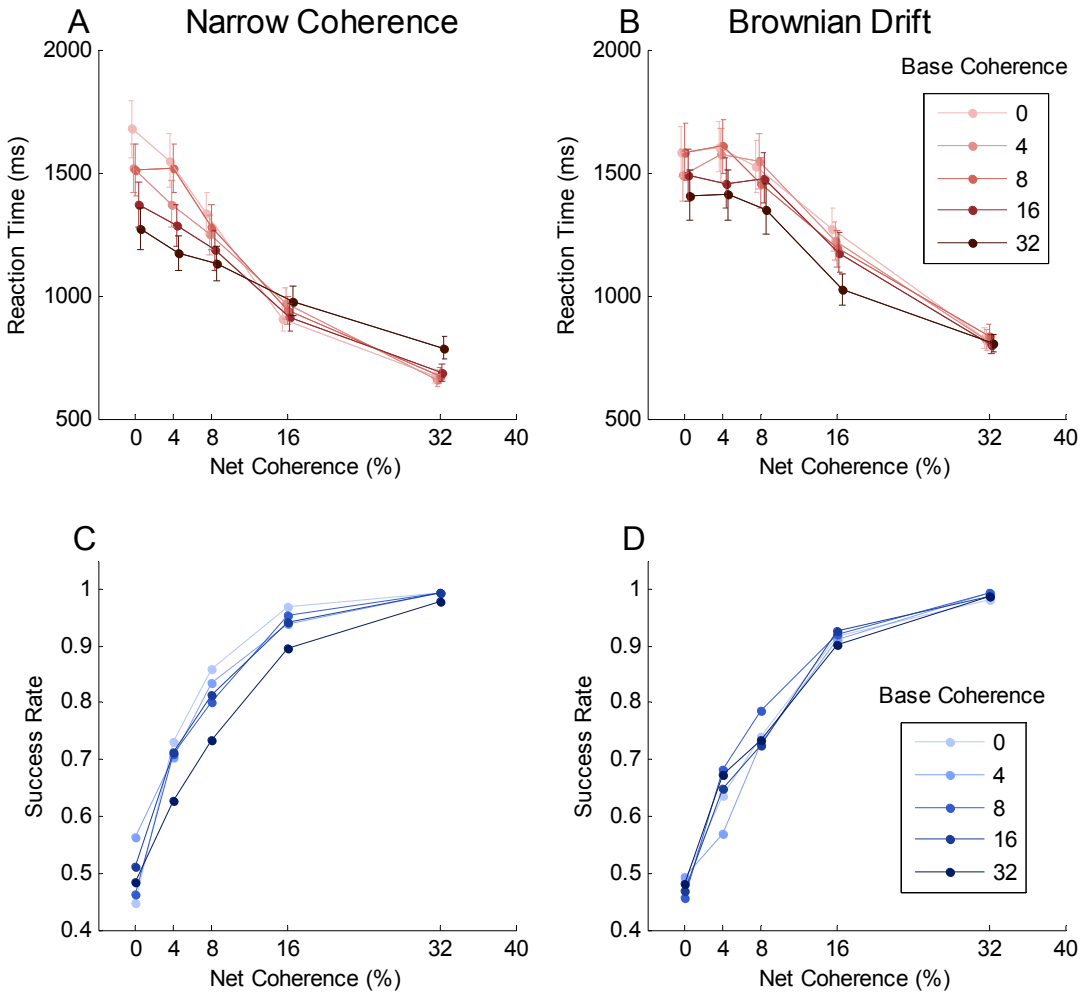

Figure 12: Psychometric curves for the remaining four subjects in Experiment 2

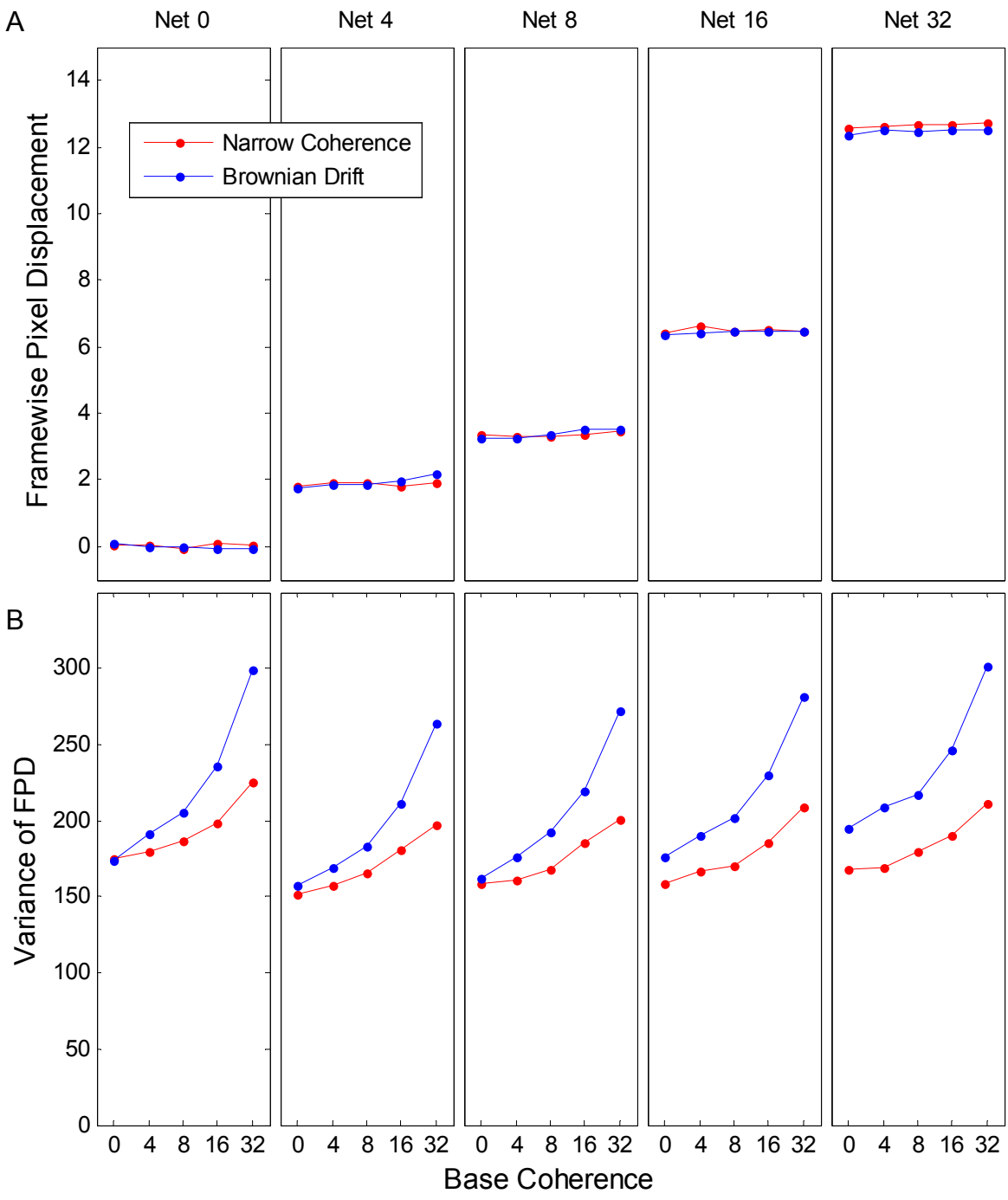

Figure 13: Framewise pixel displacement (FPD) measures for Experiment 2

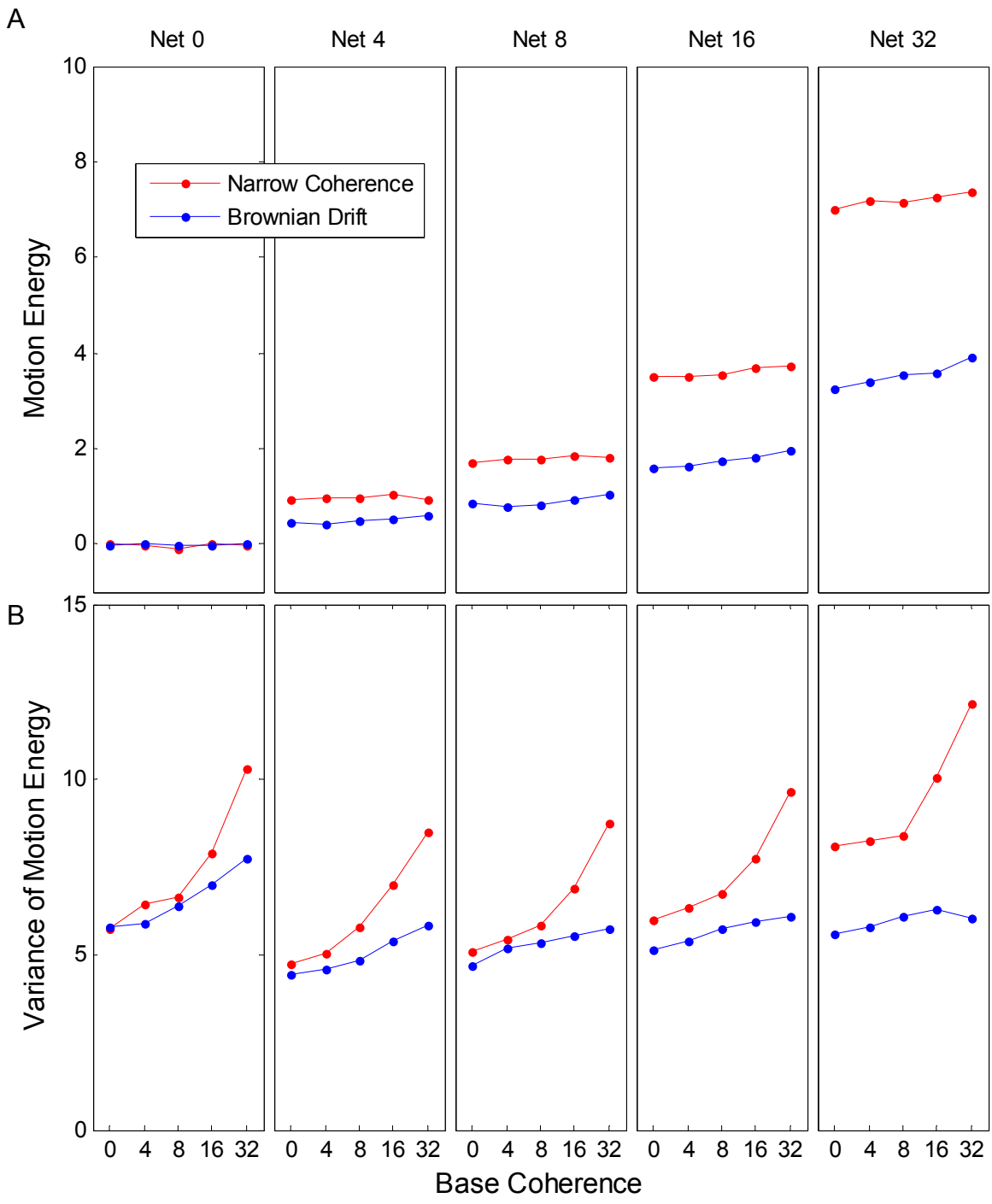

Figure 14: Motion energy measures for Experiment 2

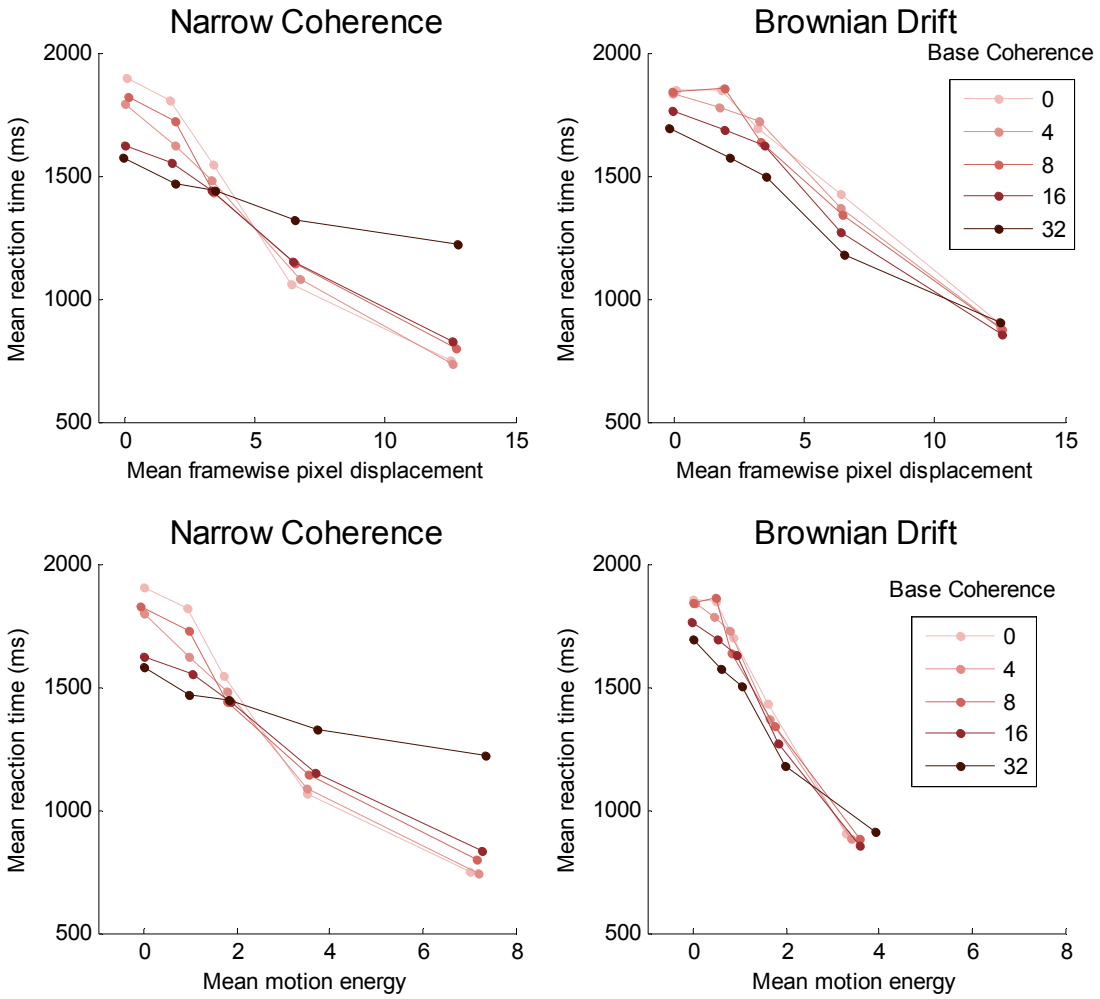

Figure 15: Reaction times as a function of measured FPD and motion energy in the NC and BD trials

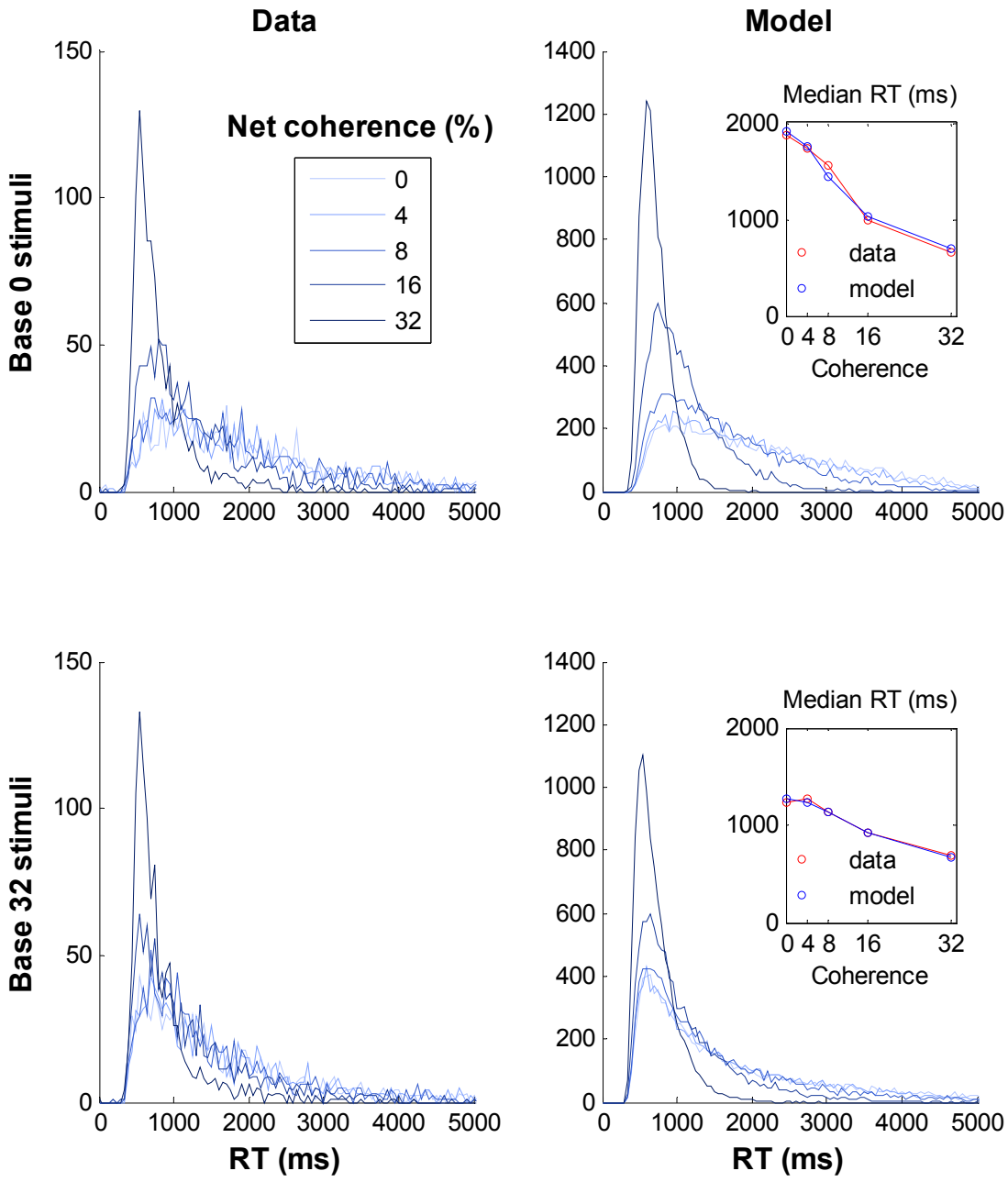

Figure 16: Dual-diffusion race model fit of the Experiment 1 reaction time data

Figure/Table Legends

Table 1. The 26 motion conditions. Each cell indicates the coherent motion in the two opposite directions. Each column groups stimuli that have the same net coherence signal (i.e. the difference in coherent motion presented in the 2 opposite directions), but different base coherence (i.e. amount of coherent motion presented equally in both directions).

Figure 1. Experimental paradigm. (A) Experimental task. Humans subjects watched a random dot kinematograms (RDK) and had to make a decision on whether there was more motion towards the right or left direction. Subjects then indicated their choice by moving a cursor from the central target one of the peripheral targets. Trial outcome and reaction times were recorded. (B) The two RDK versions. Different amounts of competing coherent motion is induced in the stimulus. In the Narrow Coherence version (left) the coherent motion is confined to the left and right directions. In the Brownian Drift version (right) the coherent motion is masked by random Brownian motion. See the Methods section for more detail.

Figure 2. Spatial distributions of dot pixel displacements for the Narrow Coherence (NC) task. Dot displacements are split into three distinct groups. The randomly moving dots form a circle of displacements equidistant from the origin. The leftward and rightward coherent dots form two oppositely oriented columns of displacements.

Figure 3. Spatial distributions of random and coherent dot displacements for the Brownian Drift (BD) task. Dot displacements are again split into three groups. The randomly moving dots form a circle of displacements equidistant from the origin. The leftward and rightward coherent dots also form a circular distribution, but shifted leftward and rightward respectively.

Figure 4. Polar histograms of the frequencies of the directions of dot displacements for the Narrow Coherence (NC) task. 0 degrees corresponds to the rightward direction and the direction of the net coherent motion. Dot displacements were sharply confined to the two opposing directions and were confined further with greater total coherent motion in the stimulus.

Figure 5. Polar histograms of the frequencies of the directions of dot displacements for the Brownian Drift (BD) task. 0 degrees corresponds to the rightward direction and the direction of the net coherent motion. Dot displacements were broadly distributed in all directions and were shifted to the right as the net coherent motion increased.

Figure 6. Auto-correlation analysis. (A) Two-dimensional histogram of vectors generated from all possible dot combinations between each pair of corresponding frames in 600 NC 64/32 trials. Displacements are measured in pixels. (B) Magnified view.

Figure 7. Ideal observer analysis. (A) Distribution of the average FPD per trial for the NC condition grouped by net coherence. (B) ROC curves for the different net coherence NC stimuli.

Figure 8. The directionally selective spatiotemporal motion filters used in the motion energy analysis. The pair of filters on the left column are selective for leftward motion, while the filters on the right are selective for rightward motion. These filters are combined and convolved with the random dot stimuli to give a measure of motion as a function of time in the stimulus.

Figure 9. Psychometric curves for Experiment 1. (A,B) Mean reaction time as a function of net coherence for the NC and BD stimuli respectively. Each line connects conditions with the same background base coherence. Values with the same net coherence are grouped into columns and are shifted slightly to increase visibility. (C,D) Success rate as a function of net coherence for the NC and BD stimuli respectively.

Figure 10. Psychometric curves for Experiment 2. (A,B) Mean reaction time as a function of net coherence for the NC and BD stimuli respectively. (C,D) Success rate as a function of net coherence for the NC and BD stimuli respectively. The dotted black line indicates how well an ideal observer would perform if it could perfectly integrate the stochastic motion information presented to the subjects. All other labelling details are identical to Figure 9.

Figure 11. Psychometric curves for the two outlier subjects in Experiment 2. (A,B) Mean reaction time as a function of net coherence for the NC and BD stimuli respectively. (C,D) Success rate as a function of net coherence for the NC and BD stimuli respectively. All labelling details are identical to Figure 9.

Figure 12. Psychometric curves for the remaining four subjects in Experiment 2. (A,B) Mean reaction time as a function of net coherence for the NC and BD stimuli respectively. (C,D) Success rate as a function of net coherence for the NC and BD stimuli respectively. All labelling details are identical to Figure 9.

Figure 13. Framewise pixel displacement (FPD) measures for Experiment 2. Top row: Mean FPD as a function of base and net coherence. Values are grouped into separate columns of equal net coherence and different base coherence within each column. Mean FPD values were identical for NC and BD stimuli. Bottom row: variance of FPD for the stimuli. The BD conditions had systematically greater variance than the corresponding NC conditions.

Figure 14. Motion energy measures for Experiment 2. Top row: Mean motion energy as a function of base and net coherence. Values are grouped into separate columns of equal net coherence and different base coherence within each column. Mean motion energy values were greater for the NC than the BD stimuli. Bottom row: variance of motion energy for the stimuli. The BD conditions had systematically lower variance than the corresponding NC conditions.

Figure 15. Reaction times as a function of motion signal measured in the NC (left column) and BD trials (right column). Top row: RTs as a function of mean framewise pixel displacement. Bottom row: RTs as a function of mean motion energy. Each line connects conditions with the same background base coherence.

Figure 16. Comparison of the observed (left column) and predicted (right column) distributions of RTs for different motion coherence levels of base-0% (top row) and base-32% (bottom row) stimuli. Inserts in the right column: the observed and predicted median RTs for the different net motion coherence levels for each base coherence level.

III. Overall Discussion

III.1. Review of the main objectives

In the following two sections, I will discuss the results from the article in the context of the two main objectives stated in the introduction.

III.1.1. Effect of directly competing motion

The first objective of this work was to determine the effect of net evidence and total relevant evidence in a 2AFC task on an observer's reaction times and success rates. We used a modified RDK stimulus design where different amounts of coherent random dot motion in both directions were combined to produce an RDK stimulus that had the same amount of net coherent motion in one of the two directions, but different amounts of simultaneous coherent motions in both opposing directions. We hypothesized that if the decision process was driven by the integration of net evidence, reaction times and success rates would be mainly driven by the net amount of coherent evidence towards the correct choice and would be independent of the total amount of motion in the stimulus. On the other hand, if the decision process was driven by two accumulators integrating evidence supporting their own preferred choice independent of each other, reaction times and success rates would be influenced primarily by the total amount of evidence for each choice rather than the net evidence.

Our results showed that observers' reaction times and success rates were primarily driven by the net coherence of the stimuli, with a smaller secondary effect of base coherence when the net evidence signal was weak. Our results therefore support the idea that the decision-making process in the brain integrates the relative difference in evidence towards

both choices. We showed that models that are based on the integration of the net evidence in the trial can predict the RT and success rate data well. On the other hand, we showed that simple race models in which two competing integrators accumulate all the evidence for their respective choices would not fit well with the data.

The stimuli that we have created are not the first to use multiple or opposite directions of motion in an RDK. Opposing motion RDK stimuli have been used to study the perception of transparent motion, in which local stimuli moving in different directions are grouped perceptually and perceived as separate transparent surfaces moving coherently in different directions (for a review, see Snowden and Verstraten, 1999). However, our stimuli do not evoke sensations of motion transparency, because dots can switch from carrying random motion to coherent motion displacements from frame to frame. Instead, our stimuli yield sensations of a bias in the direction of motion in one direction or the other. In addition, transparent motion has been studied as a visual perceptual phenomenon of itself. On the other hand, we are using opposing motion RDK stimuli in order to study the process of decision-making in the context of drift diffusion models. By manipulating the amount of coherent motion bias in two opposite directions, this experiment demonstrated that the perception of global motion direction was determined primarily by the level of net motion bias in one of the two directions, across a wide range of levels of opposing total coherent motion.

The results that we have presented add to the extensive psychophysical and neurophysiological literature showing that the decision process accumulates the difference in neuron/anti-neuron inputs (Roitman and Shadlen, 2002; Ditterich et al., 2003; Bosking and Maunsell, 2011; Bollimunta and Ditterich, 2012; Bollimunta et al., 2012). However, where in the brain does the differencing operation of opposing motion signals occur? Gold and Shadlen

(2001) proposed that sensory evidence is encoded in area MT and that opposing motion signals encoded in area MT are subtracted downstream by neurons in the parietal and frontal association cortex such as area LIP and FEF. MT neurons were thought not perform the differencing operation because MT neurons would increase their activity from baseline inter-trial levels even when coherent motion was presented in the null direction (Britten et al., 1993). The differencing operation could occur in LIP neurons, since they showed a ramping activity whose rate of rise was correlated with the net evidence in the trial (Roitman and Shadlen, 2002). The calculation of net motion coherence in LIP was further supported by a recent study by Bollimunta and Ditterich (2012) who recorded single unit activity and local field potentials (LFP) in LIP while monkeys performed the same 3-direction RDK task used by Niwa and Ditterich (2008). The monkeys showed the same psychophysics as humans, in that their choice behaviour was driven by the net motion coherence across the three motion streams. Bollimunta and Ditterich also found that single unit activity and the LFPs in LIP encoded different information about the coherent motion in the task. While single-neuron activity in LIP was best correlated with the net coherent motion in the trial, the LFP activity was better correlated with the sum of three coherent motion components. As LFPs are often presumed to reflect the synaptic input into the local circuits (Mitzdorf, 1985; Logothetis, 2003), this suggested that area LIP was receiving the full motion signals as input and that the net difference operation was being calculated locally by LIP neurons (Bollimunta and Ditterich, 2012; Bollimunta et al., 2012).

These neurophysiological recordings during a RDK motion discrimination task were used as a neural basis for the feed-forward inhibition race model proposed by Mazurek et al. (2003) (Figure I.4d), in which MT neurons play the role of sensory units encoding motion in

their preferred direction, while LIP neurons are the decision units that take the MT neuronal output and perform the differencing operation and accumulate the net evidence for the decision process.

However, one of the problems with this interpretation of these results is that the RDK stimuli used in decision making research only induce one direction of coherent motion. One could therefore not directly test how an MT neuron would respond to mutually opposing motion signals presented at the same time. In fact, evidence from studies of transparent motion indicates that MT neurons do indeed show a form of motion opponency. For example, Snowden and colleagues (1991; 1992) used RDK stimuli with transparent motion to show that MT neuronal activity was systematically suppressed as more dots drifted in the anti-preferred direction. Qian & Andersen (1994) showed that the MT motion opponency occurred in RDK stimuli in which dots with opposing vectors were paired locally. Recanzone et al. (1997) demonstrated similar motion opponency of MT neurons even when only two dots moved in different directions.

Consistent with these neurophysiological results, "motion-energy" computational models of motion perception also predict that an opponent-motion subtraction stage occurs in the early stages of the visual motion analysis pathway and usually attribute the opponent-motion process to V1 complex cells and MT motion-selective neurons (Adelson and Bergen, 1985; Snowden et al., 1991; Qian et al., 1994b; Simoncelli and Heeger, 1998). These lines of evidence suggest that the calculation of net motion evidence probably begins before area LIP, at least locally in area MT, but does not rule out the possibility of further opponent motion processing in LIP.

In summary, the reaction times and choice probabilities of observers in our task were mainly driven by the net evidence in the trial. These results support decision models which accumulate a decision variable representing the net evidence in the trial. It is unclear where in the brain this differencing operation occurs but future neurophysiological studies using competing RDK motion stimuli could fill this knowledge gap.

III.1.2. Integration of the global motion signal

The second objective of my work was to explore the effect of distributing competing coherent motion evidence across a broad range of directions in the RDK stimuli. In my experiments, I compared the psychophysics of a 2AFC task using RDK stimuli with coherent motion confined either to the two opposing directions at a constant velocity (Narrow Coherence), or spread across many different directions (Brownian Drift). The key difference between the two types of stimuli used was that in the NC stimuli, the coherent motion vectors replaced the random motion vectors of the selected coherent dot populations. The coherent motion in the NC stimuli was therefore explicitly evident in the motion stimuli. In contrast, the coherent motion vector component in the BD stimuli was added to the random-motion vector of the selected dots and was therefore implicitly embedded in a change in the distribution of dot motion directions and velocities. Our hypothesis was that if the decision process integrates motion signals from a wide range of directions and velocities (Williams and Sekuler, 1984; Smith and Ratcliff, 2004; Jazayeri and Movshon, 2006; Bosking and Maunsell, 2011), then participants should have similar reaction times and success rates for both versions of the RDK stimuli. If instead subjects were only relying on motion signals in the narrow band of left and right directions since the subjects have to make a decision between left and right to point to the correct target, then the behavioural results for the two stimuli would be different. Our

results showed that observers had similar reaction times and success rate curves for both types of stimuli across all base coherences. This suggested that participants were able to integrate motion signals with the same efficiency whether the coherent motion signal was confined to the two directly opposite directions at a constant velocity, or was spread across many directions at varying velocities. Furthermore, they could perform the task equally well with the two types of stimuli whether they were presented in separate blocks (Experiment 1) or randomly interleaved in the same trial block (Experiment 2).

The psychophysical results obtained for the NC and BD stimuli were consistent with a similar study by Niwa and Ditterich (2008), who found the subject behaviour in a three-direction discrimination task (described in Section I.3.2) was driven by the net difference between the coherent motion in the correct direction and the average of the coherent motions in the other two directions. Furthermore, the psychophysical results obtained in the BD stimuli were consistent with previous studies by Sekuler and colleagues who used stimuli that spread the local motion along a wide range of directions centered on one net motion direction (for more detail, see Section I.3.2). They showed that observers could integrate the global coherent motion from an RDK in which the coherent dots had a distributed range of directions (Williams and Sekuler, 1984; Watamaniuk et al., 1989; Watamaniuk and Sekuler, 1992). In addition to replicating these results with our BD stimuli, we also demonstrated that the integration of local motion signals still occurs when coherent motion was presented in two opposing directions in the RDK.

At the neural mechanism level, these results suggest that the pools of motion sensitive neurons used in this decision process were not limited to those with preferred directions in the left and right directions, but consisted of a broad distribution of preferred directions. The

evidence from this wide range of directions was then combined with motion evidence across different velocities as a global picture of the net evidence signal to be used in decision making process. The population of motion sensitive neurons in the middle temporal (MT) cortex exhibits a wide range of preferred motion directions (Dubner and Zeki, 1971; Zeki, 1974; Albright, 1984; Newsome et al., 1986; Mikami et al., 1986a, 1986b). In addition, MT neurons also have a diverse range of velocity tuning (Maunsell and Van Essen, 1983).

Recent theoretical modelling has suggested that the global percept of motion can be generated in the brain by sampling the activity of a large population of MT neurons with a broad range of preferred motion directions (Jazayeri and Movshon, 2006). In this model, MT neurons are thought to represent the likelihood that the presented motion stimuli are in their preferred direction of motion. This decision framework would pool the population of neuronal activity and weigh each neuron's activity based on their likelihood to contribute to the decision hypothesis. This framework makes it possible for the population of MT neurons to adapt their weighting based on the task demands towards the neurons that provide the greatest discriminatory information. During a coarse discrimination task such as the present task in which an observer must distinguish between two opposite directions 180° apart, if all the information is confined to those two directions (such as in the NC stimulus), a population code might only have to strongly weigh neurons tuned to the two opposite directions. However, if the global coherent motion is distributed across a range of local signals with different directions (such as in the BD stimulus), a population code would have to incorporate the neuronal activity of neurons with a wide range of preferred directions. The similar psychophysical profiles of the human subjects in our experiments for both the NC and BD stimuli would indicate that the pooling process was incorporating neurons with a wide range

of preferred directions. Under the framework of the Jazayeri & Movshon (2006) model and consistent with the neurophysiological results of Bosking & Maunsell (2011), these results suggest that the NC and BD stimuli activated the population of directionally selective MT neurons differently, but that the combined likelihood contributions from the MT neurons produced a similar likelihood output to the decision process.

III.2. Quantifying motion evidence in RDKs

The motion evidence given by the random dot stimuli is variable in nature due to three factors. First the dots are initialized in random locations for each trial. Second, each dot is initially assigned a random displacement vector between two frames. Third, the algorithm that determines which dots move randomly or coherently in each frame also uses a random selection process. Because of this variability, the motion signal that is presented from frame to frame and over many frames is not always exactly the percent coherence indicated for that particular trial. This results in transient deviations of the motion evidence from its intended value in a given trial that can cause an unintended bias in the motion evidence towards one or the other choice (Britten et al., 1996). To measure this trial-by-trial stimulus variation, we used two methods: the Framewise Pixel Displacement (FPD) analysis and motion energy analysis. The motion energy model that we used, developed by Adelson and Bergen (1985), attempts to simulate the motion sensitivity of an MT neuron. This model convolves four directionally oriented spatiotemporal motion filters with the RDK stimulus to give a measure of directional motion as a function of time. However, one of the limitations to the motion energy model is that the spatiotemporal filters are selective for a specific direction and speed. While this is good for stimuli that have the matching properties, such as the NC version of our stimuli, their

properties may not capture all the coherent motion component added to the dot motions in our BD version of our stimuli, in which the coherent motion component was carried implicitly by the dots that moved along all directions and with speeds of 0°/s and 4°/s. Indeed, as shown in **Figure III.1**, the motion energy values measured at 5 different angles centered on the left right axis show systematically lower motion energy values for the BD version compared to the NC version.

In order to ensure that the same amount of potential motion information was being presented in both stimulus versions, we used the FPD analysis. This analysis takes a simple sum of the horizontal components of all the displacements made by each possible pair of dots between two corresponding frames. Aside from omitting dot displacements corresponding to speeds greater than 8°/s, which were twice as large as any of the dot displacements actually controlled by the RDK algorithm, the FPD analysis captures all possible horizontal motion signals in the input regardless of the speeds and directions of actual displacement, and free of any assumptions of how those stimuli were processed centrally. The FPD measurements produced nearly identical motion values for equivalent coherent-motion conditions of NC and BD stimuli, and indicated that the same amount of coherent component motion evidence was being presented in both stimuli.

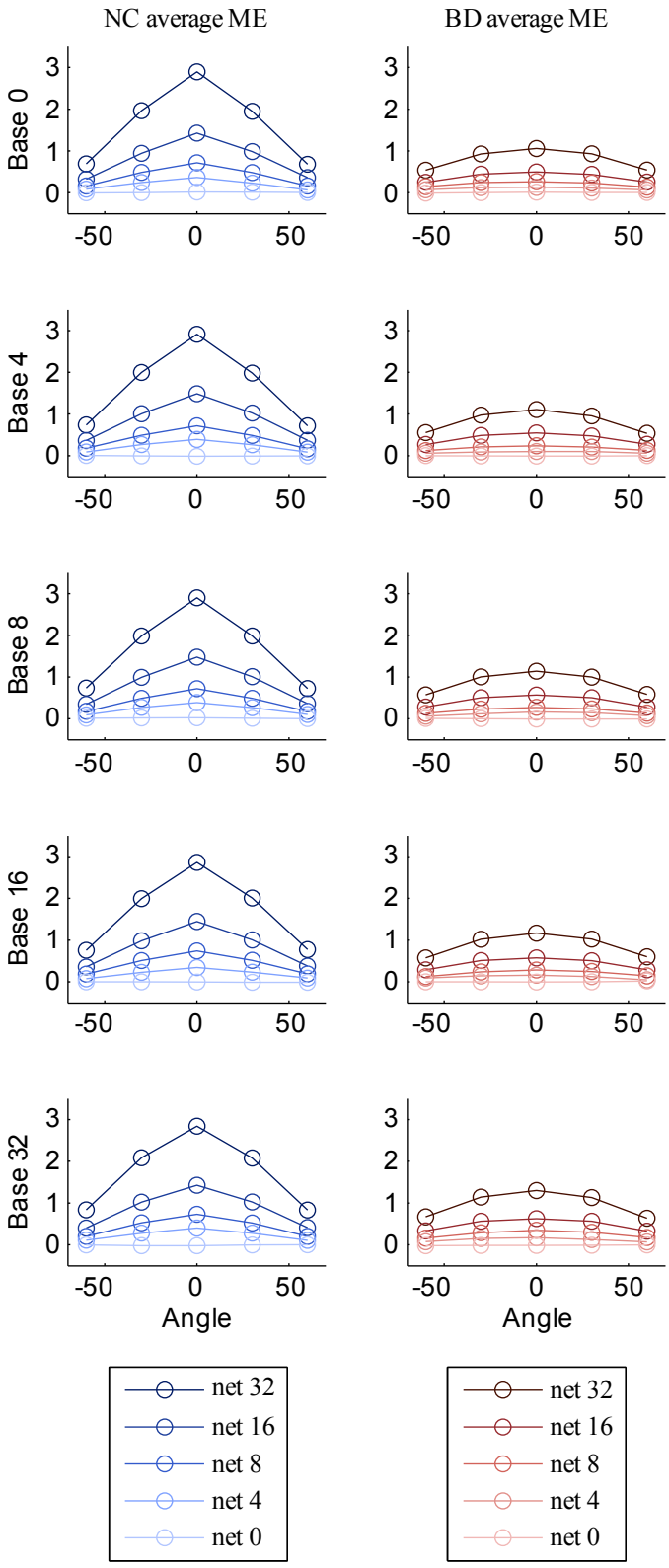

Figure III.1: Motion energy (ME) values measured at different angles from the coherent motion for the Narrow Coherence (NC) and Brownian Drift (BD) stimuli

It should be noted that the results of the motion energy analysis does not mean that the motion energy analysis is an inappropriate way to measure the relative amount of movement direction strength in RDK stimuli. Both FPD and motion energy measurements showed the same trends in the effects of net and base coherence on mean motion strength and variance for stimuli of the same stimulus type. Thus, the motion energy and FPD analysis will give comparable results when comparing levels of coherent motion strength within any one RDK algorithm.

The FPD analysis provided more consistent measures of motion strength between the NC and BD stimuli than the motion energy analysis. The key difference between the FPD and the motion energy analysis is that the FPD analysis is a global measure of motion that simply sums the directional components of the physical displacements of the dots across all directions and velocities. In contrast, the motion energy analysis uses spatiotemporal filters that extract a measure of motion strength with a specific directional and velocity tuning, and that incorporate a number of known non-linear properties of MT neuron responses to visual motion stimuli, including temporal and spatial integration and facilitation of the local motion stimuli in their spatiotemporal "receptive fields". As the motion evidence in the BD stimuli is distributed across many directions and velocities, there are fewer local motion stimuli at any given time and spatial position that optimally activate the filters, with the result that less motion energy is captured by the motion energy filter in the BD stimuli than the NC stimuli. It is possible that similar motion energy read-outs might be attained for the BD and NC stimuli if we used a large population of motion energy filters tuned for multiple velocities and all the spatio-temporal filter combinations that would be tuned to those velocities (Simoncelli and Heeger, 1998). This would further support the idea that the decision mechanism must integrate

from a pool of neurons with a wide distribution of directional and velocity tunings to perform the task at a similar level in the NC and BD stimuli.

III.3. Limitations to the stimuli used

One of the potential caveats in our work is that in the NC and BD stimuli, dots that were chosen to move randomly between a pair of image frames were not then randomly replaced to another location in the next frame of the image sequence like some conventional RDK stimuli (Roitman and Shadlen, 2002; Palmer et al., 2005; Kiani et al., 2008; Niwa and Ditterich, 2008; Pilly and Seitz, 2009). Instead, they were continuously displaced in a random direction in a form of Brownian motion. Because of this, the dots had a sustained lifetime for the entire duration of the trial, unless they disappeared behind the edge of the masking circular aperture. This raises the possibility that subjects could ignore the moment-to-moment motions of the dots and instead monitor the progressive changes in position of the dots across time, since the position of each dot is the cumulative result of the entire sequence of frame-to-frame displacements from the start of the trial. Furthermore, because each dot can be part of any of the three subgroups of dots (coherent left, coherent right, or random), its change in position over extended periods of time would approximate the net motion evidence in the stimulus. At the extreme, subjects could attempt to track the changing position of a single dot and try to base their directional choice on that single-dot evidence. However this would not be a very effective strategy for several reasons. First the single-dot displacements were rapid and noisy; dots frequently "collided" in crossed paths, making it difficult to track a single dot reliably. Furthermore, at low net motion coherences, the probability of any single dot showing a reliable change in position across time that is perceptually distinguishable from all of its

moment-to-moment movement changes in motion direction is low. This suggests that if the subjects were basing their perceptual decisions primarily on the basis of progressive changes in position across time, they would have to monitor the position trends of many dots simultaneously.

However, our subjects did not seem to gain substantial additional evidence from the long lifetime of dots. If they were indeed primarily using the temporal evolution of dot positions across extended periods of time to make their perceptual decisions, our results show that the psychophysics of their motion perception decisions is remarkably similar to that for subjects who presumably had to depend primarily on the global directional signals available in RDK motion stimuli with short dot lifetimes (Niwa and Ditterich, 2008). This result is also consistent with studies that have directly compared the responses of subjects to RDK stimuli with short and long dot lifetimes and have found that subjects do not utilize the information given by the progressive changes in position of the dots across time but instead monitor the distribution of motion displacements from frame to frame in order to obtain a global percept of motion (Watamaniuk et al., 1989; Pilly and Seitz, 2009).

Finally, it must be noted that the question of the degree to which subjects use instantaneous direction versus progressive position changes is inevitably confounded by the design of motion energy filters used to model the early processing of visual motion. These filters inherently incorporate information about the temporal evolution of the positions of dots in RDK stimuli since they are optimally activated by dots that move in a consistent direction over time across their spatio-temporal "receptive fields" (Adelson and Bergen, 1985; Qian et al., 1994b; Simoncelli and Heeger, 1998).

One additional feature of the BD stimuli is that the velocity of the dots carrying the coherent motion was not constant but varied as a function of the resultant direction of the vector sum of the coherent and random vector components. Another modification to the random dot algorithm could be used to eliminate this velocity variability. Instead of adding the coherent motion vector to the random displacement of the dot, the magnitude of the coherent motion steps could remain constant while the dot's direction would be selected from a predefined uniform or Gaussian distribution of directions. In this way, the motion would be spread out along different directions, centered on one net direction, but have the same velocity. This method has been used previously by Sekuler and colleagues (Williams and Sekuler, 1984; Watamaniuk et al., 1989; Watamaniuk and Sekuler, 1992), in which dot directions were selected from a uniform or Gaussian distribution with a mean in the direction of global motion. However, while the motion signal was distributed in many directions, the Sekuler stimuli only contained one component of global coherent motion, instead of two distributed components of global motion with opposing mean directions as in our stimuli. One prediction with these stimuli would be that the FPD measurements would be lower for the new BD stimuli compared to the NC stimuli, because moving dots off the main axis would reduce the horizontal component of the coherent motion. The motion energy values would remain lower in the BD stimuli compared to the NC stimuli. It would be interesting to see if subjects would still have similar psychophysics with these new BD stimuli and the more conventional NC stimulus, assuming that less motion evidence will be shown in the BD stimuli.

III.4. Future Directions

In the current work, we found that in low net-coherence trials, subjects' reaction times shortened as the base coherence increased. This effect was paired with an increase in the measured variability of the motion signal presented in the different base coherence conditions. We suggested that increasing the base coherence increased the magnitude of momentary biases of motion signal away from the intended net motion coherence. Under the context of drift-diffusion models, this could be represented as an increase in the gain of the noise in the accumulation process, which could lead to faster decision times. Using a very simple generative drift-diffusion model, we showed that we could simulate not only the observed median RTs of subjects to different combinations of met and base coherence but also the overall RT distributions simply by increasing the gain of the stochastic noise term in the model without any other changes in the model parameters. This also implied that the momentary fluctuations could have an effect on subject choice. In the next few sections I will detail some of the more recent analyses that I have conducted in order to examine to what degree the trial-to-trial variability of the observed visual RDK stimuli could explain the trial-to-trial variability in the subjects' choice selection.

Drift-diffusion models predict that if the accumulation process is perfect, without any leak or other loss of accumulated evidence, then the average signal presented to subjects on each trial should determine their subject choice. **Figure III.2** shows a scatterplot of the single-trial RTs as a function of the mean FPD in the trial. Each dot in the figure represents one trial plotted as a function of its average motion signal in the stimulus and the reaction time of the subject. Trial conditions were grouped by net coherence and collapsed over base coherence.

The solid horizontal lines show the average FPD signal for the two groups in each scatterplot. For the net 4-32% coherence conditions, the two groups represent success (black) and error (cyan) trials. There is a small shift in the mean motion displacements between the correct and error trials, whereby the average motion signal in trials in which the subjects made the correct choice was slightly stronger than in trials in which they made incorrect choices. This shift is also apparent in the net 0% conditions, where the two groups represent trials in which the subject selected the leftward (blue) or rightward (red) target. However, the distributions overlap extensively, and so it is not apparent that the average motion signal had a strong causal impact on choice selection on a trial-to-trial basis.

To illustrate how moment-to-moment fluctuations could influence the amount of motion evidence being presented over the course of a trial, we measured the FPD values as a function of time for each trial. **Figure III.3** shows the accumulation over time of FPD motion evidence presented for single trials. Each line represents the cumulative sum of momentary FPD motion evidence measured in one trial as that trial progressed. Lines are aligned to the start of the trial and are colored by the direction of coherent motion and the outcome of the trial. For example, in the net 4% column, the red and orange lines represent trials in which the net coherent motion was towards the right. Red lines indicate that the subject successfully chose the correct rightward target, while the orange lines indicate that the subject incorrectly chose the leftward target. There is extensive overlap in the cumulative information for the correct and incorrect trials.

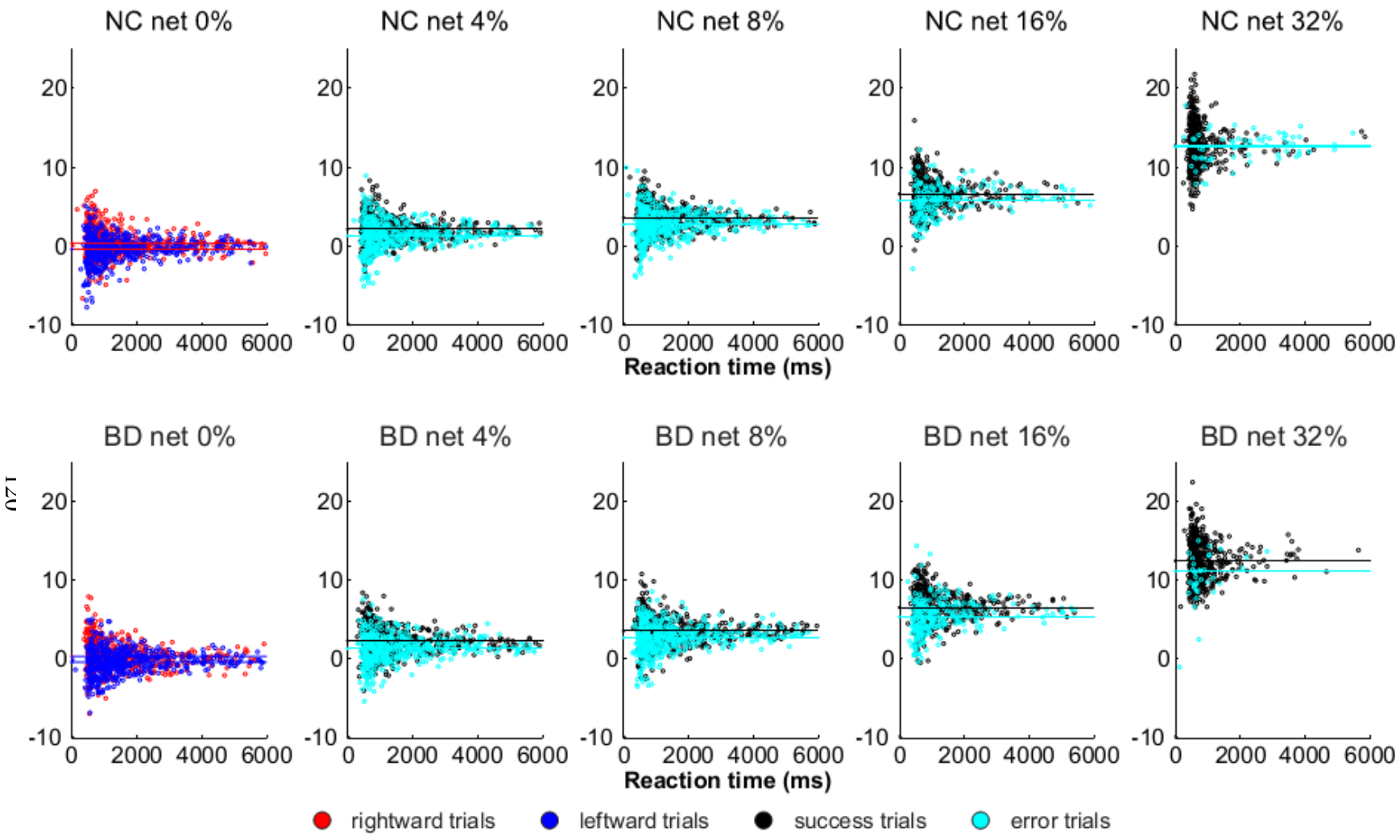

Figure III.2: Scatterplot of single-trial reaction times as a function of mean Framewise Pixel Displacement

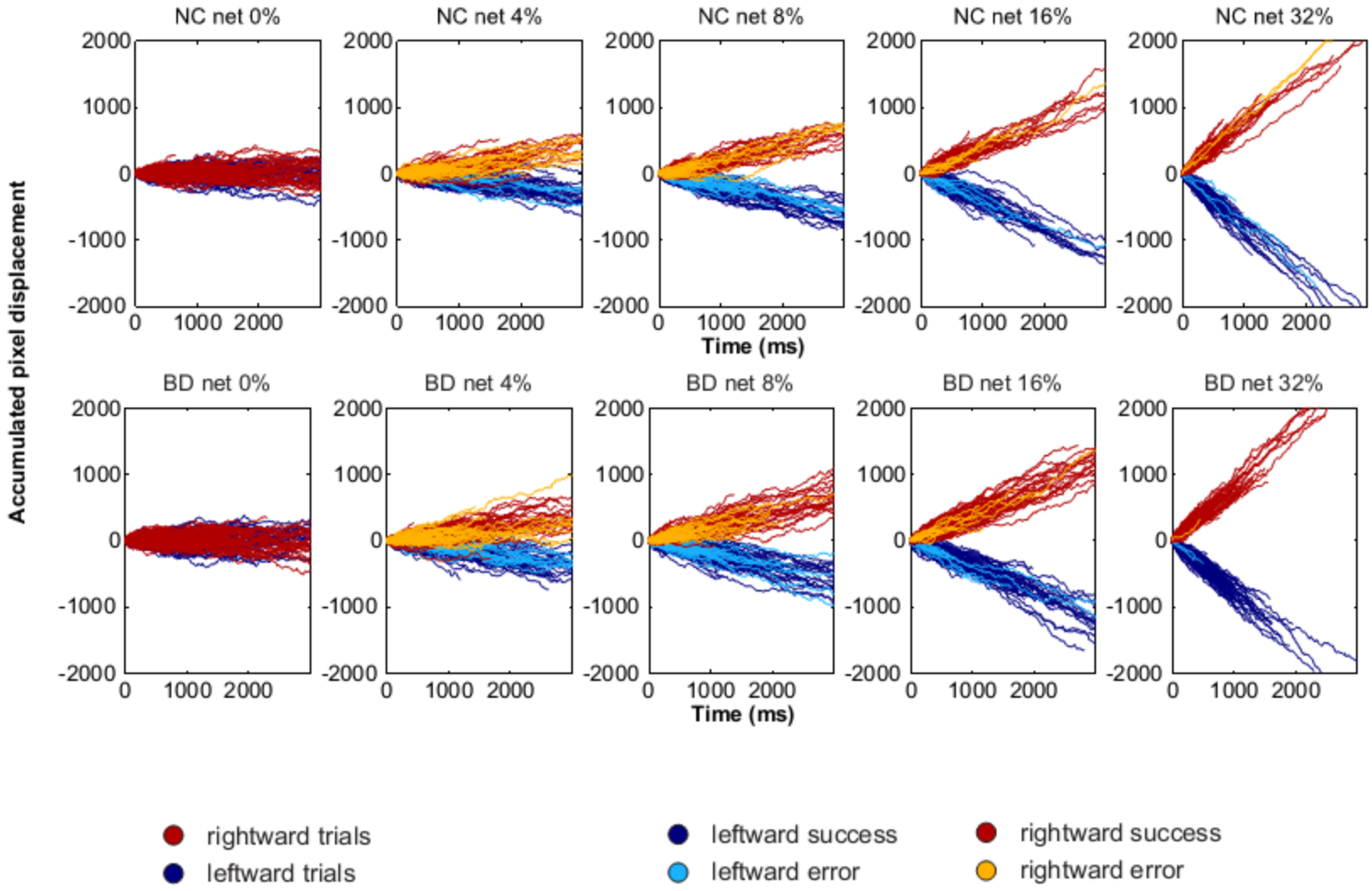

Figure III.3: Integration of single-trial FPD aligned to the start of the trial

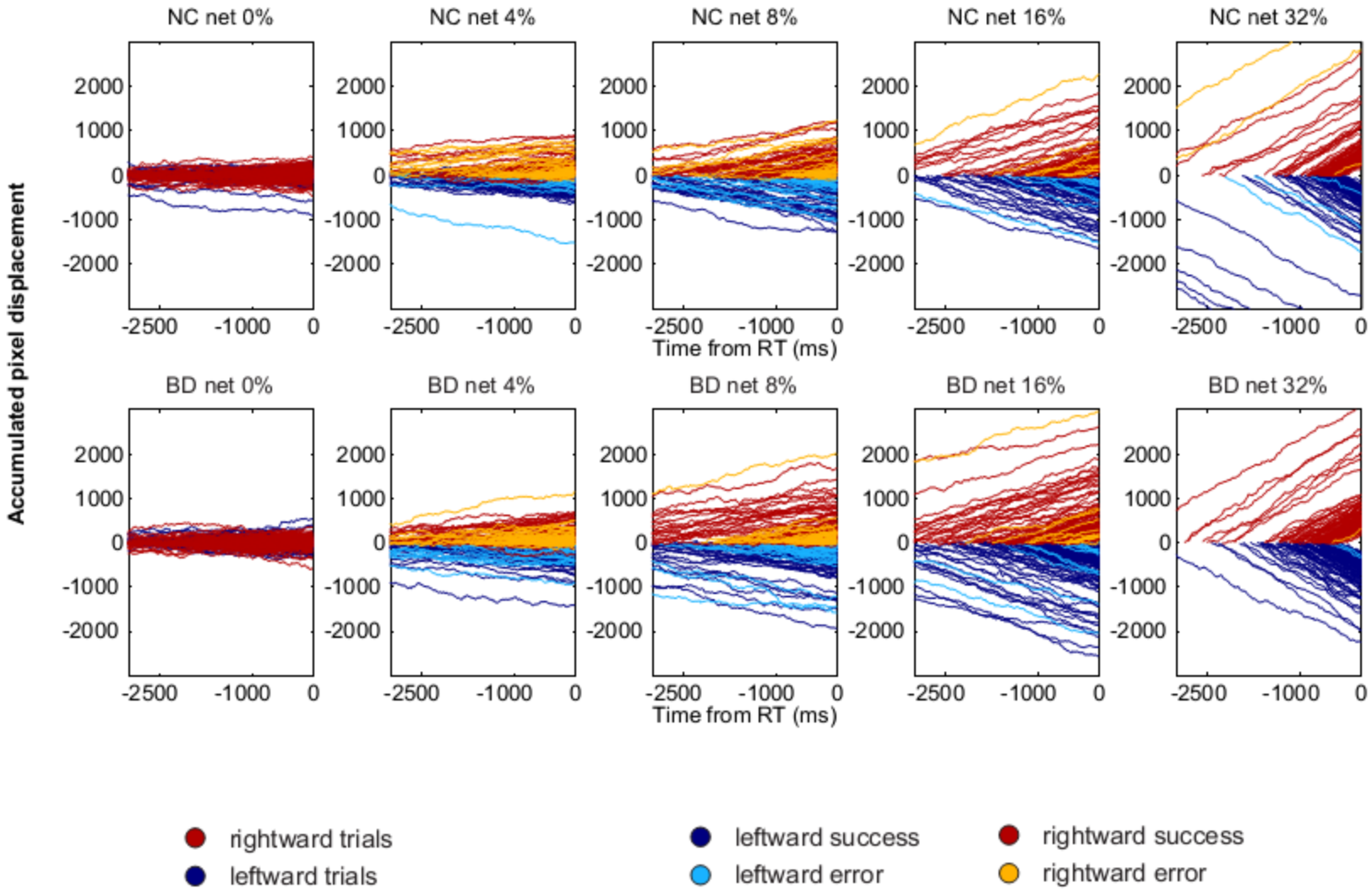

Figure III.4: Integration of single-trial FPD aligned to the end of the trial

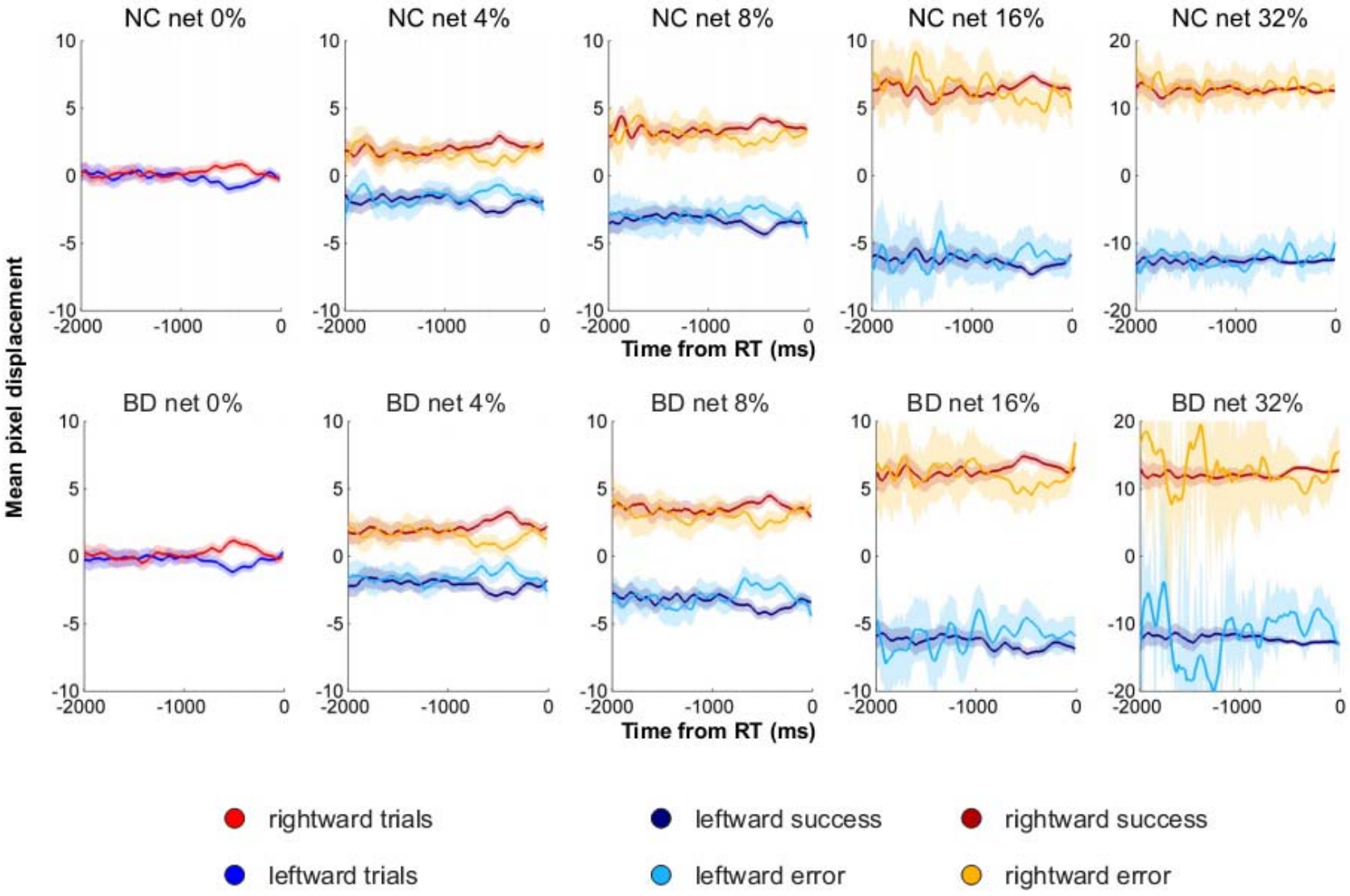

Figure III.5: Reverse correlation analysis of trial FPD averaged and aligned to the end of the trial

Assuming that the decision process is modeled by a perfect integrator of the motion presented in the stimuli, there should be far fewer errors than observed in Figure III.3, even for the net 4% coherent stimuli as there is a clear bifurcation in the accumulated evidence for rightward and leftward trials. Furthermore, when the same cumulative motion evidence is aligned to the reaction time (**Figure III.4**), one can see that the final cumulative evidence presented in a trial can vary greatly between trials not only with different net evidence, but also for trials with the same net coherence. This is not consistent with the prediction of drift diffusion models that the evidence in the decision process is accumulated towards a bounded threshold and that a decision is made once the accumulating evidence exceeds that constant threshold across all stimulus conditions. Figures III.3 and III.4 therefore suggest that the integration process does not perfectly accumulate the motion evidence presented. There must be a neural source of variability in the accumulation of evidence that has a major impact on evidence accumulation in the decision process.

While our data show that a central source of variability must have a major impact accumulation of evidence during the trial, we also found evidence that momentary fluctuations of motion evidence in the stimuli presented had an effect on subjects' choice selections. **Figure III.5** show a reverse correlation analysis of trial motion displacements averaged and aligned to the reaction time. There is a clear difference in observed motion displacements in a 500 ms window before the RT in trials with different response outcomes for the 0%-8% net motion coherences. For example in a rightward net 4% trial, the average motion signal increased just before the subjects responded in trials where the subjects correctly picked the rightward target (red line), but decreases just before subjects incorrectly picked the leftward

target (orange line). This suggests that small momentary fluctuations may have a significant impact on both what choice the subjects made and when they halted the decision process.

There are several possible explanations for this striking effect. One possibility is that the integration process is not perfect. There may be a leaky process which puts a greater weight on later evidence in the trial. Another possibility is that this is an effect of the termination process. Subjects might be waiting for a strong piece of motion information in the random dot kinematogram for stimuli with low net coherence before terminating their decision process and picking a target.

To my knowledge this is the first time that the reverse correlation analysis has been applied to a RT version of the 2AFC task in which subjects are free to view the RDK stimulus until they have sufficient information to make a decision. Other studies used the reverse correlation analysis but with a fixed duration version of the RDK task. Zylberberg et al. (2012) used a RDK task with a fixed duration of 700ms and found that early information had a greater influence on subject choice. Interestingly, the window in which motion energy fluctuations were most correlated with subject choice was also around 500ms, similar to our results.

In Kiani et al. (2008), monkeys were presented with a RDK 2AFC direction discrimination task in which the stimulus duration was experimentally controlled to vary between 80-1500 ms. Kiani et al. reported that in their experiment, the earlier evidence had a disproportionate impact on decisions while later evidence was discounted. However, this effect could likely be explained by the design of the task. The distribution of stimulus durations was out of control of the observing monkeys. As a result, the monkeys were confronted with a task environment with considerable uncertainty at the start of each trial

about the duration of the motion stimulus. It would seem reasonable to expect that this uncertainty would lead the monkeys to pay more attention evidence early in the trial because they did not know when the trial would end. The different results from the reverse correlation analysis between fixed duration and RT versions of the RDK direction discrimination task suggests that the decision process can flexibly weigh momentary evidence differently depending on the design and requirements of the task, and on expectations about the duration of available motion evidence.

In summary, the average motion signal presented to subjects on each trial does not have a strong effect on their choices. The extensive overlap of the accumulated motion evidence in trials in which the subjects made correct and error choices suggests that a central source of stochastic neural activity is a major source of variability. Nevertheless, momentary fluctuations in the motion signal in a time window of 500 ms before subjects terminate their decision correlates with their eventual choice selection. The preliminary analysis presented in this section has the potential to address the validity of some of the fundamental features used in decision making models that rely on the accumulation of noisy evidence. This avenue of research will be one our objectives for a future publication.

IV. Conclusion

In conclusion, we have developed a novel RDK paradigm that tested how simple perceptual decisions are formed when two opposing motion signals are presented in one visual stimulus. Using this stimulus we have shown that the decision making process is based on the net difference of these two opposing signals. Furthermore, similar psychophysical performance on the NC and BD versions of the experiment demonstrate that the decision process can integrate motion signals from a wide distribution of directions in order to obtain a global percept of coherent motion.

References

Adelson EH, Bergen JR (1985) Spatiotemporal energy models for the perception of motion. J Opt Soc Am A 2:284-299.

Albright TD (1984) Direction and orientation selectivity of neurons in visual area MT of the macaque. J Neurophysiol 52:1106-1130.

Asrress K, Carpenter R (2001) Saccadic countermanding: a comparison of central and peripheral stop signals. Vision Res 41:2645-2651.

Baker C, Hess RF, Zihl J (1991) Residual motion perception in a" motion-blind" patient, assessed with limited-lifetime random dot stimuli. J Neurosci 11:454-461.

Ball K, Sekuler R (1979) Masking of motion by broadband and filtered directional noise. Percept Psychophys 26:206-214.

Barlow H, Tripathy SP (1997) Correspondence noise and signal pooling in the detection of coherent visual motion. J Neurosci 17:7954-7966.

Bogacz R, Brown E, Moehlis J, Holmes P, Cohen JD (2006) The physics of optimal decision making: a formal analysis of models of performance in two-alternative forced-choice tasks. Psychol Rev 113:700-765.

Bollimunta A, Ditterich J (2012) Local computation of decision-relevant net sensory evidence in parietal cortex. Cereb Cortex 22:903-917.

Bollimunta A, Totten D, Ditterich J (2012) Neural dynamics of choice: single-trial analysis of decision-related activity in parietal cortex. J Neurosci 32:12684-12701.

Bosking WH, Maunsell JH (2011) Effects of stimulus direction on the correlation between behavior and single units in area MT during a motion detection task. J Neurosci 31:8230-8238.

Braddick O (1974) A short-range process in apparent motion. Vision Res 14:519-527.

Brainard DH (1997) The psychophysics toolbox. Spat Vis 10:433-436.

Britten KH, Shadlen MN, Newsome WT, Movshon JA (1992) The analysis of visual motion: a comparison of neuronal and psychophysical performance. J Neurosci 12:4745-4765.

Britten KH, Shadlen MN, Newsome WT, Movshon JA (1993) Responses of neurons in macaque MT to stochastic motion signals. Vis Neurosci 10:1157-1169.

Britten KH, Newsome WT, Shadlen MN, Celebrini S, Movshon JA (1996) A relationship between behavioral choice and the visual responses of neurons in macaque MT. Vis Neurosci 13:87-100.

Brody CD, Hernández A, Zainos A, Romo R (2003) Timing and neural encoding of somatosensory parametric working memory in macaque prefrontal cortex. Cereb Cortex 13:1196-1207.

Brown S, Heathcote A (2005) A ballistic model of choice response time. Psychol Rev 112:117-128.

Brown S, Heathcote A (2008) The simplest complete model of choice response time: linear ballistic accumulation. Cogn Psychol 57:153-178.

Busemeyer JR, Townsend JT (1993) Decision field theory: a dynamic-cognitive approach to decision making in an uncertain environment. Psychol Rev 100:432.

Bushnell M, Goldberg M, Robinson D (1981) Behavioral enhancement of visual responses in monkey cerebral cortex. I. Modulation in posterior parietal cortex related to selective visual attention. J Neurophysiol 46:755.

Carpenter R (1981) Oculomotor procrastination. In: Eye movements: Cognition and visual perception, pp 237-246.

Carpenter R, Williams M (1995) Neural computation of log likelihood in control of saccadic eye movements. Nature 377:59-62.

Churchland AK, Kiani R, Shadlen MN (2008) Decision-making with multiple alternatives. Nat Neurosci 11:693-702.

Cisek P, Kalaska JF (2002) Simultaneous encoding of multiple potential reach directions in dorsal premotor cortex. J Neurophysiol 87:1149-1154.

Cisek P, Kalaska JF (2005) Neural correlates of reaching decisions in dorsal premotor cortex: specification of multiple direction choices and final selection of action. Neuron 45:801-814.

Cisek P, Kalaska JF (2010) Neural mechanisms for interacting with a world full of action choices. Annu Rev Neurosci 33:269-298.

Coallier E, Kalaska JF (2014) Reach target selection in humans using ambiguous decision cues. (submitted).

Cook EP, Maunsell JH (2002) Dynamics of neuronal responses in macaque MT and VIP during motion detection. Nat Neurosci 5:985-994.

Ditterich J (2006) Stochastic models of decisions about motion direction: behavior and physiology. Neural Netw 19:981-1012.

Ditterich J (2010) A Comparison between Mechanisms of Multi-Alternative Perceptual Decision Making: Ability to Explain Human Behavior, Predictions for Neurophysiology, and Relationship with Decision Theory. Front Neurosci 4:184.

Ditterich J, Mazurek ME, Shadlen MN (2003) Microstimulation of visual cortex affects the speed of perceptual decisions. Nat Neurosci 6:891-898.

Donovan PW (2014) Alan Turing, Marshall Hall, and the Alignment of WW2 Japanese Naval Intercepts. Notices Amer Math Soc 61:258.

Downing CJ, Movshon JA (1989) Spatial and temporal summation in the detection of motion in stochastic random dot displays. Invest Ophthalmol Vis Sci 30:72.

Dubner R, Zeki S (1971) Response properties and receptive fields of cells in an anatomically defined region of the superior temporal sulcus in the monkey. Brain Res 35:528-532.

Eckhoff P, Holmes P, Law C, Connolly P, Gold J (2008) On diffusion processes with variable drift rates as models for decision making during learning. New J Phys 10:015006.

Fechner G (1966) Elements of psychophysics. Vol. I.

Gescheider GA (2013) Psychophysics: the fundamentals: Psychology Press.

Gnadt JW, Andersen RA (1988) Memory related motor planning activity in posterior parietal cortex of macaque. Exp Brain Res 70:216-220.

Gold JI, Shadlen MN (2001) Neural computations that underlie decisions about sensory stimuli. Trends Cogn Sci 5:10-16.

Gold JI, Shadlen MN (2007) The neural basis of decision making. Annu Rev Neurosci 30:535-574.

Good IJ (1979) Studies in the history of probability and statistics. XXXVII AM Turing's statistical work in World War II. Biometrika 66:393-396.

Green DM, Swets JA (1966) Signal detection theory and psychophysics: Wiley New York.

Hanks TD, Ditterich J, Shadlen MN (2006) Microstimulation of macaque area LIP affects decision-making in a motion discrimination task. Nat Neurosci 9:682-689.

Hernández A, Zainos A, Romo R (2000) Neuronal correlates of sensory discrimination in the somatosensory cortex. Proc Natl Acad Sci U S A 97:6191-6196.

Hernández A, Zainos A, Romo R (2002) Temporal evolution of a decision-making process in medial premotor cortex. Neuron 33:959-972.

Hernández A, Nácher V, Luna R, Zainos A, Lemus L, Alvarez M, Vázquez Y, Camarillo L, Romo R (2010) Decoding a perceptual decision process across cortex. Neuron 66:300-314.

Hirsh IJ, Watson CS (1996) Auditory psychophysics and perception. Annu Rev Psychol 47:461-484.

Horwitz GD, Newsome WT (1999) Separate signals for target selection and movement specification in the superior colliculus. Science 284:1158-1161.

Horwitz GD, Newsome WT (2001) Target selection for saccadic eye movements: prelude activity in the superior colliculus during a direction-discrimination task. J Neurophysiol 86:2543-2558.

Huk AC, Shadlen MN (2005) Neural activity in macaque parietal cortex reflects temporal integration of visual motion signals during perceptual decision making. J Neurosci 25:10420-10436.

Huk AC, Meister ML (2012) Neural correlates and neural computations in posterior parietal cortex during perceptual decision-making. Front Integr Neurosci 6.

Jazayeri M, Movshon JA (2006) Optimal representation of sensory information by neural populations. Nat Neurosci 9:690-696.

Kiani R, Hanks TD, Shadlen MN (2008) Bounded integration in parietal cortex underlies decisions even when viewing duration is dictated by the environment. J Neurosci 28:3017-3029.

Kiani R, Churchland AK, Shadlen MN (2013) Integration of Direction Cues Is Invariant to the Temporal Gap between Them. J Neurosci 33:16483-16489.

Kim J-N, Shadlen MN (1999) Neural correlates of a decision in the dorsolateral prefrontal cortex of the macaque. Nat Neurosci 2:176-185.

LaBerge D (1962) A recruitment theory of simple behavior. Psychometrika 27:375-396.

Laming DRJ (1968) Information theory of choice-reaction times. Oxford, England: Academic Press.

Lappin JS, Bell HH (1976) The detection of coherence in moving random-dot patterns. Vision Res 16:161-168.

Leach J, Carpenter R (2001) Saccadic choice with asynchronous targets: evidence for independent randomisation. Vision Res 41:3437-3445.

Linschoten MR, Harvey LO, Eller PM, Jafek BW (2001) Fast and accurate measurement of taste and smell thresholds using a maximum-likelihood adaptive staircase procedure. Percept Psychophys 63:1330-1347.

Liston DB, Stone LS (2013) Saccadic brightness decisions do not use a difference model. J Vis 13.

Logothetis NK (2003) The underpinnings of the BOLD functional magnetic resonance imaging signal. J Neurosci 23:3963-3971.

Macmillan NA, Creelman CD (1996) Triangles in ROC space: History and theory of "nonparametric" measures of sensitivity and response bias. Psychon Bull Rev 3:164-170.

Maunsell JH, Van Essen DC (1983) Functional properties of neurons in middle temporal visual area of the macaque monkey. I. Selectivity for stimulus direction, speed, and orientation. J Neurophysiol 49:1127-1147.

Mazurek ME, Roitman JD, Ditterich J, Shadlen MN (2003) A role for neural integrators in perceptual decision making. Cereb Cortex 13:1257-1269.

Mikami A, Newsome W, Wurtz R (1986a) Motion selectivity in macaque visual cortex. I. Mechanisms of direction and speed selectivity in extrastriate area MT. J Neurophysiol 55:1308.

Mikami A, Newsome W, Wurtz R (1986b) Motion selectivity in macaque visual cortex. II. Spatiotemporal range of directional interactions in MT and V1. J Neurophysiol 55:1328.

Mitzdorf U (1985) Current source-density method and application in cat cerebral cortex: investigation of evoked potentials and EEG phenomena. Physiol Rev 65:37-100.

Mountcastle VB, Talbot WH, Darian-Smith I, Kornhuber HH (1967) Neural basis of the sense of flutter-vibration. Science 155:597-600.

Newsome W, Mikami A, Wurtz R (1986) Motion selectivity in macaque visual cortex. III. Psychophysics and physiology of apparent motion. J Neurophysiol 55:1340.

Newsome WT, Pare EB (1988) A selective impairment of motion perception following lesions of the middle temporal visual area (MT). J Neurosci 8:2201-2211.

Newsome WT, Britten KH, Movshon JA (1989) Neuronal correlates of a perceptual decision. Nature.

Niwa M, Ditterich J (2008) Perceptual decisions between multiple directions of visual motion. J Neurosci 28:4435-4445.

Noorani I, Carpenter R (2011) Full reaction time distributions reveal the complexity of neural decision-making. Eur J Neurosci 33:1948-1951.

Noorani I, Gao MJ, Pearson B, Carpenter R (2011) Predicting the timing of wrong decisions with LATER. Exp Brain Res 209:587-598.

Palmer J, Huk AC, Shadlen MN (2005) The effect of stimulus strength on the speed and accuracy of a perceptual decision. J Vis 5:376-404.

Pelli DG (1997) The VideoToolbox software for visual psychophysics: Transforming numbers into movies. Spat Vis 10:437-442.

Pilly PK, Seitz AR (2009) What a difference a parameter makes: a psychophysical comparison of random dot motion algorithms. Vision Res 49:1599-1612.

Platt ML, Glimcher PW (1997) Responses of intraparietal neurons to saccadic targets and visual distractors. J Neurophysiol 78:1574-1589.

Platt ML, Glimcher PW (1998) Response fields of intraparietal neurons quantified with multiple saccadic targets. Exp Brain Res 121:65-75.

Purushothaman G, Bradley D (2005) Neural population code for fine perceptual decisions in area MT. Nat Neurosci 8:99.

Qian N, Andersen RA (1994) Transparent motion perception as detection of unbalanced motion signals. II. Physiology. J Neurosci 14:7367-7380.

Qian N, Andersen RA (1995) VI responses to transparent and nontransparent motions. Exp Brain Res 103:41-50.

Qian N, Andersen R, Adelson E (1994a) Transparent motion perception as detection of unbalanced motion signals. I. Psychophysics. J Neurosci 14:7357.

Qian N, Andersen RA, Adelson EH (1994b) Transparent motion perception as detection of unbalanced motion signals. III. Modeling. J Neurosci 14:7381-7392.

Ratcliff R (1978) A theory of memory retrieval. Psychol Rev 85:59.

Ratcliff R, McKoon G (2008) The diffusion decision model: Theory and data for two-choice decision tasks. Neural Comput 20:873-922.

Ratcliff R, Cherian A, Segraves M (2003a) A comparison of macaque behavior and superior colliculus neuronal activity to predictions from models of simple two-choice decisions. J Neurophysiol 90:1392-1407.

Ratcliff R, Thapar A, Mckoon G (2003b) A diffusion model analysis of the effects of aging on brightness discrimination. Percept Psychophys 65:523-535.

Ratcliff R, Hasegawa YT, Hasegawa RP, Smith PL, Segraves MA (2007) Dual diffusion model for single-cell recording data from the superior colliculus in a brightness-discrimination task. J Neurophysiol 97:1756.

Recanzone G, Wurtz R, Schwarz U (1997) Responses of MT and MST neurons to one and two moving objects in the receptive field. J Neurophysiol 78:2904-2915.

Reddi B, Carpenter R (2000) The influence of urgency on decision time. Nat Neurosci 3:827-830.

Reddi B, Asrress K, Carpenter R (2003) Accuracy, information, and response time in a saccadic decision task. J Neurophysiol 90:3538.

Resulaj A, Kiani R, Wolpert DM, Shadlen MN (2009) Changes of mind in decision-making. Nature 461:263-266.

Robinson D, Goldberg M, Stanton G (1978) Parietal association cortex in the primate: sensory mechanisms and behavioral modulations. J Neurophysiol 41:910.

Roitman JD, Shadlen MN (2002) Response of neurons in the lateral intraparietal area during a combined visual discrimination reaction time task. J Neurosci 22:9475-9489.

Romo R, de Lafuente V (2013) Conversion of sensory signals into perceptual decisions. Prog Neurobiol 103:41.

Romo R, Hernández A, Zainos A (2004) Neuronal correlates of a perceptual decision in ventral premotor cortex. Neuron 41:165-173.

Romo R, Brody CD, Hernández A, Lemus L (1999) Neuronal correlates of parametric working memory in the prefrontal cortex. Nature 399:470-473.

Salinas E, Hernandez A, Zainos A, Romo R (2000) Periodicity and firing rate as candidate neural codes for the frequency of vibrotactile stimuli. J Neurosci 20:5503-5515.

Salzman CD, Murasugi CM, Britten KH, Newsome WT (1992) Microstimulation in visual area MT: effects on direction discrimination performance. J Neurosci 12:2331-2355.

Scase M, Braddick O, Raymond J (1996) What is noise for the motion system? Vision Res 36:2579.

Schütz AC, Braun DI, Movshon JA, Gegenfurtner KR (2010) Does the noise matter? Effects of different kinematogram types on smooth pursuit eye movements and perception. J Vis 10:26.

Shadlen MN, Newsome WT (2001) Neural basis of a perceptual decision in the parietal cortex (area LIP) of the rhesus monkey. J Neurophysiol 86:1916-1936.

Shadlen MN, Kiani R (2013) Decision making as a window on cognition. Neuron 80:791-806.

Shadlen MN, Britten KH, Newsome WT, Movshon JA (1996) A computational analysis of the relationship between neuronal and behavioral responses to visual motion. J Neurosci 16:1486-1510.

Simoncelli EP, Heeger DJ (1998) A model of neuronal responses in visual area MT. Vision Res 38:743-761.

Sinha N, Brown JT, Carpenter RH (2006) Task switching as a two-stage decision process. J Neurophysiol 95:3146-3153.

Smith AT, Snowden RJ, Milne AB (1994) Is global motion really based on spatial integration of local motion signals? Vision Res 34:2425-2430.

Smith PL, Ratcliff R (2004) Psychology and neurobiology of simple decisions. Trends Neurosci 27:161-168.

Snowden R, Braddick O (1989) The combination of motion signals over time. Vision Res 29:1621-1630.

Snowden RJ, Verstraten FA (1999) Motion transparency: making models of motion perception transparent. Trends Cogn Sci 3:369-377.

Snowden RJ, Treue S, Andersen RA (1992) The response of neurons in areas V1 and MT of the alert rhesus monkey to moving random dot patterns. Exp Brain Res 88:389-400.

Snowden RJ, Treue S, Erickson RG, Andersen RA (1991) The response of area MT and V1 neurons to transparent motion. J Neurosci 11:2768-2785.

Stone M (1960) Models for choice-reaction time. Psychometrika 25:251-260.

Story GW, Carpenter R (2009) Dual LATER-unit model predicts saccadic reaction time distributions in gap, step and appearance tasks. Exp Brain Res 193:287-296.

Swets JA (1961) Is there a sensory threshold. Science 134:168-177.

Swets JA (1986) Indices of discrimination or diagnostic accuracy: their ROCs and implied models. Psychol Bull 99:100.

Takemura H, Tajima S, Murakami I (2011) Motion integration and segregation modulated by surrounding motion. J Vis 11:739-739.

Talbot W, Darian-Smith I, Kornhuber H, Mountcastle V (1968) The sense of flutter-vibration: comparison of the human capacity with response patterns of mechanoreceptive afferents from the monkey hand. J Neurophysiol 31:301.

Thura D, Cisek P (2014) Deliberation and Commitment in the Premotor and Primary Motor Cortex during Dynamic Decision Making. Neuron 81:1401-1416.

Thura D, Beauregard-Racine J, Fradet C-W, Cisek P (2012) Decision making by urgency gating: theory and experimental support. J Neurophysiol 108:2912-2930.

Tripathy SP, Barrett BT (2004) Severe loss of positional information when detecting deviations in multiple trajectories. J Vis 4:4.

Uhlenbeck GE, Ornstein LS (1930) On the theory of the Brownian motion. Phys Rev 36:823.

Usher M, McClelland JL (2001) The time course of perceptual choice: The leaky, competing accumulator model. Psychol Rev 108:550-592.

Vickers D (1970) Evidence for an accumulator model of psychophysical discrimination. Ergonomics 13:37-58.

Wald A (1945) Sequential tests of statistical hypotheses. Ann Math Stat 16:117-186.

Wald A (1973) Sequential analysis: Courier Corporation.

Watamaniuk S, McKee S, Grzywacz N (1995) Detecting a trajectory embedded in random-direction motion noise. Vision Res 35:65.

Watamaniuk SN, Sekuler R (1992) Temporal and spatial integration in dynamic random-dot stimuli. Vision Res 32:2341-2347.

Watamaniuk SN, Sekuler R, Williams DW (1989) Direction perception in complex dynamic displays: the integration of direction information. Vision Res 29:47-59.

Webb BS, Ledgeway T, Rocchi F (2011) Neural computations governing spatiotemporal pooling of visual motion signals in humans. J Neurosci 31:4917.

Werner G, Mountcastle VB (1965) Neural activity in mechanoreceptive cutaneous afferents: Stimulus-response relations, Weber functions, and information transmission. J Neurophysiol.

Williams DW, Sekuler R (1984) Coherent global motion percepts from stochastic local motions. Vision Res 18:24-24.

Zeki SM (1974) Functional organization of a visual area in the posterior bank of the superior temporal sulcus of the rhesus monkey. J Physiol 236:549-573.

Zohary E, Scase M, Braddick O (1996) Integration across directions in dynamic random dot displays: vector summation or winner take all? Vision Res 36:2321.

Zylberberg A, Barttfeld P, Sigman M (2012) The construction of confidence in a perceptual decision. Front Integr Neurosci 6:79.